An Acoustical Study of the Playing Characteristics of Brass Wind Instruments

Shona Mary Logie

A thesis submitted in fulfilment of the requirements
for the degree of Doctor of Philosophy
to the
University of Edinburgh
August 2012

Abstract

When assessing the quality of a brass instrument the player must consider a number of factors, the main consideration being the playability of the chosen instrument. The playability of an instrument is a broad term used to describe how well the instrument plays; this includes how in tune the resonant modes are, how easy it is to start and move between notes, how easy it is to bend notes and the degree of spectral enrichment during a crescendo that is able to be produced.

The starting transient is known to be of crucial importance for both the musician and listener, and previous work in the field has been mainly concerned with such starting transients; this work focusses on inter-note transitions. Transitions between notes include both starting and finishing transients as the initial note is ended and the next begun. Using high speed photography images synchronised with pressure signals from the mouthpiece and bell end, the inter-note transitions are explored. Results from these experiments are compared with those from a simple one dimensional time domain model.

Other techniques used to determine the playability of a specific instrument include the rate at which the instrument timbre becomes 'brassy' due to nonlinear effects, that are a consequence of loud playing. The relative significance of viscothermal wall losses and nonlinear effects within realistic brass instruments have been explored here using experiments on cylindrical tubes of different internal diameters. These experimental results are compared with results from a computational model that uses weakly nonlinear wave propagation theory and includes viscothermal losses. It is also possible on some brass instruments, when playing loudly, to achieve what are known as super high notes; these notes are above the frequency where the instrument has well defined resonances. Experimental results are presented here using optical techniques to visualise the motion of the player's lips during playing of these super high notes.

Declaration

Except where otherwise stated, the research undertaken in this thesis was the unaided work of the author. Where the work was done in collaboration with others, a significant contribution was made by the author.

Shona Mary Logie
August 2012

Acknowledgements

I firstly would like to thank Murray Campbell for his unfaltering energy, enthusiasm, support and guidance throughout my PhD. He has not only supported me for the last 4 years, but also sparked my interest in acoustics right at the start of my undergraduate degree. I really can't thank him enough for being a truly amazing supervisor and lecturer.

I also owe a very big thank you to John Chick for all his help and support and for always being on the other end of the phone in times of panic over the last few years, even if his teethy horn playing has caused me numerous headaches. I'd also like to think that all those times he told me "it'll be good for you" have paid off, and were good for me in the end.

Joël Gilbert has been a great help in many ways, not to mention his enthusiasm - it is impossible to not get excited about cylindrical tubes, of all things, when Joël and Murray are in the lab together. He has always made time to help me whether it be here in Edinburgh or over Skype. Thank you.

Thank you to Stefan Bilbao for being very patient with all my computational questions, and being a great help throughout the last few years.

I would like to also thank Jonathan Kemp for all his help with experiments, theory, computing, and for always being there to answer any acoustics question. Arnold Myers has been the provider of many instruments for study, and has been there to provide a slightly different take on acoustics. Richard Smith has also provided me with ideas, allowed me to visit his workshop, and loaned me one of his super duper, super high note trumpets.

Everyone who has been part of the office has made such a difference to my time doing this PhD. Although this lot were only here for the first few months - Sam Stevenson provided me with some very useful instructions to get me going, and gave me lots of ideas as to where my work could go along with Rob MacDonald

and Mike Newton. Alan Wooley has always been on hand to remind me how long things really do take, and give me an evil eye if thesis writing seemed to have slowed. Darren Hendrie provided some awesome live office music, and has made sure that I know I have to do something that makes me happy and not be an actuary.

The two people who have been there through it all and in the same boat are Lisa Norman and Adam Apostoli - we've certainly had PhD ups and downs together. Lisa has been a great friend and always there to listen to me moaning about whatever it happens to be on the day. She has also been my on-hand brass advisor for all things to do with instruments and playing. Adam has been my LaTeX, Matlab, C++, Labview help and my traveling buddy - I won't be forgetting the freezing outdoor Lituus concert, in Switzerland, anytime soon.

Other computer support has came from Alan Watt. He has supported and revived not one but two 'comedy laptops' in my time here. He also provided some non-acoustics banter in the office for a while, along with Liz McIvor.

Lauren Keddie has been the best friend anyone could ask for. She has always supported me and showed so much dedication to my PhD that she accompanied me all the way to Australia...just to listen to my presentations I'm sure.

My parents have supported me through a lot during my time at university and I sincerely thank them for everything they have done for me. My Dad deserves a special thank you for copious amounts of teeth colouring in, proof reading of basically everything I have ever written, and showing such a keen interest in all my work, whether he understands it or not.

Lastly, I would like to thank my boyfriend Pete. He has put up with a lot, especially over the last months. Without his support, and love, stressful times would have been much worse. Thank you for everything.

Financial support was provided by EPSRC.

Nomenclature

General symbols

Symbol	Explanation
z	specific acoustic impedance
ω	angular frequency
$p(\omega)$	acoustic pressure
$u(\omega)$	acoustic particle velocity
Z	acoustic impedance
S	cross sectional area
$U(\omega)$	acoustic volume flow
ν_n	frequency
n	harmonic number
l	effective length
c	speed of sound in air
D	tube diameter
a	bore radius
x	distance along bore from input
Γ	flare rate
F	nonlinear function
ΔP	pressure difference
$U(t)$	volume velocity
ρ	density of air
$h(t)$	lip opening height
c_0	small signal speed of sound
γ	ratio of specific heat at constant pressure to specific heat at constant volume
X_s	distance to shock wave formation
P_{atm}	atmospheric pressure
p_{in}	input pressure
L	tube length
B	brassiness potential parameter

L_{ecl}	equivalent conical length
f_1	nominal fundamental frequency
p_{out}	output pressure
Q	monopole source strength
d	distance from monopole source to point of measurement
$u(bell)$	acoustic particle velocity at bell exit plane
T	transfer function
α	viscothermal attenuation coefficient
Z_L	radiation impedance
Z_0	characteristic impedance of tube
Ψ	velocity potential
Ψ_l^n	grid function
Γ	Gold'berg number
M	Mach number

Abbreviations

Abbreviation	**Explanation**
FFT	Fast Fourier Transform
RMS	Root Mean Square
FDTD	Finite Difference Time Domain
$T14$	Transfer function between microphones 1 and 4
$SC1$	Spectral Centroid at microphone 1

Musical Dynamics

pp	*pianissimo*	'very soft'
p	*piano*	'soft'
mp	*mezzo-piano*	'moderately soft'
mf	*mezzo-forte*	'moderately loud'
f	*forte*	'loudly'
ff	*fortissimo*	'very loudly'

Contents

List of Figures

List of Tables

Chapter 1

Introduction

The brass instrument family has developed throughout history to contain many weird, and wonderful instruments, along with the well known modern selection of instruments commonly available today. Although brass instruments in their present form are well recognised, there is a common misconception that the instruments are categorised, and so called, because of the material used in their manufacture. Firstly, not all brass instruments are made from brass (their main material could be silver, copper, wood or even plastic), and secondly, they are categorised based on the manner in which they are sounded. Brass instruments can also be called *labrosones* which literally means 'lip-vibrated instruments' [Baines 93]. The player's lips are pressed over the input end of the instrument and when 'buzzed' together the air blown through the lips is modulated in such a way as to excite the air column within the instrument, and thus produce the sounded notes. It is this common excitation method that leads to the classification of such instruments.

When thinking about brass instruments in a simple conceptual manner, they do not strike one as being particularly complex; the player's lips open and close periodically, which provides the instrument with a periodic oscillating pressure wave. If the lips are vibrating at a frequency close to one of the resonant modes of the instrument, the pressure wave is reinforced within the instrument. When the pressure wave reaches the end of the instrument, some of the sound is radiated to the atmosphere, while a portion will be reflected back towards the input end and create a standing wave. The realities of this simple concept are not quite as simple however.

The nature of the lip motion is one of the most complex parts of a brass instrument system, and one of the most difficult to study. In many cases the lips have been modelled as a mass on a spring approximation, and this has been successful up to a point. The lips do not, however, move in just one dimension, as with a one mass/spring model, and it has been found that the lip motion is in all three dimensions [Cullen 00b]. It can also be the case that simultaneously different parts of the lips are moving in different directions. Therefore to model the lip motion correctly the model would need to consist of more than one mass and spring. To assist in understanding the lip motion, the use of high speed photography of the lips has proved to be a non-intrusive way to view the lip motion during playing. Even with the best understanding of the instrument, and the physics of what is happening inside it during playing, we do not have a full understanding of the complete system until we understand the nature of the motion of the lips and the coupling between them and the instrument itself.

The nature of the lip motion is further complicated by the fact that it is part of a nonlinear coupled system. The lips control the air flow into the instrument, which in turn affects the behaviour of the lips as there is a complicated feedback system between these components. The pressure wave which leaves the player's lips is subject to a number of factors as it propagates to the end of the instrument, and back to the lips, where it can then reinforce the lip motion. At high amplitudes, the pressure wave is subject to highly nonlinear effects as it propagates down the instrument [Fletcher 99a]; this acts to increase the amplitude of the higher harmonics and hence increase spectral enrichment. There is also an opposing reduction in the higher harmonics due to the frequency dependent viscothermal losses that the wave is subject to during propagation.

The complex system of a brass instrument is not yet fully understood, but in studying this it also has a further reaching goal than to satisfy scientists with increased knowledge. Players assess instruments by their 'playability'; this is a term which generally means how well the player perceives an instrument to play. The playability of a specific instrument can be determined by its tonal qualities, the ease with which notes can be started and moved between, how easy it is to bend notes around the resonant modes using the lips to make slight alterations to the played frequency, and the degree of spectral enrichment that can be produced during a crescendo. Players are very sensitive to how an instrument plays and

how they can gain the most appealing sound from the instrument; this however is very hard to quantify. Brass instrument playing involves much feedback from the instrument which is interpreted by the player as feel and sound, again both are difficult quantities to verbalise and quantify. To be able to rank instruments by their playability would lessen the need for players to express their feelings on an instrument, when assessing it, and give a more direct comparative factor between instruments.

With a fuller understanding of the mechanics and physics behind brass instruments and them being played, it should be possible to determine a playability factor for instruments, and be able to theoretically assess the overall quality of a given instrument. With this understanding, manufacturers will hopefully be able to use this knowledge to optimise instruments for the best playability.

1.1 Aims

The broad aim of this thesis is to carry out a series of experimental studies, along with comparisons to computational simulations, that are aimed at trying to broaden the understanding of some of the playability issues discussed above, specifically the following aims:

- Explore slurred transients on brass instruments through high speed filming of the player's lips, synchronised with pressure data from inside the mouthpiece and radiated from the bell.
- Use a forced oscillation excitation source to explore the behaviour of the pressure in the mouthpiece and radiated from the bell of the instrument during a slurred transient.
- Compare experimentally determined player and forced oscillation results with a time domain computational model.
- Use transfer function measurements and high speed photography of the player's lips to determine if there is significant reinforcement for the lips at extremely high frequencies on the trumpet.
- Use transfer function and spectral centroid measurements to explore the relative significance of nonlinear effects and viscothermal losses within cylindrical tubes as simple brass instruments.
- Compare cylindrical tubes measurements with a computational simulation to determine whether the nonlinear effects or viscothermal losses are the dominant factor in brass instruments.

1.2 Contents

Chapter 2 gives an overview of the relevant acoustic theory for this thesis. The role of the player's lips and associated behaviour is discussed. This chapter also includes a discussion of the 'brassy' sound of brass instruments, and the relevant importance of the nonlinearities and losses in the system.

Chapter 3 presents experimental work on transients. The transients work is concerned with slurred transitions between two resonant modes of the instrument. The experimental techniques used in this chapter include high speed photography of the player's lips and forced oscillation of the system by means of a loudspeaker.

Chapter 4 details the computational investigation into transients, as discussed experimentally in Chapter 3. A one dimensional finite difference time domain model is used and results compared directly with player and loudspeaker data presented in Chapter 3.

Chapter 5 discusses extreme high notes on trumpets. Some expert players are able to play notes well above the normal playing range of the trumpet; this chapter presents some preliminary results of the transfer function of a trumpet/mouthpiece combination used for playing extreme high notes.

Chapter 6 gives a discussion of the relative importance of nonlinear effects and viscothermal losses. Experiments and results are presented using cylindrical tubes as a simple brass instrument to explore these effects. Experimental results are also compared with those from a computational simulation based on weakly nonlinear propagation theory.

Chapter 7 presents a summary of the conclusions from this thesis, along with suggestions for further work in this area.

Appendix A contains extra figures of slurred transients on a horn, relating to those in Section 3.3.2.

Appendix B shows extra figures relating to the individual tubes spectral centroid results as discussed in Section 6.5.2.

Chapter 2

Brass wind instrument acoustics

There are a number of textbooks on musical acoustics that give detailed descriptions of the theory of brass instrument acoustics; such as [Backus 77, Benade 76, Campbell 87, Fletcher 98]. An overview of the experimental and theoretical research in the field of brass instrument work was presented in [Campbell 04]. A thorough review of the theory that is relevant to this work and mention of the associated literature is presented in this chapter.

2.1 Overview

Brass instruments all operate under the same principle and generally have the same components which make it possible for the instrument to produce sound. In a simplistic manner it is possible to think of the instrument as comprising of three main parts: the lips which act as a mechanical oscillator; the air column within the instrument which acts as the acoustic resonator; and the airflow which couples these two parts together.

Figure 2.1 shows the three parts of the system combined to form a feedback loop. This feedback loop is created as the player induces a pressure difference across the lips as they blow. This pressure difference causes the lips to oscillate which in turn creates an acoustic pressure signal at the input of the instrument. The lips act as a valve in the system and are referred to as a lip-reed with regards to brass instruments, serving the same purpose as a cane reed in woodwind acoustics. The player's lips receive acoustical feedback from the resonating air column within the instrument, which itself affects the behaviour of the lips.

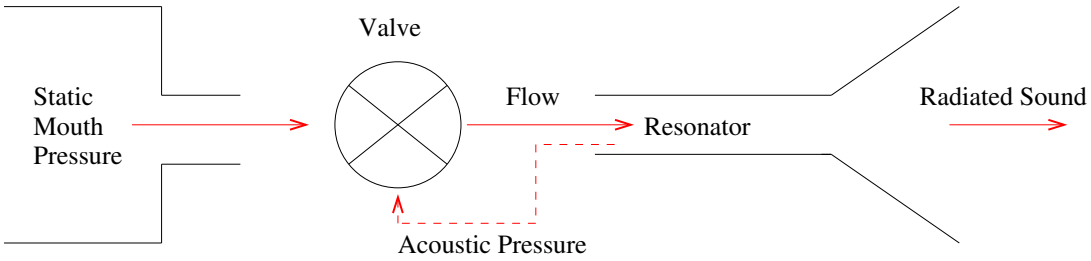

Figure 2.1: A basic model of a wind instrument. A brass instrument can be thought of as three parts: resonator, pressure controlled valve and the air flow through the system. The air column acts as the resonator, and the lips as the valve which controls the air flow.

At this point it is convenient to split the study of brass instruments into four sections [Carrall 06], these being:

- Behaviour of the resonator (air column or instrument bore)
- Behaviour of the mechanical oscillator (lip reed)
- Coupling between instrument and lip reed
- Nonlinearities in the system.

2.2 The resonator - the air column

2.2.1 Impedance

The specific acoustic impedance, z, is a useful place to begin when wishing to describe the acoustics of brass instruments. Here z is a function of angular frequency, ω, and is defined as the ratio of acoustic pressure $p(\omega)$ to the acoustic particle velocity $u(\omega)$.

$$z(\omega) = \frac{p(\omega)}{u(\omega)} \tag{2.1}$$

The acoustic impedance Z at a surface, S, is defined as the ratio of the acoustic pressure, $p(\omega)$, to the acoustic volume flow through the surface $U(\omega)$:

$$Z(\omega) = \frac{p(\omega)}{U(\omega)} \tag{2.2}$$

where $U(\omega) = u(\omega)S$.

The input impedance of a brass instrument is defined as the acoustic impedance, Z, at the entrance plane of the instrument. It is also a function of angular frequency and describes the strength of pressure variation for a given amount of alternating flow of air through the player's lips and into the instrument. The input impedance can be measured experimentally and an input impedance curve produced using the Brass Instrument Analysis System [BIAS 13], as shown in Figure 2.2. Each resonance of the air column within the bore of the instrument corresponds to a peak on the impedance curve [Fletcher 98]. Generally the playing frequencies of the instrument are very close to one of those resonances; with the exception of the pedal note, the lowest note that can be played, where the playing frequency cannot be assigned to the lowest resonance peak as it lies around a musical fifth higher [Gilbert 08a], the input impedance peaks give the frequencies at which the instrument will sound.

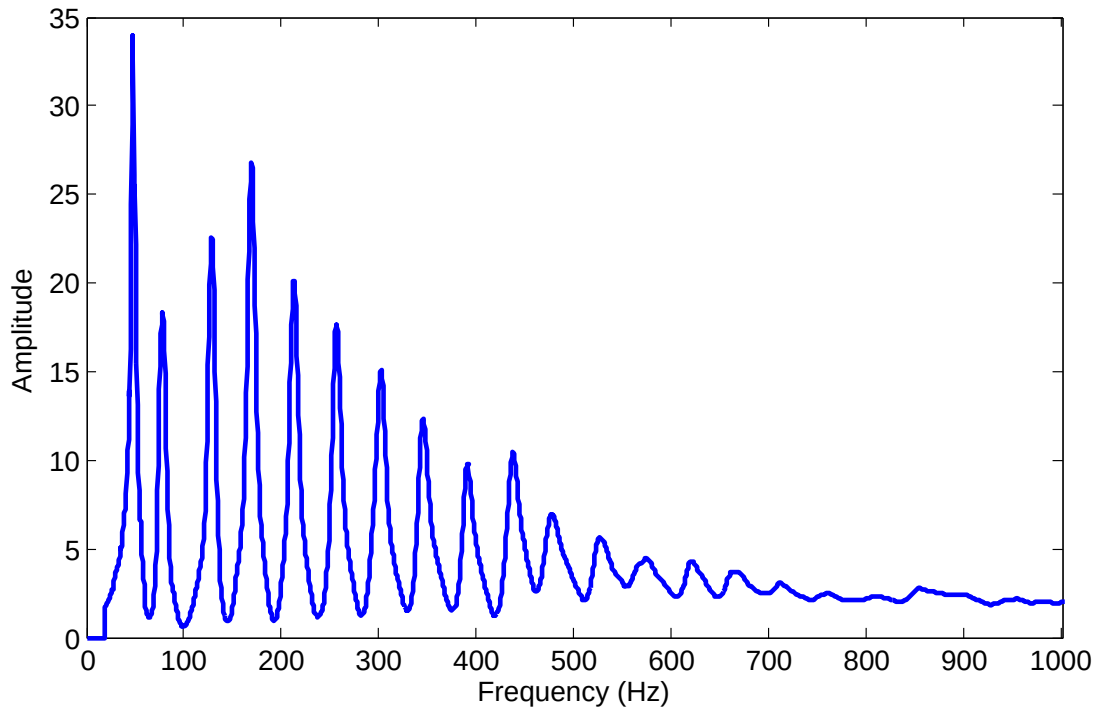

Figure 2.2: Typical input impedance of a brass instrument. This example is of a 5-valve tuba in F.

2.2.2 Simple resonator approximation

The player's lips modulate the air flow into the instrument; this allows a periodic modulation of high and low pressures. The pressure wave that is produced can be taken, as a first approximation, to be a plane wave. This resulting pressure wave propagates along the air column within the instrument and is partially reflected at any changes in acoustic impedance. Impedance changes, and hence partial reflections, could occur where there is a change in the cross section of the bore, a tone hole, a joint in the wall material and also at the end of the instrument. While some of the pressure wave is reflected at the end of the instrument, some of the sound is radiated to the surrounding atmosphere. A standing wave will be set up within the instrument if the air column has a resonance close to the frequency of the pressure wave.

Some brass instruments are largely cylindrical in design, for at least a considerable proportion of their length. This is true for the trombone, trumpet and (to a lesser extent) the horn.

As the instrument has the player's lips at one end, this effectively makes the instrument a cylinder closed at one end. As a result of this the air column inside the instrument has a pressure antinode at the lips and a pressure node at the bell. In the ideal case of a perfect cylinder closed at one end the instrument would have a harmonic series of resonances at frequencies:

$$\nu_n = \frac{2n-1}{4l}c \tag{2.3}$$

where n is the harmonic number (1,2,3...), l is the effective length of the cylinder, and c is the speed of sound in air. The effective length denoted here is not equal to the physical length of the tube. The anti-node at the end of the tube is approximately *D/3* outside the end of the tube, where D is the tube diameter; hence making the effective length, l, longer than the physical length of the instrument by *D/3* [Campbell 87].

This simple instrument would only be able to play the odd harmonics, (1,3,5...) and so would be of limited use [Fletcher 98]. Real brass instruments, however, are not this simple, and have a more complicated shape and design.

2.2.3 Real brass instrument shape

There are many shapes and sizes of brass wind instruments, but the majority share a number of common features: a section of tubing that is made up from cylindrical and conical sections (with approximately circular cross section), a rapidly flaring bell and a cup shaped mouthpiece. Most instruments have a means to change the sounding length of the tubing by valves, a slide or even tone holes (this is uncommon however). Some instruments such as the natural trumpet are of fixed length. All of these features contribute to determining the actual resonances of the instrument and mean that real instruments cannot be treated as a simple closed cylinder. It is fundamental to the playability of the instrument that these components are designed correctly to achieve the most beneficial set of resonances [Benade 76]. Equation 2.3 gives the series of resonances of a simple cylinder; to play an instrument with only these resonances would produce only odd-numbered members of a harmonic series. In a real brass instrument the combination of the effects of the mouthpiece and bell give a series of resonances that are close to a complete harmonic series apart from the fundamental [Campbell 87].

2.2.4 Mouthpiece effect

A brass instrument mouthpiece consists of two main parts; the cup and the shank. The player places the lips into the cup of the mouthpiece and the shank is the tapered tube which fits into the instrument. Ideally there should be a smooth join between the end of the shank and the instrument bore so the shank radius is approximately equal to that of the bore at this end, whereas at the mouthpiece end the shank radius is much smaller than the instrument bore. When the player has placed the lips inside the mouthpiece a volume of air is enclosed which acts as a simple Helmholtz resonator [Campbell 87] and therefore has its own resonance determined by the volume of air that is enclosed and the area of the opening in the shank of the mouthpiece. The mouthpiece acting as a Helmholtz resonator has two resulting effects; it reduces the frequencies of the higher modes of the instrument [Backus 77] along with strengthening some of the resonances of the instrument around the mouthpiece resonant frequency [Benade 76].

2.2.5 Bell effect

The bell of a brass instrument has a dual effect on the sound produced. The flaring bell acts as a high pass filter, which improves the radiation of higher frequency components of the sound; this is what gives brass instruments their distinctive sound and timbre. Because of this high pass filter effect brass instruments are highly directional with the majority of the sound being radiated in the direction that the bell is pointing. The other effect that the bell has on the sound is that it raises the frequency of the lower modes in the instrument. The shape of a brass instrument can be approximated to that of a Bessel horn [Benade 59, Benade 74] and can be described using:

$$a = b(x + x_0)^{-\Gamma} \tag{2.4}$$

where a is the bore radius, x is the distance along the bore from the mouth of the horn which is located at position x_0. b and x_0 are chosen to give the correct radii at each end of the horn, and Γ defines the rate of flare (where 0.7 is a realistic value for instruments such as trumpets and trombones [Young 60]). Benade [Benade 76] calculated the approximate resonance frequencies, ν_n, for this model at the throat in the following:

$$\nu_n \approx \frac{c}{4(l + x_0)} \left\{(2n - 1) + \beta[\Gamma(\Gamma + 1)]^{1/2}\right\} \tag{2.5}$$

where c is the speed of sound, l is the horn length, and β is a parameter equal to approximately 0.6 for $\Gamma < 0.8$ and 0.7 for $\Gamma > 0.8$ [Fletcher 98].

In effect, the effective length of the air column is shorter at low frequencies, where the wavelength is longest, and cannot 'see' the bell [Campbell 87] as the bell radius is smaller than the wavelength; this has the effect of raising the frequency of the lowest modes.

Taking into account the effects of both the mouthpiece and bell we can see that the higher mode frequencies are lowered and the lower mode frequencies are raised. Therefore, the combined effect of the whole instrument and components creates resonances which are very close to a complete harmonic series. Nevertheless, the fundamental mode of the instrument is still an exception to this statement. The fundamental mode exhibits some very interesting different behaviour [Gilbert 08a].

2.3 The lips - mechanical oscillator

Much of the mechanics of brass instrument playing and the motion of the lips is driven by the player's intuition rather than conscious manipulation of the lips. When players wish to sound a note on a brass instrument they force their lips to periodically open and close. In many ways, modelling the lips in the way of a mass on a spring has been successful; this is the most basic approximation that can be associated with the oscillatory motion of the lips. The lips, however, move in a more complicated way than this one mass model can describe. The lips are made up of soft tissue and muscle, and players have great control over many aspects of their lip motion; they can greatly vary the tension, shape and mechanical properties of their lips. The lips do not just move in one dimension but in all three; it is entirely possible that adjacent parts of the lip are moving in different directions simultaneously. Studies [Martin 42] have shown that the lips exhibit motion in the vertical plane of lip opening and also horizontally perpendicular to this plane. It is the horizontal motion of the lips that causes the air to be displaced by the lips. However, it is assumed that this horizontal motion does not significantly affect the air flow through the lip channel and it is the overall open area of the lips that control the flow [Cullen 00b]. Both lips are interacting with the air column within the instrument, the rim of the mouthpiece, the teeth, the opposing lip and the air flow through the lips, resulting in a complicated system.

2.3.1 Pressure controlled valve

The player's lips are the component that allows the air flow from the lungs into the instrument to be regulated; this is in the form of an oscillating flow which couples to the instrument producing a self-sustaining oscillation. The lip-reed's oscillation is controlled by the air flow into the instrument as well as itself controlling this air flow. For this self-sustained oscillation to be produced, the lip-reed must add energy to the system in such a way as to balance the energy lost to friction and radiation etc.

Like most reeds, the lip-reed acts as a closed end for the instrument; this means there is a pressure anti-node at the input of the instrument. At this pressure anti-node the pressure fluctuates above and below a mean value. The geometry of the

reed determines the way in which the reed responds to the pressure fluctuations and this leads to how the reed is classified.

2.3.2 Inward and outward striking reeds

A musical reed can be thought of as a valve mechanism, controlled by the pressure change that happens across the valve. In a brass wind instrument the player places the mouthpiece on the lips and then blows into the mouthpiece; this creates a static overpressure upstream of the reed, hence giving a pressure difference over the valve.

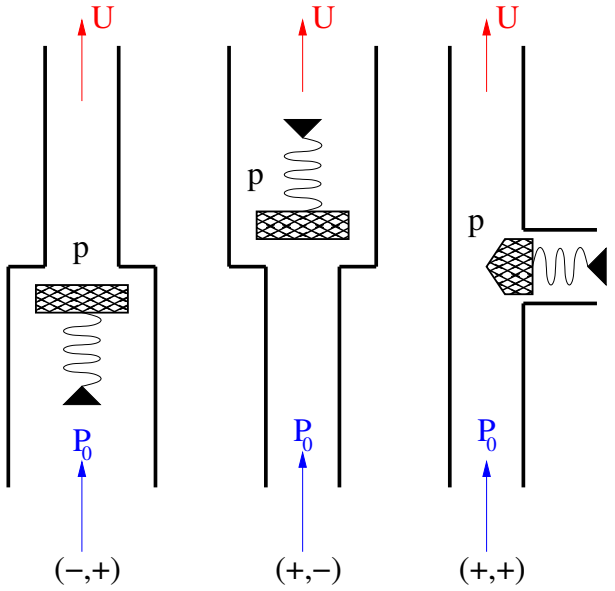

Figure 2.3: Simplified models of pressure controlled valves. From left to right: inward striking reed, outward striking reed, sideways striking reed. Adapted from [Fletcher 98].

Helmholtz [Helmholtz 77] was responsible for the majority of the earliest work into the physical properties of wind instruments, including brass wind instruments. The first attempt at classifying musical valves was made by Helmholtz; he attempted to classify valves (reeds) by their response to change in pressure. Helmholtz description of the reed behaviour was expanded by Fletcher [Fletcher 93, Fletcher 98]. Fletcher and Rossing [Fletcher 98] use the notation (σ_1,σ_2) to classify the types of reeds. σ_1 has the classification of $+1$ if there is a larger pressure at the inlet side of the valve and it tends to open, and -1 if

it tends to close. Likewise, σ_2 shows the effect of the pressure at the outlet of the valve, again having +1 and -1 classifications. Helmholtz called the (−1,+1) valve the 'inward-striking' reed and the (+1,−1) as the 'outward-striking' reed. There is another combination which has been called the 'sideways-striking' or 'sliding-door' reed and this is (+1,+1). There doesn't appear to be any musical use for the combination (−1,−1). The 3 types of reed are shown schematically in Figure 2.3.

In instruments such as the saxophone or clarinet, with cane reeds, the valve mechanism has been decidedly classified as being 'inward-striking'. 'Inward-striking' means that the reed closes in response to an increase in static pressure at the input and these instrument reeds can be well represented by the mass on a spring one-mass model, as shown in [Bilbao 08, Dalmont 95, Dalmont 03]. The lip-reed in brass instruments, however, has not yet been able to be classified in the same way [Yoshikawa 95, Chen 96, Newton 08, Cullen 00a]. Due to this uncertainty it makes it extremely difficult to describe the lip-reed using a single degree-of-freedom model.

There have been some very successful attempts at modelling the lip-reed in this manner; these studies generally approximate the lip-reed to be mostly 'outward-striking'. A number of the most successful attempts are detailed in [Adachi 96, Vergez 00, Msallam 00].

2.3.3 Photographic study of the lips

Photographic techniques to view brass player's lip motion have been pursued for many years with work beginning in the 1940s by Martin [Martin 42]. Martin used a stroboscopic technique to photograph the lip motion of a cornet player. This work by Martin led to more attempts at viewing and recording the motion of the lips during playing [Yoshikawa 95, Copley 95, Richards 03, Bromage 07, Stevenson 09b]. These investigations have proved very successful in broadening the understanding of the lip-reed and its behaviour under near real playing circumstances. Along with this work in photographing real human lips while playing, a substantial amount of work has been done using artificial lips. The first development of an artificial mouth is detailed in [Gilbert 97]. There have been a number of further artificial mouth designs and experiments using these to sound brass instruments [Gilbert 98, Neal 01, Bromage 03, Petiot 03, Newton 08].

Also a substantial amount of work has been done on photographing steady state behaviour of the brass player's lips, as discussed above, but a slightly newer area of interest is the transient behaviour of the lips. The steady state behaviour of the lips has to be initiated and this cannot be instantaneous; there is a finite time when the various parts of the system begin to cooperate and then eventually settle on a stable behaviour which is self sustaining. Many studies, including [Berger 64, Saldanha 64, Luce 67], have verified that the beginning and end of a note, the transients, are extremely important when trying to identify characteristics of a note, such as timbre. When the transient section of a note is removed, it can be difficult or often not possible to identify the instrument which produced the note in question.

Transients are also very important to musicians in determining the quality of an instrument; the ease for a player of starting a note on an instrument may distinguish a good instrument from a bad one. When developing a note there are two main areas of instrument design that should be taken into consideration [Benade 69, Benade 76]. Firstly, in the same way that this factor is important in sustaining a note, the fact that there has to be harmonically related resonances affects the initial development of a note also. For an oscillation and coupled regime to be sustained in the instrument the frequency must be close to a resonance of the air column. Secondly, there is a finite time taken for the initial disturbance to travel from the lips along the bore of the instrument and be reflected at the bell and return to the lips. Within this finite time the lips start oscillating without knowing anything about the instrument and its resonances and before they are able to couple to the rest of the system.

2.4 Nonlinearity

The volume flow of air passing through the lip-valve has a nonlinear relationship with the pressure difference across the valve . This volume flow is determined by the pressure difference over the valve, the lip-reed, along with the open area of the lips. The result of this nonlinear relationship is the cause of the pressure waveform measured in the mouthpiece being non-sinusoidal [Backus 71, Elliot 82, Fletcher 99a]. Even if the player's lips were to open and close sinusoidally the airflow through them is not usually sinusoidal itself, because of the nonlinearity

of the valve. When playing at low and moderate levels, the harmonic content of the sound is produced mainly due to the lip-reed's nonlinearity.

2.4.1 Basic lip model

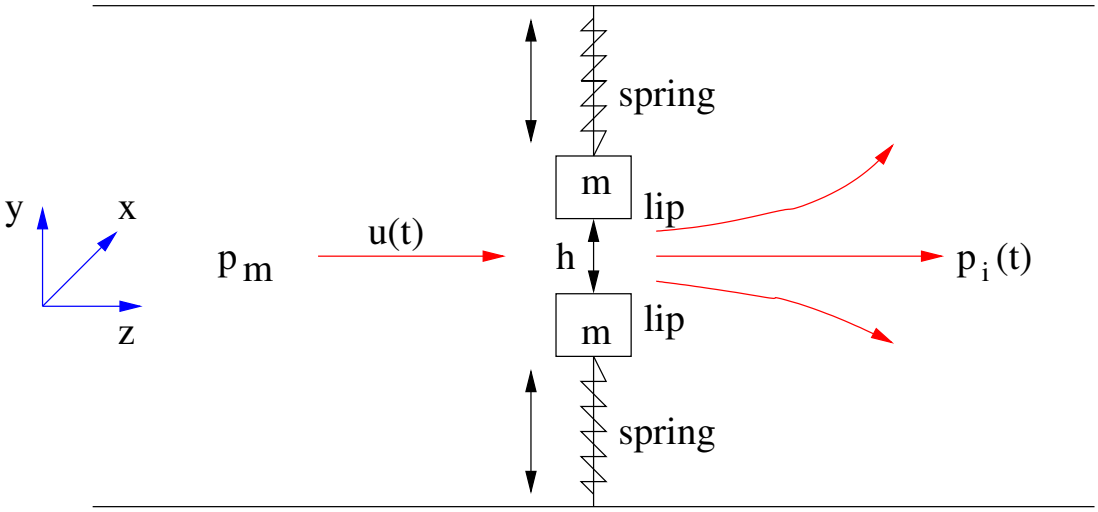

Figure 2.4: Basic one mass lip reed model, where the lips behave as masses on springs. P_m is the pressure inside the mouth, P_i is the pressure in the mouthpiece and the height of the lip opening is denoted by h.

Figure 2.4 shows a diagram of the basic lip-reed model that was first proposed by Elliot and Bowsher [Elliot 82]. Knowing that there is a nonlinear relationship between the pressure difference across the lip-reed and the flow through this valve, the volume flow rate $U(t)$ of the air passing into the instrument can be described using some nonlinear function F of the pressure difference:

$$U(t) = F(\Delta P) \tag{2.6}$$

where ΔP is the pressure difference across the reed, and is given by:

$$\Delta P = P_m - P_i(t) \tag{2.7}$$

where P_m is the pressure in the mouth, and $P_i(t)$ is the pressure in the mouthpiece. The volume velocity (volume flow rate) is given by the product of the particle velocity $u(t)$ and the open area $S(t)$:

$$U(t) = S(t)u(t) \tag{2.8}$$

Elliot and Bowsher [Elliot 82] assumed that the pressure inside the player's mouth was constant, that the flow through the lip channel could be described by the Bernoulli equation, and that there was no downstream pressure recovery. Therefore, using these assumptions the volume flow across the lips may be written as:

$$U(t) = S(t)\sqrt{\frac{2\Delta P}{\rho}} \tag{2.9}$$

The result of combining equations 2.9 and 2.7 gives the following:

$$U(t) = S(t)\sqrt{\frac{2(P_m - p_i(t))}{\rho}} \tag{2.10}$$

From this equation it is clear that the behaviour of the lip open area as a function of time is directly related to the volume flow entering the instrument. For this type of model the open area is modelled as a rectangular space as shown in Figure 2.5.

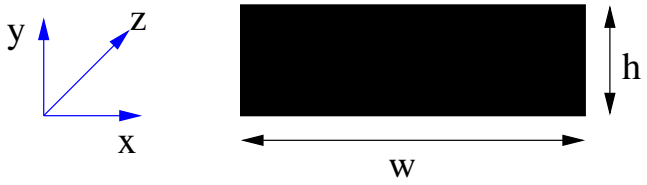

Figure 2.5: Lip open area of one mass model (shown in Figure 2.4). The width of the channel is shown as w and the height of the open area as h.

It has been shown, in a number of works, that a basic one degree of freedom lip model can be used to successfully produce realistic synthesised tones [Adachi 96, Dietz 95, Msallam 00]. However, it was shown in [Yoshikawa 95] that real player's lips are able to produce a number of features that are not possible in this one degree of freedom model; for example - players are able to 'lip' notes both up *and* down from the resonant mode frequency of the air column [Cullen 00a, Cullen 00b, Neal 01, Campbell 04]. For this particular feature of a real musician's playing technique a two degree of freedom model is needed [Richards 03].

2.4.2 Lip opening area

As described above in Section 2.4.1 it is important, for computational modelling, to understand the mechanics of the player's lips, and specifically how the lip opening area varies with time. The opening area can be considered as a function of the opening height, *h(t)*, of the lips. The simplest form of this function is to assume that the relationship between the parameters is linear, resulting in

$$S(t) \propto h(t) \tag{2.11}$$

This linear relationship has been used in a number of models, such as [Adachi 96, Elliot 82, Saneyoshi 87]. It is also possible to assume that the width also varies with height, which gives the commonly used power law relationship

$$S(t) \propto h(t)^n \tag{2.12}$$

with $n \geq 1$. When $n = 1$, the width of the opening area remains constant throughout the cycle, where the open area is a rectangle of constant width and gives the relationship in Equation 2.11.

The case where $n = 2$ was used in [Msallam 00] and produced considerably more accurate results than had been shown with the simpler linear relationship. In this case the width of the lip opening increases directly as the height is increased.

It has been shown in [Richards 03] that the realistic behaviour of the lip opening area lies somewhere between the two cases described above, that is - $1 < n < 2$. Bromage [Bromage 07] has since suggested that there may be two separate values of n used at different points in the motion.

2.4.3 Harmonic Generation

It was shown by Martin [Martin 42] that on the cornet, the lip motion was almost sinusoidal; however, studies of trombone lip motion, [Copley 95], showed a more asymmetric area function when playing loudly. This area function alone is not adequate to account for the high frequency components of the characteristic sound of a brass instrument. Backus and Hundley [Backus 71] carried out a detailed experimental and theoretical investigation into the physical mechanism in brass instruments behind harmonic generation.

The results of this study showed that nonlinear effects did not significantly contribute to harmonic generation, and that the input impedance did not significantly change with different input pressures. It was concluded that the main mechanism responsible for harmonic generation was the relationship between the time-varying impedance of the lip opening and the input impedance of the instrument. The lip opening behaviour of the pressure valve is intrinsically nonlinear, but the flow through this valve is also determined by a combination of the input impedance of the instrument and the time varying impedance created by the lips. When the open area of the lips is small, the lip impedance is much greater than that of the input impedance of the instrument. When the lip opening is at its maximum, the open area is much greater than the cross sectional area of the narrowest part of the instrument's bore (the mouthpiece throat), and therefore the lip impedance is far smaller than the input impedance of the instrument. This means that the volume flow into the instrument, for parts of the cycle, is controlled by the lips; for the other parts of the cycle the volume flow is controlled by the instrument. Backus and Hundley used these results to simulate the pressure then created within the mouthpiece. Although the basis of these results still hold, it has been shown in [Elliot 82, Hirschberg 96] that Backus and Hundley underestimated the effect of the nonlinear behaviour on the system.

2.4.4 Co-operative regimes of oscillation

In brass wind instrument playing the player is able to modify the embouchure (the shaping of the lips) within the mouthpiece. The player sets the embouchure such that the lips start vibrating at a particular desired frequency and so that the flow into the instrument is modulated appropriately. To obtain a self-sustaining oscillation regime the frequency at which the lips are vibrating must be close to a resonance of the air column.

If the air flow through the lips was purely linear it would be sufficient to have a set of resonances for the notes the player wished to play. The vibration of the lips and therefore the pressure fluctuations would generate a standing wave at this resonance. The air column within the instrument can be described as a linear acoustic oscillator, but the valve controlling the flow complicates the system with its nonlinear nature. Because of this it is not sufficient to only consider the fundamental frequency of oscillation as the resonator is coupled to the flow valve

which is nonlinear. It is known [Benade 76] that if the air column has no other resonances harmonically related to the fundamental frequency then energy is lost and the note is hard to sustain, it is because of this that it is desirable to have harmonically related resonances within an instrument.

2.5 The Brassy Sound

Brass instruments have a very distinctive sound quality when played at high dynamic levels: a 'brassy' or 'cuivré' sound, which is utilised by musicians and composers as musical expression. In a brass instrument the harmonic content of a sound played at quiet or moderate playing levels can be explained by the primary nonlinearity of the lip-reed which is the origin of the non-sinusoidal waveforms of the pressure and flow measured in the mouthpiece [Backus 71, Elliot 82, Fletcher 99a]. However, when a brass instrument is played at the loudest dynamic levels there is a distinct change in timbre to a 'brassy' sound. This 'brassy' sound is characterised by the significant increase in the strength and number of upper harmonics. The nonlinear propagation of the waveform along the bore of the instrument produces an energy transfer from the low harmonics to the high harmonics [Fletcher 99a] and it is generally accepted that this is the origin of the 'brassy' sound [Campbell 99]. The effect of nonlinear propagation in increasing the amplitude of higher harmonics is more dominant in some instruments than others; for example, the trombone is generally considered to be more 'brassy' than the tuba. There have been attempts to assign a 'brassiness coefficient' to instruments as a method of musical taxonomy [Gilbert 07]. There are several effects that have been suggested as being possible contributions to the production of the 'brassy' sound, as are discussed in the following sections.

2.5.1 Lip motion

One factor that some researchers [Fletcher 99b, Widholm 05, Moore 05] have suggested could contribute to the brassy sound is that as you increase the playing dynamic the player's lip opening area can become 'saturated' at extremely loud dynamics. This saturation comes from the lips being constrained by the rim of the mouthpiece and the cup walls. If saturation of the lips were present under

these loud playing conditions this would contribute significantly to the change in timbre of the sound produced by the instrument. As discussed in Section 2.4.3 measurements were carried out by [Martin 42] which showed that the lip opening area was almost sinusoidal with respect to time for *mezzo forte* playing on the cornet. There have been other studies, however, that have used trombones and shown that the lip opening area does not vary sinusoidally. Copley and Strong [Copley 95] and Bromage *et al.*, [Bromage 06] have both shown that the lip motion is split into two phases; the opening and closing phases of one cycle, then the closing phase takes longer than the opening phase. It was shown that at loud playing levels this effect was more apparent.

2.5.2 Wall vibrations

It is well known that as a sound is produced on a brass instrument the walls vibrate [Knauss 41] and as the dynamic level of the sound increases so does the amplitude of the wall vibrations. There have been many works debating whether these wall vibrations contribute considerably to the sound produced by the instrument [Kausel 08, Whitehouse 08, Nief 08, Moore 07, Pyle 98].

It was found by Smith, in 1978, that in trumpets the wall thickness was the dominant factor affecting the timbre of the instrument, rather than the wall material [Smith 78]. Smith published further work showing holograph images of bell eigenmodes and that the vibration amplitude is inversely proportional to the fourth power of the wall thickness [Smith 87]. It was found by Moore *et al.* [Moore 05] that the effect of bell vibrations varies between instruments; work on trombones showed that the bell vibrations have little effect on the radiated sound [Smith 86], and conversely, work on trumpets and horns showed that the bell vibrations do effect the radiated sound [Lawson 85].

More recently, more work on horns showed that wall vibrations do indeed matter and that it is quite difficult to attribute this to one single mechanism [Kausel 08]. The same authors have since proved that there is no longer any doubt that the vibrations of the bells of brass wind instruments affect the sound produced during play [Kausel 10]. This work used both experimental and theoretical approaches, with results indicating that audible effects of the radiated sound can be attributed to the presence of strain oscillations in the bell and the interaction of these with the air column within the instrument.

2.5.3 Waveform distortion

In 1971 Backus and Hundley [Backus 71] were the first to seriously attempt to identify the physical mechanism by which the harmonics of a brass instrument were created. This work concludes that the nonlinear behaviour of the air column within the instrument is not a major factor in the production of harmonics, accounting for only a minor percentage of the total harmonic distortion. This work was challenged by Beauchamp [Beauchamp 80] which suggested that the air column within the instrument became more important when an instrument is played loudly and there is nonlinear propagation down the instrument, this was further confirmed by Elliot and Bowsher [Elliot 82]. Hirschberg *et al.* [Hirschberg 96] verified that shockwaves were formed within the bore of instruments; these shockwaves were responsible for the nonlinear effects in the instrument. These nonlinear effects have been verified since, both theoretically [Thompson 01, Msallam 00] and experimentally [Pandya 03].

We first consider a large amplitude plane wave in a lossless fluid, propagating within a cylindrical tube [Blackstock 97, Hamilton 98]. Figure 2.6 shows the initial waveform in the solid curve, a sinusoidal waveform. The propagation speed of this wave, dx/dt, at a point x relative to a fixed observer is given by:

$$\frac{dx}{dt} = c + u \tag{2.13}$$

where c is the speed of sound, and u is the particle velocity.

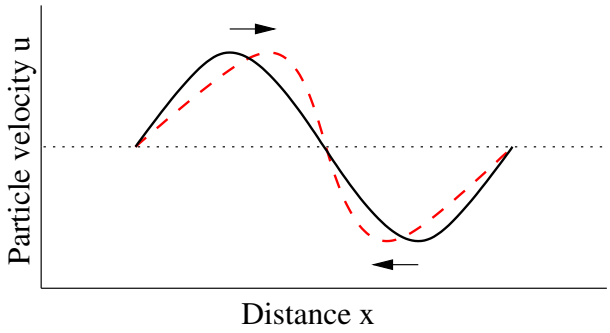

Figure 2.6: Sound wave propagation from left to right. Solid line showing one cycle of initial sine wave, dashed line showing how the wave distorts. Arrows indicating the particle velocity direction.

As the wave is propagating, the local air temperature is affected because of the sound pressure. c is increased as the air is compressed and decreased as the

air is rarefied. This gives:

$$c = c_0 + \frac{\gamma - 1}{2}u \tag{2.14}$$

where γ is the ratio of specific heat at constant pressure to specific heat at constant volume, and c_0 is the small signal speed of sound. Therefore, combining Equations 2.13 and 2.14 gives:

$$\frac{dx}{dt} = c_0 + \frac{\gamma + 1}{2}u. \tag{2.15}$$

This equation shows that the propagation speed varies at different points on the waveform. The overall speed of the propagating wave is c_0, but the points where u, the particle velocity, is positive move faster than c_0, and the points where u is negative move slower than c_0. Figure 2.6 shows how this effect causes the waveform to steepen, shown as the dashed curve. As this effect becomes more and more pronounced the rate of change of the waveform, *du/dt* tends towards infinity and hence a shock wave is formed.

2.5.4 Distance to shockwave formation

The distance X_s needed for a shock wave to be generated in a cylindrical tube, using a lossless approximation, is shown in [Hirschberg 96] to be:

$$X_s \approx \frac{2\gamma P_{atm} c}{(\gamma + 1)(\delta p(in)/\delta t)_{max}} \tag{2.16}$$

where *p(in)* denotes the input pressure, P_{atm} atmospheric pressure, c the speed of sound in air and γ the ratio of specific heats for air. It is clear from Equation 2.16 that X_s is not dependent on the internal diameter of the tube D; this implies that tubes/instruments with the same length and different internal bore diameters should have the same rate of nonlinear distortion for the same input pressure waveform.

2.5.5 Brassiness potential

We now consider a flaring horn, or a brass instrument, with length L and diameter *D(x)*, where $0 \leq x \leq L$. The input/mouthpiece end is defined as $x = 0$ and the output/bell end is defined as $x = L$.

As the sound wave propagates down the horn, the cross-sectional area increases, and hence, the sound energy is spread over a larger area and the particle velocity decreases. If we neglect viscothermal wall losses inside the horn and assume that the sound energy is constant throughout, conservation of energy dictates the following relationship:

$$\frac{u(x)}{u_0} = \frac{D_0}{D(x)} \tag{2.17}$$

where *D(x)* is the bore diameter and *u(x)* is the particle velocity at position x. D_0 and u_0 are *D(x)* and *u(x)* at a reference point.

The speed of sound is changed for the various parts of the waveform as it propagates within the horn. Combining Equation 2.17 and Equation 2.15, for a plane wave propagating within a tube, gives

$$\frac{dx}{dt} = c_0 + \left(\frac{\gamma + 1}{2}\right)\frac{D_0 u_0}{D(x)}. \tag{2.18}$$

In an outward flaring horn the sound wave has to travel further than it would in a cylindrical tube if the same amount of nonlinear distortion is to be seen; this leads to an effective 'stretch' in the x coordinate for the same input particle velocity.

It is possible to find the length of a cylindrical tube that will have the same nonlinear distortion as an instrument with a much more complicated flaring bore; this can be done by integrating Equation 2.18 over the entire length of the instrument. The length of the cylinder will be less than that of the instrument as almost all brass instruments flare outwards. The *brassiness potential parameter* B is defined as the ratio of the length of the cylinder and L_{ecl}, the equivalent conical length of the instrument [Gilbert 07, Myers 07]:

$$B = \frac{1}{L_{ecl}} \int \frac{D_0}{D(x)} dx \tag{2.19}$$

where *D(x)* is the bore profile of the instrument, and the equivalent conical length is the length of a cone where $L_{ecl} = c/2f_1$, f_1 being the nominal fundamental frequency of the instrument. Therefore, the equivalent conical length, L_{ecl}, is the same for instruments that are pitched in the same key, but the physical length, L, of these instruments will vary depending on the bore profile.

B is a dimensionless parameter that lies between zero and one for brass

instruments, where $B = 1$ denotes a cylindrical tube. Therefore, instruments with a higher proportion of cylindrical tubing, such as the trombone and trumpet, have a higher value of B than instruments with more expanding tubing, such as euphoniums and flugelhorns. Instruments with a higher value of B will show more nonlinear distortion, and hence sound more 'brassy', than instruments with a lower value of B if the instruments are excited by the same input signal.

2.5.6 Linear regime transfer function

Musicians generally agree that a brassy timbre will be developed at a lower dynamic level in narrow bored instruments than in an instrument with a wider bore, but similar bore profile. This can be justified if we take into account the radiated pressure at the bell end of the instrument. The player will be using this radiated pressure wave to determine the overall dynamic level they are playing and will not have an indication of the level of the pressure waveforms inside the instrument. Assuming linear acoustics, for a given sine wave input pressure, *p(in)*, there will be a radiated sine wave pressure that corresponds to *p(out)* = T *p(in)*, where T is the transfer function between the input of the instrument and the point in the radiation field where measurements are taken. The radiation can be approximately treated as a monopole source centred on axis, at the bell exit, when the frequency is significantly low enough that the wavelength will be much greater than the diameter of the bell, resulting in radiation given by [Myers 12]:

$$p(out) \approx \frac{j\rho_0\omega Q}{4\pi d}\exp(j(\omega t - kd)) \approx \frac{\rho_0\omega S u(bell)}{4\pi d}\exp(j(\pi/2 - kd)) \tag{2.20}$$

where Q is the monopole source strength, d is the distance from the monopole source to the point of measurement, S is the bell opening area, and *u(bell)* the acoustic particle velocity at the bell exit plane. Being able to calculate the output pressure, *p(out)*, allows the transfer function to be calculated using the following:

$$T = \frac{p(out)}{p(in)} = \frac{\rho_0\omega S}{4\pi d}\exp(j(\pi/2 - kd))\frac{u(bell)}{p(in)} \tag{2.21}$$

If we neglect viscothermal wall losses within the tube, the ratio *u(bell)/p(in)* will not be affected by a uniform scaling of the bore by a factor σ. Knowing that T is proportional to the cross sectional area of the bell, S, this means that it will

increase by a factor of σ^2. The minimum diameter of the bore, D_0 will increase by a factor of σ, and therefore the lossless approximation predicts that $T \propto D_0^2$.

The inclusion of wall losses acts to reduce *u(bell)/p(in)*, and the amount of reduction increases as the internal diameter is reduced. This therefore, further increases the dependance of T on D_0. In the case of a cylindrical tube of length L and the input at $x = 0$ the effect of losses on the transfer function can be incorporated by introducing the complex wave vector $k' = \omega/\nu$ - $j\alpha$, where ν is the internal propagation velocity. The viscothermal attenuation coefficient α is given by

$$\alpha \approx \frac{3 \times 10^{-5} f^{1/2}}{r} \tag{2.22}$$

where r is the internal tube radius, f is the frequency in Hertz, and α is given in $(\text{metres})^{-1}$ if r is in metres [Fletcher 98]. This relationship shows that viscothermal losses are also frequency dependent, increasing with frequency.

The sound field inside the tube/instrument can be treated as the sum of the forward and backward propagating waves, which can be expressed as $p_+ = A\exp(j(\omega t - k'x)$ and $p_- = B\exp(j(\omega t + k'x)$ respectively. Therefore, the input pressure and particle velocity can be expressed as

$$p(in) = (A + B)\exp(j\omega t), \tag{2.23}$$

$$u(out) = (\rho_0 c)^{-1}[A\exp(-jk'L) - B\exp((jk'L)]exp(j\omega t) \tag{2.24}$$

Equation 2.21 can then be expressed in the form

$$T = \frac{kS\exp(j(\pi/2 - kd))}{2\pi d[(Z_L/Z_0 + 1)\exp(jk'L) + (Z_L/Z_0 - 1)\exp(-jk'L)]} \tag{2.25}$$

where Z_L is the radiation impedance and Z_0 is the characteristic impedance of the tube, $Z_0 = \rho_0 c/S$.

2.5.7 Nonlinear regime transfer function

When examining the case of the linear transfer function and its dependence on bore diameter this implies that the player is required to generate a higher

amplitude input pressure, *p(in)*, in a narrow bored instrument than in a wide bore instrument to produce the same radiated sound intensity. It can then be seen from Equation 2.16 that the narrow bore instrument will have a higher rate of nonlinear distortion.

This linear regime argument is not wholly sufficient to quantify this effect as when the output waveform is significantly distorted then the linear regime transfer function is no longer applicable. A sinusoidal input will result in an output wave whose spectral enrichment will increase with the amount of nonlinear distortion, up until the point where a shock wave is formed. It is also known that the higher frequency components are more efficiently radiated because of the frequency dependance of the radiation impedance, therefore the total radiated sound power for a given input pressure will increase with the amount of nonlinear distortion. While this boost of amplitude in the upper harmonics is acting to increase the radiated sound power, there is some degree of counteraction to this by the increased wall losses with increasing frequency.

In the nonlinear distortion case the simplified effective transfer function can be used to take into account these subtleties and can be defined as:

$$T_{eff} = p(out)_{rms}/p(in)_{rms} \tag{2.26}$$

Wave steepening, due to nonlinear distortion, and shock wave formation are widely accepted as the dominant factors behind the brassy sound produced by brass instruments. However, there are other mechanisms which are believed could be responsible for the creation of the brassy sound, or which reinforce that produced by the nonlinear distortion.

Chapter 3

Analysis of the mechanics of slurred transients

This chapter will explore the motion of the player's lips during transients, in particular slurred transients between different resonant modes of the instrument. Two different experimental techniques were used; high speed filming of the lips during playing and the use of a forced oscillation input to the instrument. In Chapter 4 these results will be compared with a time domain computational model.

3.1 Introduction

It is widely acknowledged that the starting transient of a note is of paramount importance for the listener in determining which instrument is being sounded, and giving an instrument its characteristic sound [Grey 77, Berger 64, Saldanha 64]. The mechanics of such transients have been explored in a number of more recent works [Bromage 07, Stevenson 09a], using optical techniques with both human players and an artificial mouth. Leading on from this work on starting transients, the natural progression is to explore the mechanics of transitions between different notes once a note has been started and sustained.

In music, a 'slur' indicates a smooth transition between two notes; on a brass instrument, if these two notes are both resonant modes of the instrument, the player achieves this slur by a combination of changing the tension in the lips, mouthpiece pressure, and air flow rate. This is often referred to as a lip-slur.

Previous exploration in this area includes impedance measurements for slurred transients in valved instruments [Widholm 97, Widholm 05].

When sounding a note on a brass instrument the player's lips open and close periodically. The initial frequency with which the lips vibrate is determined by the player's choice of embouchure, which influences the mechanical properties of the lips. When a player sounds a note on a brass instrument there is a strong coupling between the vibration of the lips and the resonant modes of the instrument air column. During a lip-slur the player is attempting to change the lip vibration from one strongly coupled steady state vibration to another. It is expected that as the player changes the frequency of the lips in order to reach the target second note there will be a finite time during which the oscillations of the lips and air-column will no longer be coupled.

The time taken for the lip oscillation and the air column resonance to couple is determined by the period of the acoustic wave within the instrument and the frequency at which the lips are vibrating. Say, for example, that the lips are vibrating at the frequency of a high number mode of the air column e.g. the 6^{th} mode - the player is aiming to play at the 6^{th} mode frequency of the instrument. The period of the acoustic wave for a fixed length of tube is constant with respect to frequency, so in the time it takes for the wave to propagate to the end of the instrument and back, the lips will have completed 6 cycles; therefore for the 6^{th} mode it will take approximately 6 cycles of the lips before the system is coupled to establish a stable regime of oscillation.

When assessing the qualities of a note sounded on a musical instrument the transient, either in starting a note or between slurred notes, is one of the most important features. This is true not only for the listener but also for the player. For a brass player evaluating a new instrument, he or she will be concerned with issues such as intonation and timbre, the responsiveness of the instrument to start a note, and also the ease with which the player can move between notes, including slurred intervals. A fuller understanding of the mechanics behind this complex coupled system, during a transition, is of great importance in the wider explanation of what makes one particular instrument easier, and more enjoyable, to play than any other instrument.

3.2 Visualisation of the lips - Experimental technique

With the use of a high speed digital camera it was possible to capture the lip motion of a player during playing. This optical data was synchronised with different measured pressure signals to enable analysis of the lip motion during note transitions.

3.2.1 Instruments

A number of different brass instruments have been used in this study of slurred transients. The high speed photography experiments used three different orchestral horns - an early 20^{th} century narrow bore horn by Boosey and Hawkes, a modern wide bore Conn 8D, F/Bb double horn, c.2000, and a Meinl & Lauber/Paxman 'baroque' horn modelled after an 18^{th} century instrument by Huschauer, Vienna c.1770.

All players used in this study were skilled players with many years of playing experience. Each of the transitions shown here were performed well and decided by the players and listeners in the room to be musically satisfactory.

3.2.2 Experimental setup

A Vision Research Inc. [Vision Research Inc 13] Phantom v4.1 digital high speed camera was used to capture the motion of the lips. The camera resolution was normally set to 256×128 pixels, and a recording rate of 5000 frames per second. The exposure time and aperture setting of the camera were varied to give the maximum depth of focus while maintaining the quality of the images produced.

The filming of the lips required a strong light source to produce video footage appropriate for computational analysis. A Schott KL1500 LCD swan-neck fibre optic cold light source was used to create the desired illumination; this type of light source was necessary because of its use in close proximity to the player's face.

The mouthpiece pressure was measured using a 106B PCB Piezotronics dynamic pressure transducer with a probe attachment that was inserted into a small hole drilled in the rim of the mouthpiece. The radiated sound was measured

using a Bruël and Kjær 4192 pressure-field microphone which was placed one bell radius from the bell of the instrument. The microphone pressure signals were fed into a Bruël and Kjær PULSE system [Bruël and Kjær 13] for data acquisition and synchronisation with the high speed video data. The instruments were mounted using retort stands. The horn mounting is shown in Figure 3.1; the horn is mounted upside down to allow the best optical access possible.

Figure 3.1: Boosey and Hawkes early 20^{th} century narrow bore horn as mounted for experiment.

Although this orientation of the horn is not at all a normal position for playing the players were able to play the horn suitably well and comfortably. With the horn in this position it was still possible for the players to have the right hand positioned in the bell as they would for playing in a conventual position. The full experimental setup is shown in Figure 3.2.

3.2.3 Transparent mouthpiece

Specially designed transparent mouthpieces were used to allow optical access to the player's lips, based on an original design by Ayers [Ayers 98]. These

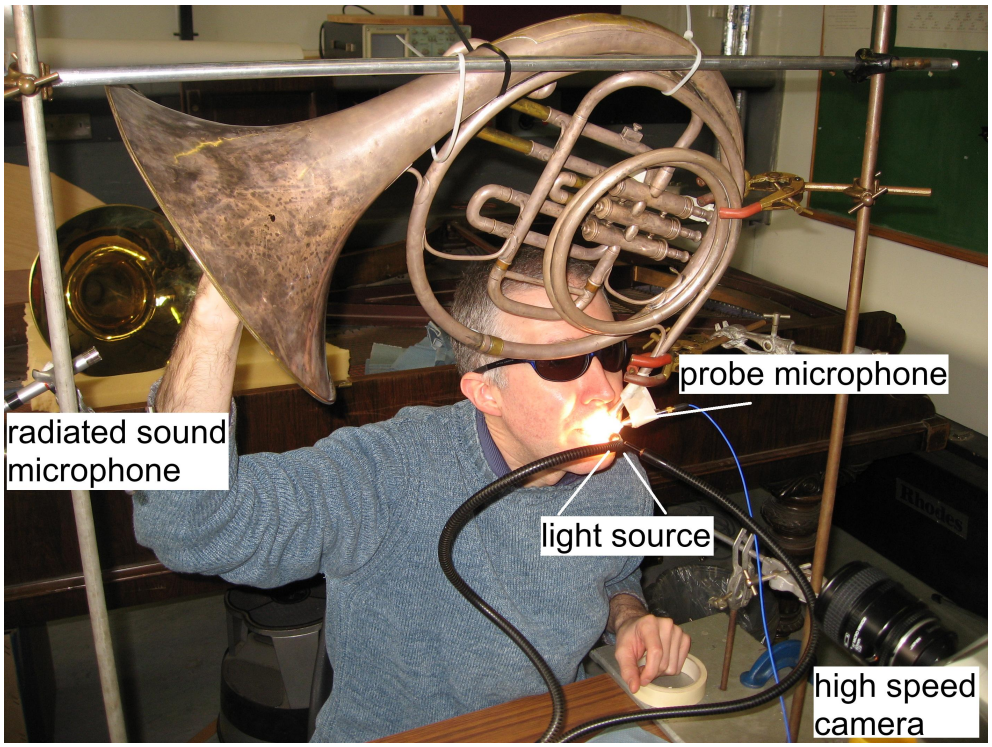

Figure 3.2: Experimental setup for high speed filming of the player's lips, with simultaneous recording of the pressure inside the mouthpiece and the radiated sound.

transparent mouthpieces have been developed and used at the University of Edinburgh in various works on brass instruments [Richards 03, Bromage 07, Newton 09, Stevenson 09a]. The cups of the mouthpieces are machined from perspex with an optical glass window that is approximately parallel to the face of the player. The mouthpieces can have this optical window in this position as the shank extends sideways from the cup instead of forwards. Figure 3.3 shows a schematic diagram of the transparent horn mouthpiece, and Figure 3.4 shows a photograph of the same.

In the case of the horn mouthpiece the optical window is angled slightly, and not perpendicular to the rim. This design feature was used as it has been found with horn measurements that the top lip can 'overhang' the lower lip slightly. The angled optical window allows the lips to be filmed from slightly below the straight-on position. The dimensions of the rim, cup, volume, and shank (including the throat and backbore) are based on commercially available models of mouthpiece. The horn mouthpiece properties were taken from a Paxman 4C.

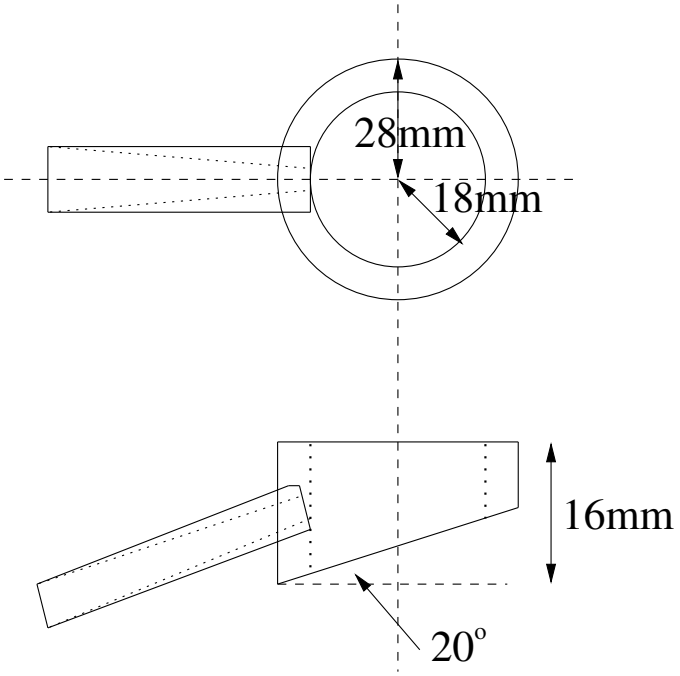

Figure 3.3: Schematic of horn transparent mouthpiece with angled optical window.

Figure 3.4: Photo of horn transparent mouthpiece with angled optical window.

While the dimensions of the commercial mouthpieces can be replicated, it is clear that the shape of the cup is very different from the commercial models. It has been assumed that the cup volume and not shape is the most important design feature [Plitnik 99].

3.2.4 Data analysis

The (greyscale) video footage obtained from the high speed camera was edited such that one bitmap (*.bmp) image was produced for each frame of the video; this was done using VideoMach software package [Gromada 13]. The images were cropped as to only show the relevant parts of the lips. These sets of images were then analysed in MATLAB [Mathworks 13] using a technique developed by Richards [Richards 03] and Bromage [Bromage 07] and also used by Stevenson [Stevenson 09a].

The individual frames are loaded into MATLAB, and the first image is used to set the greyscale threshold level. Because the high speed camera produces greyscale footage the user is able to set a threshold level, in which each pixel that has a greyscale level above the threshold is set to white, and all that are below the threshold are set to black. The open area of the lips will correspond to the black pixels if the correct threshold is set and the inner edge of the lips is then well defined. Figure 3.5 shows one cropped frame from the video footage on the left and the final 'binarised' image on the right. The number of black pixels are then counted, again using a MATLAB program, for each image and the opening area plotted as a function of time.

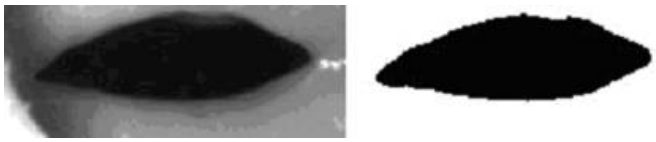

Figure 3.5: An image of the lip open area from the video footage (**Left**) and the corresponding 'binarised' image (**Right**). The opening area appears black.

The instantaneous frequency of the pressure signals and the lip open area were calculated using YIN, a fundamental frequency estimator program which is detailed in [Cheveigne 02]. This analysis program uses the well-known autocorrelation method that may be used on signals with a degree of aperiodicity. There are a small number of parameters that require to be tuned including

upper and lower fundamental frequency, F_0, search bounds, window size, and the absolute threshold. The absolute threshold determines the proportion of aperiodic power tolerated within a periodic signal. When choosing the upper and lower limits of F_0, they were bounded as closely as possible to the expected fundamental frequencies of the notes in the transitions as determined from the input impedance of the instrument. The window size and threshold must be chosen carefully as the signals being analysed in this work have quickly varying fundamental frequencies, within one period the frequency can change. It is worth noting that when the frequency changes in a time shorter than one period, it can be difficult to accurately define the fundamental frequency. The rate of change of the phase is a more accurate definition of the a quickly varying signal in terms of frequency. If the window size is too large the frequency estimation will be overly smoothed, whereas if the window size is too small there is a risk of a full period not being encapsulated in the window. It is fair, in this work, to have a threshold value slightly higher than would be used for a steady state signal as the signals considered here can become very complex and aperiodic during the transitions. Even after the tuning of these parameters there can be points in the frequency analysis that are not 100% reliable; these points occur where there are unexpected aperiodic inconsistencies in the signal.

3.3 Visualisation of the lips - Results

3.3.1 Different approaches to slurring

The study of starting transients on brass instruments has shown that the time for a transient is typically around 50ms; this was first reported by Luce and Clark [Luce 67]. A slurred transient consists of a finishing transient followed by a starting transient as the player's lips are decoupling from one cooperative regime, and then become coupled to the new cooperative regime that is set up.

Different players have different approaches to producing a smooth sounding slur. For example, the well known horn teacher Philip Farkas advocates a technique in which the player practises a glissando, 'catching' the intermediate resonances en route from the first note to the second as shown in Figure 3.6. The speed of the glissando is increased until a smooth musical slur is achieved [Farkas 56]. An alternative approach is to effectively stop the first note and

discreetly start the second note as quickly as possible, producing the aural illusion of one note moving smoothly to the next.

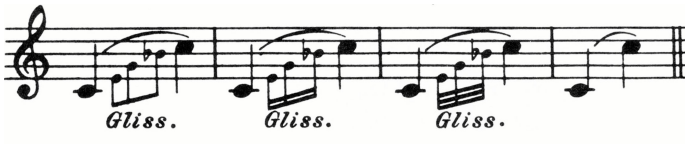

Figure 3.6: Philip Farkas' pedagogic exercise for the production of "full sounding, velvety slurs" [Farkas 56].

The approach with which each of the players used in this study takes to playing lip-slurs is different. Player A practises slowly playing each of the resonant modes of the instrument between the two slurred notes, and then builds up the speed to hopefully create a portamento type transition, as taught by Philip Farkas and described above. Player B, however, takes the opposite approach to lip-slurring, in aiming to make the transition as fast as possible and latch immediately onto the second note of the slur. When asked about their approach to carrying out this type of slur, Player B stated that there was no conscious intent to stop the first note in order to restart on the second note, and that the sensation was actually one of continuously sounding (or blowing through) the instrument during the transition.

3.3.2 Typical characteristics of slurred transitions

All results presented in this section were performed on the Conn 8D, which is the modern wide bore horn.

Figure 3.7 shows the synchronised opening area data and pressure signals for an octave lip-slur by Player A. This particular slur was an octave interval between the 4^{th} and the 8^{th} resonant modes of the horn in open D, which corresponds to the notes D_3 and D_4.

It can be seen in the middle plot of Figure 3.7 that the open area of the lips, shown in red, decreases relatively steadily in amplitude until around 0.1s. There are then around 15 cycles of the lip motion where the amplitude is significantly smaller until around 0.18s; at this point the amplitude starts to build up steadily to the second steady state motion of the new resonant mode. The instantaneous frequency of the open area, shown in blue, begins to increase at

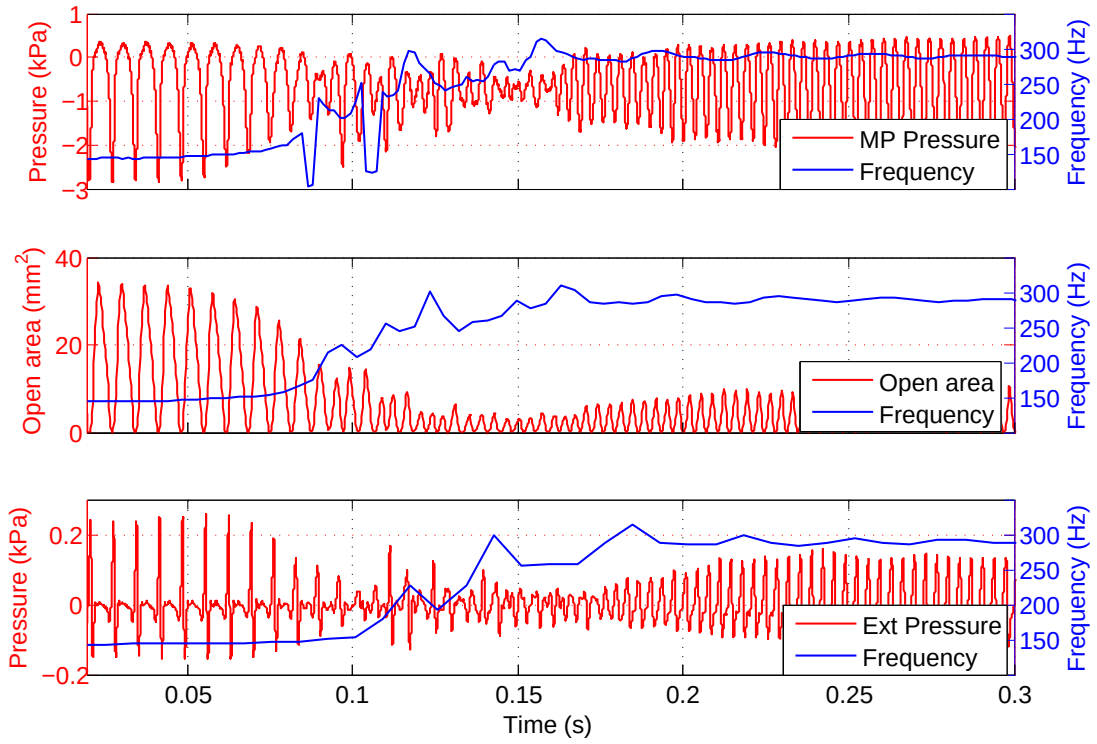

Figure 3.7: Synchronised signals for lip-slur from D_3 to D_4 by Player A, on modern wide bore horn by Conn. **Top**: Mouthpiece pressure **Middle**: Lip open area **Bottom**: Radiated pressure.

around 0.08s, showing that the amplitude of the opening area begins to decrease before the lip frequency begins to increase. It can be seen that the time between steady frequencies i.e. between the two slurred notes, is around 100ms. There are a number of peaks/shoulders within the instantaneous frequency transition period; these peaks are rather erratic and do not correspond to the intermediate resonances.

During this lip-slur transition period the pressure in the mouthpiece, shown in the top plot of Figure 3.7, also has rather erratic behaviour in both amplitude and frequency. The amplitude decreases from the steady state behaviour at around 0.05s, as with the lip opening area, and then begins to build up to the second steady state at around 0.16s. The instantaneous frequency shows similar characteristics to that of the lip opening area also, with a number of peaks during the transition. There are also two significant dips in the frequency at approximately 0.08s and 0.11s; these can be explained as a result of the fundamental frequency analysis failing to predict the instantaneous frequency

correctly at these points. It can be seen in the pressure signal that there are small secondary peaks around both these dips that the frequency analysis program is not taking into account appropriately.

The external pressure signal and instantaneous frequency are shown in the bottom plot of Figure 3.7. In this case the amplitude of the pressure signal begins to decrease at around 0.07s and begins to build up to the steady state at around 0.17s; we would expect the external pressure signal to have a small delay in beginning to decouple from the cooperative regime, as the pressure signal has to travel the length of the instrument before any change will be recorded at the external microphone. There is no break in the radiated sound as the amplitude remains significant throughout the transition, albeit rather unpredictable in amplitude. The instantaneous frequency shows similar results to those of the mouthpiece pressure and lip opening area. In this work the transition time is defined as the time between steady state frequencies of the radiated pressure; therefore in the case of this slur the transition time is around 100ms. These values were determined by inspection of the radiated pressure instantaneous frequency plots.

The synchronised signals for the same octave slur, between the notes D_3 and D_4, on the same horn, by Player B are shown in Figure 3.8. This figure shows some of the same characteristics as that of Player A, but the transition time is shorter at approximately 70ms. The external pressure signal also differs from that of Player A significantly; during the transition, between 0.14s and 0.17s, the amplitude of the pressure signal is extremely small indicating that there was more of a break in the radiated sound between the two slurred notes. This break in the sound was not audible and did not make this slur sound less musically satisfactory than the corresponding slur by Player A.

The number of small amplitude peaks in the open area plot is also significantly less than seen in the results from Player A. There is a steady decrease in amplitude of the lip open area from 0.08s, but there are only 5-6 peaks which are significantly smaller in amplitude. The instantaneous frequency of the lip opening area only begins to increase around 0.14s; this is when the amplitude is almost at its lowest point, showing that the player has tapered down the opening of the lips before changing the frequency at which they are oscillating. The frequency is shown to increase dramatically within one cycle of the lip motion, thereafter the frequency

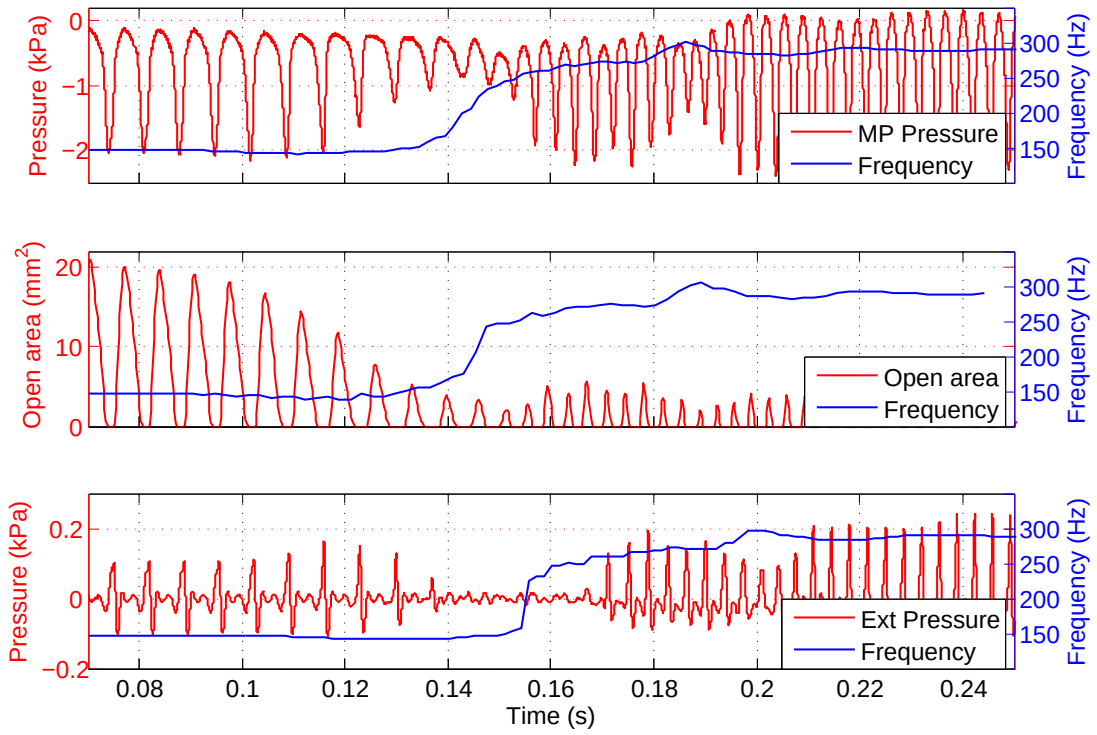

Figure 3.8: Synchronised signals for lip-slur from D_3 to D_4 by Player B, on modern wide bore horn by Conn. **Top**: Mouthpiece pressure **Middle**: Lip open area **Bottom**: Radiated pressure.

increases steadily until is has reached the frequency of the upper note. The instantaneous frequencies for both the radiated and mouthpiece pressure signals show similar characteristics.

The mouthpiece pressure signal for Player B is much less erratic than that of Player A during the transition between the two notes, although between 0.12s and 0.15s the amplitude of the signal is relatively small. Although the pressure amplitude is small between these times it is still greater than that of the radiated pressure during the transition.

Measurements were also carried out on a perfect fourth transition, between the 3^{rd} and 4^{th} resonant modes of the open F horn, which corresponds to the notes C_3 and F_3. The results for Player A performing this slur on the same wide bore horn by Conn are shown in Figure 3.9.

It can be seen here that the amplitude of the lip opening area decreases very uniformly from the steady state, as is the case in the octave slur, until around 0.1s where there is a small peak before the amplitude fluctuates in an unsteady

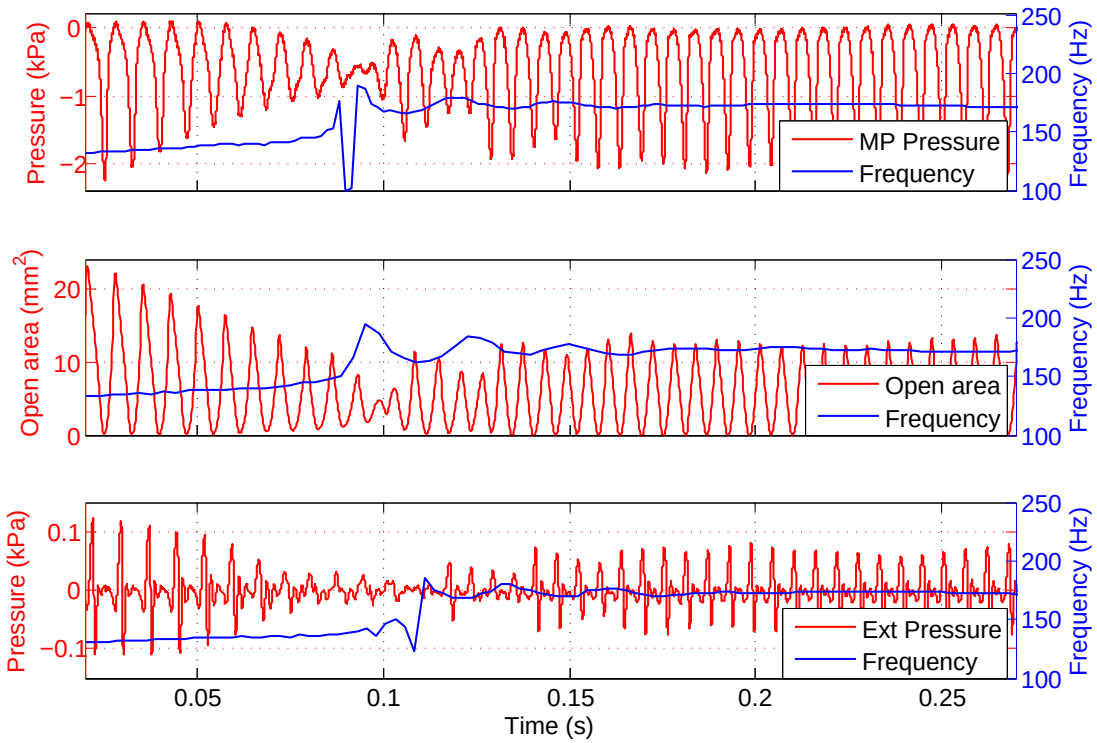

Figure 3.9: Synchronised signals for lip-slur from C_3 to F_3 by Player A, on modern wide bore horn by Conn. **Top**: Mouthpiece pressure **Middle**: Lip open area **Bottom**: Radiated pressure.

manner until 0.15s; it is at this point that the lip opening area increases steadily to the new steady state regime. The frequency of the lip opening area appears to overshoot the frequency of the second note, then fluctuates around the frequency of the new note before settling at this frequency at around 0.15s.

The mouthpiece pressure signal shows similar behaviour to that of the lip opening area in that there is a steady decrease in amplitude, a short section of unsettled oscillation of pressure around 0.1s, and the amplitude then increases slightly to the steady state situation. Both the lip opening area and mouthpiece pressure signals show similar behaviour as the corresponding signals shown in Figure 3.7, for the octave slur on the same instrument with the same player. The octave slur results show more cycles over the transition period as the frequency of these notes are higher than those played in the perfect fourth transition; this apart the results for each of the different interval slurs show similar characteristics. This is also broadly true for the radiated pressure signals but in the perfect fourth slur it can be seen that the pressure amplitude drops at around 0.1s. The frequency of

both the mouthpiece and radiated pressure signals are similar to the lip opening area, with a fluctuation around the second note frequency. The instantaneous frequency of the mouthpiece signal shows a dip at around 0.09s which can be attributed again to the analysis program faltering over the secondary peak that can be seen in the pressure signal.

Figure 3.10 shows the results for Player B performing the perfect fourth transition, again on the wide bore horn by Conn. Comparing the results shown here with those in Figure 3.8 of the Player B playing an octave slur on the same instrument it can be seen that the amplitude results have very similar characteristics. The lip open area and the mouthpiece pressure signal show the same smooth decrease and then increase in amplitude throughout the slur as was seen in the octave slur. The radiated pressure signal is also similar for both intervals, with a pressure of almost zero for the majority of the transition time. The instantaneous frequency for all three signals here also show a similar quick increase, over the time of a cycle or two, and then the frequency takes a short time to come to the steady state of the second note. As with Player A, it seems that the frequency overshoots the top note slightly before settling at the correct frequency.

All of these results show that in this register the interval in which the player slurs over does not affect the typical characteristics of the slur. It can be seen for all slurs performed by Player B that the radiated pressure effectively disappears for some time during each transition between notes, but the lips are still oscillating and there is still a small oscillating pressure in the mouthpiece. This could be attributed to the fact that the pressure seen in the mouthpiece is small in amplitude, and as this pressure wave propagates down the instrument it will be subject to viscothermal losses, leaving little pressure amplitude to be radiated at the bell end of the instrument. If we examine the case of Player B playing an octave slur on the modern wide bore Conn horn, as shown in Figure 3.8, it can be seen that the amplitude of the mouthpiece pressure never drops below 0.5kPa, meaning that there is always a significant pressure in the mouthpiece. The frequency of the lip opening area starts to change at around 0.14s, but the player has already began tapering the note down, in terms of reducing the amplitude of the lip opening area while keeping the lips oscillating at the frequency of the first note until around 0.14s. We can assume that as the lip opening amplitude

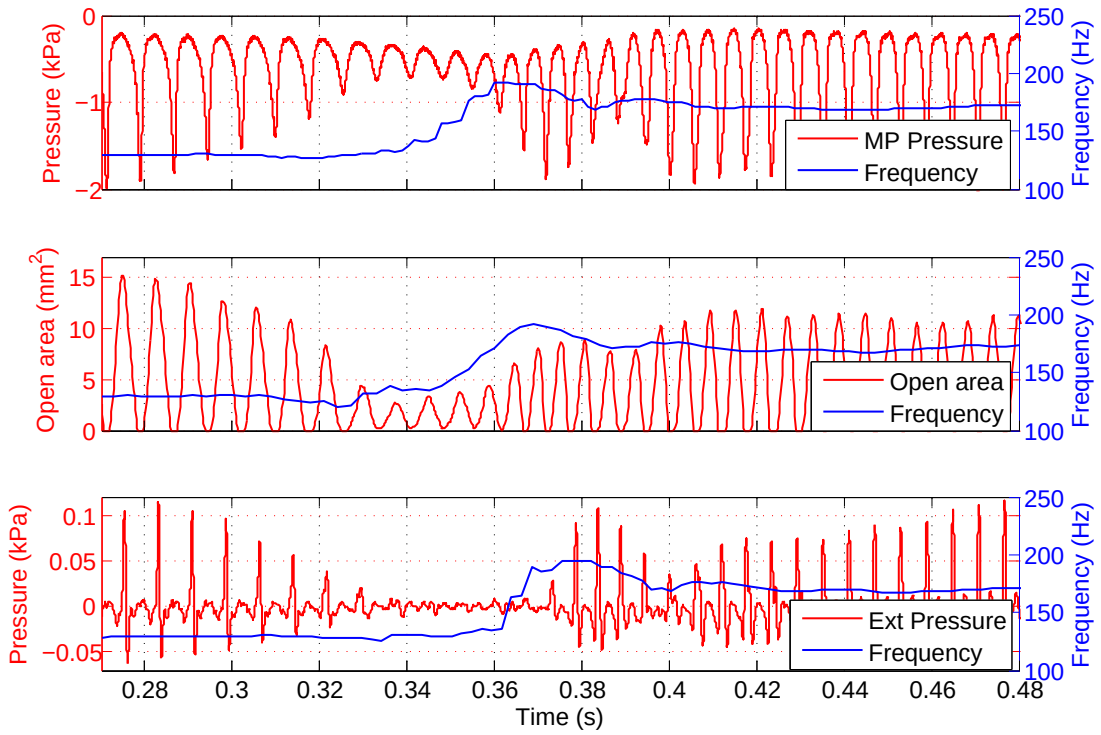

Figure 3.10: Synchronised signals for lip-slur from C_3 to F_3 by Player B, on modern wide bore horn by Conn. **Top**: Mouthpiece pressure **Middle**: Lip open area **Bottom**: Radiated pressure.

is becoming increasingly small, the backward going wave is predominant within the instrument and this is what is providing the lips with reinforcement to keep oscillating at the frequency of this first note. The frequency at which the lips are oscillating then suddenly changes; within one cycle the frequency has changed dramatically. There are then a small number of cycles where the lip frequency is a little unstable before settling at the new frequency. We can assume that if the behaviour of the lips changes almost instantaneously, the time where there is no radiated pressure is the time it takes for the sound to propagate to the end of the instrument. In the case of this instrument, a 4.42m D horn, the time for the wave to propagate to the end of the instrument is around 10ms. It can be seen in Figure 3.8 that the radiated pressure begins again to show a significant amplitude at around 0.17s, which is almost 20ms after the lip opening frequency suddenly changed from the first note. So for this particular slur we see that around 20ms after the lips instantaneously change the radiated sound amplitude dramatically increases from almost zero to around 0.1kPa amplitude; this will be around the

same time that the first pressure wave at the new frequency will be returning to the lips.

Although the lip frequency appears to change within one cycle, it will take the time of several cycles for the new frequency pressure wave to propagate to the end of the tube, and in the same way it will take twice as long for the returning wave to reach the lips and establish a new cooperative regime. This could explain the time of unsettled lip frequency between 0.17-0.20s as the time where the new frequency wave is propagating down the instrument and back, before the new steady state regime is completely formed. There is therefore a time where the backward going pressure wave, within the instrument, is at the frequency of the first note, but the lips are oscillating at the frequency of the second note, and therefore creating a forward going pressure wave at this new frequency. The reduction in the amplitude of the lip opening area could act to lessen the complication of two different frequency waves propagating simultaneously, as the reduction in open area results in a reduction in the amplitude of the wave propagating from the lips.

It was found that there were no notable differences in measurements taken on the second horn, the narrow bore Boosey and Hawkes instrument. The main characteristics that were shown in the results, for both players, were consistent across both types of horn. The results for both players on the narrow bore horn can be seen in Appendix A.

The transition time is defined here as the time between the steady state frequencies of the radiated sound pressure. It was found that the transition times for the octave slurs, for both players, were generally longer than the perfect fourth slurs, as shown in Table 3.1. The transition times shown here have not been found to be strictly double the time of a starting transient, which was found to typically be around 50ms [Luce 67], but between 70ms and 100ms.

Instrument	**Interval**	**Player**	**Transition Time**
Conn	octave	A	100 ms
Conn	octave	B	70 ms
Boosey and Hawkes	octave	A	90 ms
Boosey and Hawkes	octave	B	100 ms
Conn	perfect 4^{th}	A	70 ms
Conn	perfect 4^{th}	B	70 ms
Boosey and Hawkes	perfect 4^{th}	A	70 ms
Boosey and Hawkes	perfect 4^{th}	B	80 ms

Table 3.1: Transition times between steady state instantaneous frequencies of the radiated sound pressure. Table shows transition times for two different horns - modern wide bore by Conn, and early 20^{th} century narrow bore by Boosey and Hawkes. The two players have different approaches to slurring - Player A attempts to 'catch' the intermediate resonances and Player B attempts to move directly from one note to the next. The octave interval was played between the 4^{th} and 8^{th} resonant modes on the D horn, which corresponds to the notes D_3 and D_4, and the perfect fourth interval was played between the 3^{rd} and 4^{th} resonant modes on the F horn, which corresponds to the notes C_3 and F_3.

3.3.3 Upward and downward slurred transients

In Section 3.3.2 the typical characteristics of upward lip-slurs were explored, i.e. slurring from the lower to the higher pitched note. In music there are obviously many more types of transitions between two notes that are called for; this section will explore the similarities and differences between slurring upwards and downwards over octave intervals, again on the horn. The results presented in this section were obtained using the same high speed filming setup as previously described and are using the same two players, but in a different laboratory session. The instrument used for all results in this section was the modern wide bore horn, by Conn.

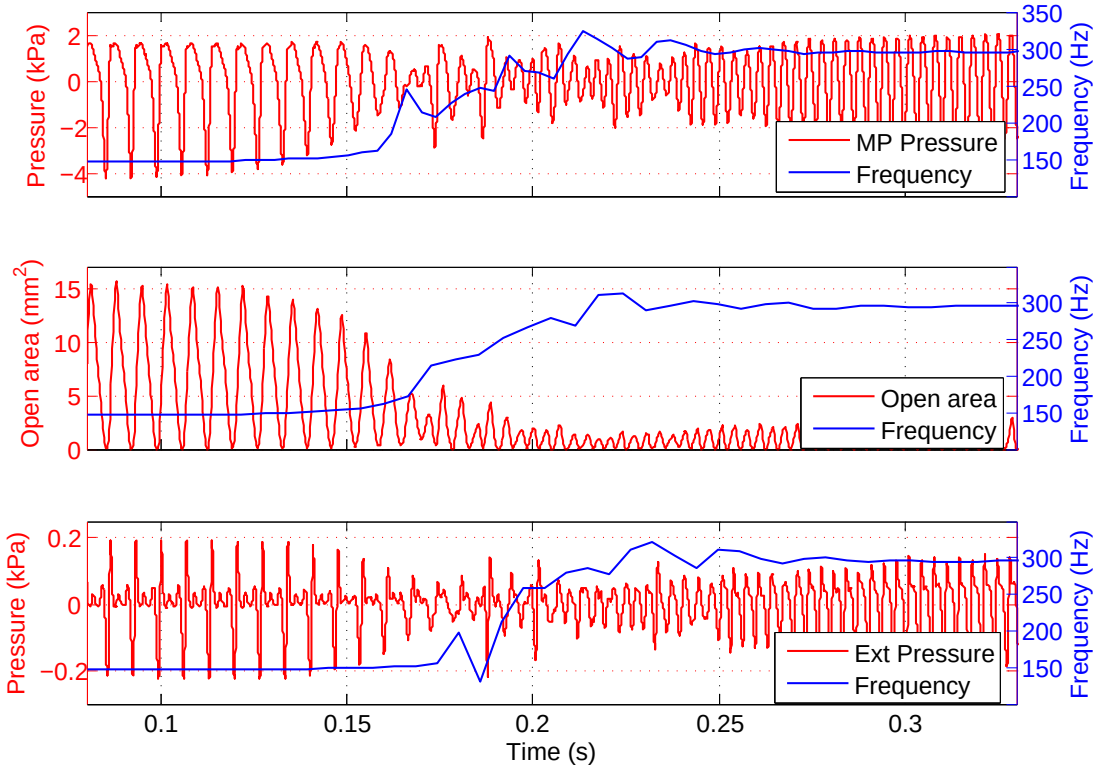

Figure 3.11: Synchronised signals for lip-slur from D_3 to D_4 by Player A, on modern wide bore horn by Conn. **Top**: Mouthpiece pressure **Middle**: Lip open area **Bottom**: Radiated pressure.

Examples of the measured data for an upward slur between notes D_3 and D_4 as played by Player A are shown in Figure 3.11. Player A is the player who employs the technique of attempting to catch the intermediate resonances during a lip-slur. This figure shows much the same results as the same upward

octave, performed in a different session, shown in Section 3.3.2. The transition time is again around 100ms and the amplitude of the sound pressure for both the mouthpiece and radiated sound remains significant throughout the transition. There is again some unevenness in the instantaneous frequency of all three signals during the transition, but the frequency does move progressively between the two notes. Careful inspection of the frequency data revealed no discernable sounding of the intermediate resonances. The dip in the external pressure frequency at around 0.18s is believed to be an artifact of the analysis method, as described for some results in Section 3.3.2.

Player B is the player who adopts the other technique of trying to jump straight from one note to the next. Figure 3.12 shows the results for Player B performing an octave slur, and shows the player's technique very clearly.

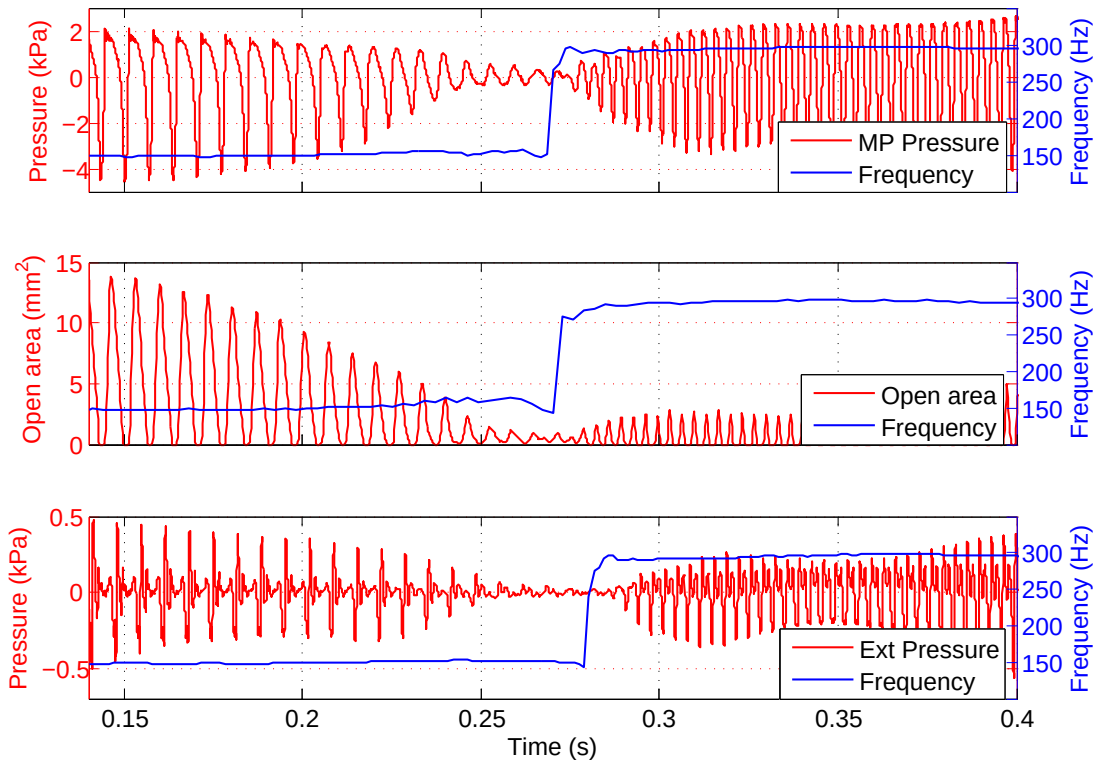

Figure 3.12: Synchronised signals for lip-slur from D_3 to D_4 by Player B, on modern wide bore horn by Conn. **Top**: Mouthpiece pressure **Middle**: Lip open area **Bottom**: Radiated pressure.

This slur is similar to the corresponding octave slur described in Section 3.3.2, Figure 3.8, but appears much 'cleaner' from the results, bearing in mind that both

slurs were deemed good and musically satisfactory. The amplitude data shown here, in Figure 3.12, shows for all three signals a smooth decrease towards the point where the frequency suddenly changes. The mouthpiece pressure amplitude has around 3 cycles at the smallest value before the frequency changes from the first note to the second. The lip opening area shows similar behaviour and both of these signals still have a small amplitude throughout the transition. The radiated pressure amplitude, however, becomes almost zero for a period of around 20ms before the second note begins to sound. These results show that there is definitely no sign of any of the intermediate resonances or any erratic behaviour of the amplitude or frequency during the transition, as is the case in the slur performed by Player A.

Here we have clearly seen that for upward octave slurs between the notes D_3 and D_4 the technique adopted by the player makes a significant difference to the results. The corresponding downward slur results are now shown. These were performed in the same session as the upward results, by the same players and on the same instrument.

Figure 3.13 shows the slur between the notes D_4 and D_3 performed by Player A. The behaviour of the lips and pressure signals are different from those observed during upward slurs. Here, the frequency of the opening of the lips is almost monotonically decreasing, with little or no decrease in amplitude of oscillation. The pressure signals for both the mouthpiece and radiated sound show similar erratically varying amplitudes during the transition as for the upward slur by Player A. However, the instantaneous frequency for the two pressure signals do not replicate those results for the upward octave slur. During the transition the frequency results show much less erratic behaviour, and with some evidence of steps in the frequency. On careful inspection of these frequency signals, three small plateaus can be seen; these are more clearly seen in the mouthpiece signal. As this transition is between the 8^{th} and the 4^{th} resonant modes there are three intermediate resonances that this player is trying to catch during the transition. Table 3.2 shows the frequency of these small plateaus and the difference, in cents, between these frequencies and the expected frequency of the intermediate resonances, as determined from the input impedance of this instrument/mouthpiece input impedance curve. All three of these intermediate frequencies are lower than the expected values, assuming these correspond to the

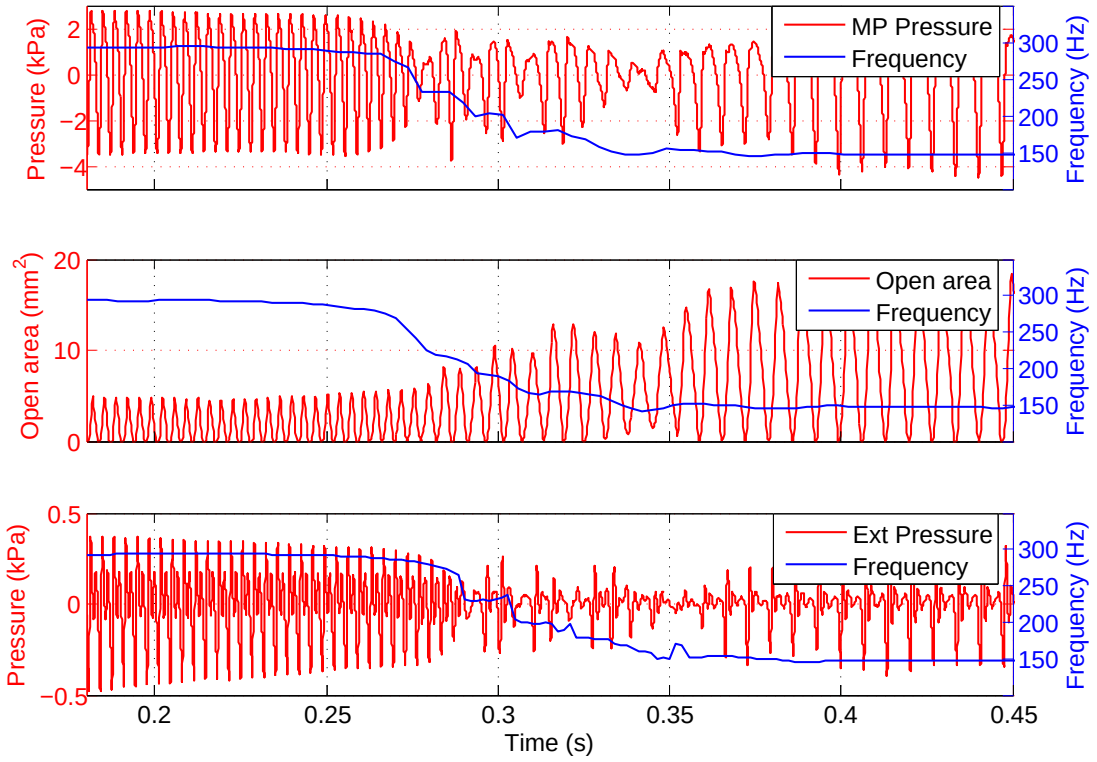

Figure 3.13: Synchronised signals for lip-slur from D_4 to D_3 by Player A, on modern wide bore horn by Conn. **Top**: Mouthpiece pressure **Middle**: Lip open area **Bottom**: Radiated pressure.

intermediate resonances. The 6^{th} resonant mode frequency is the furthest from the expected value at 165 cents, which corresponds to this mode being slightly more than one and a half semitones flat.

The expected resonant mode frequencies were obtained from the input impedance curve shown in Figure 3.14. In the horn not all of the natural resonant mode frequencies of the instrument are 'in tune' with the expected harmonic series tuning, for example the 7^{th} mode in inherently flat. Accomplished players can bend these resonant mode frequencies to sound more 'in tune' with the harmonic series; this can be done by adjusting the lips or using the placement of the right hand in the bell of the instrument. Therefore, it would be expected that if intermediate resonances are seen in lip-slurs that the frequency of these would correspond more closely to the natural resonances of the instrument as the player does not have time to adjust the pitch of the notes. It is for this reason that the true frequencies of the instrument's resonant modes are used for comparison.

Resonant Mode	**Resonant Mode Frequency**	**Player Frequency**	**Difference in Cents**
8	289 Hz	293 Hz	+ 22
7	255 Hz	233 Hz	- 156
6	219 Hz	199 Hz	- 165
5	184 Hz	178 Hz	- 56
4	146 Hz	147 Hz	+ 12

Table 3.2: Radiated intermediate resonance frequencies of an octave lip-slur from D_4 to D_3 by Player A. The resonant mode frequency is the expected frequency, the player frequency is the frequency of the steps in the instantaneous frequency. Difference in cents is the difference between the expected and player frequencies.

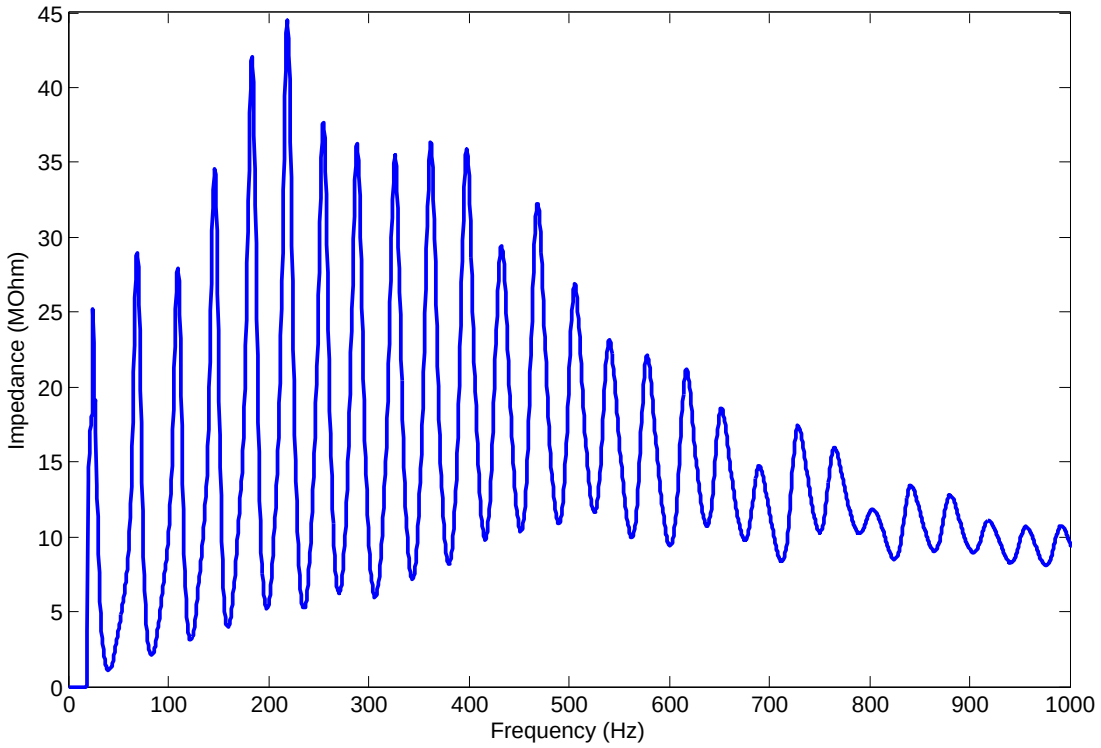

Figure 3.14: Input impedance of the modern wide bore horn by Conn in open D used for this work.

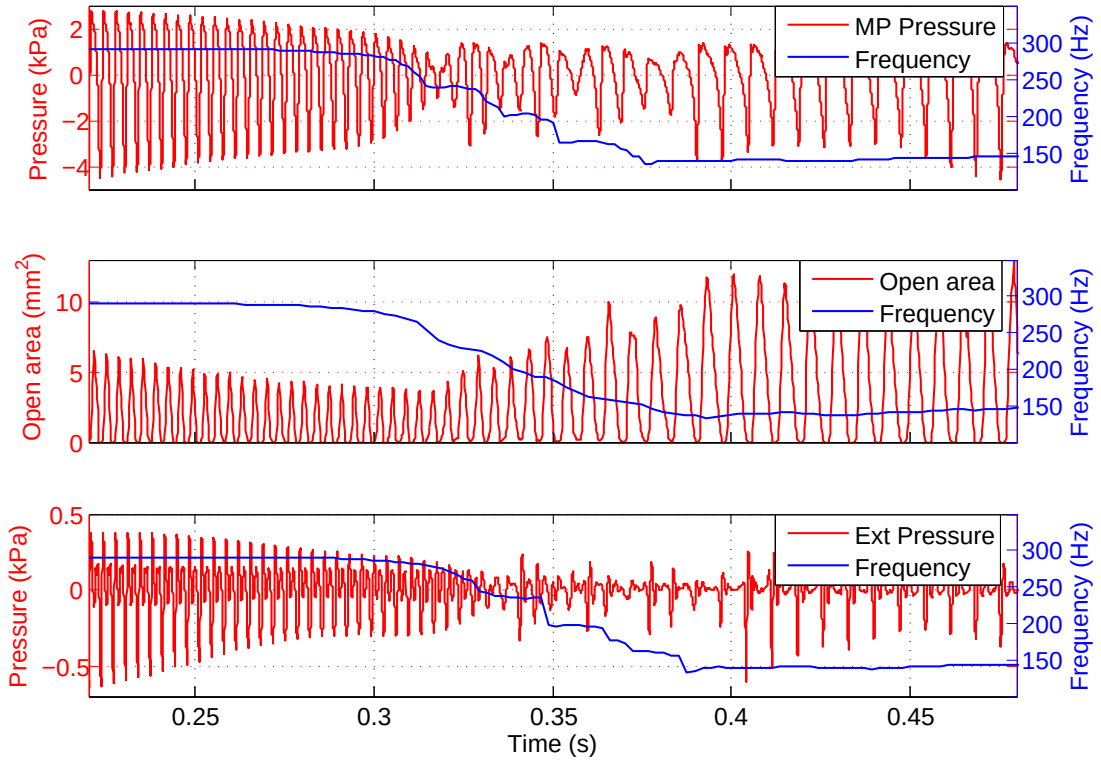

Figure 3.15: Synchronised signals for lip-slur from D_4 to D_3 by Player B, on modern wide bore horn by Conn. **Top**: Mouthpiece pressure **Middle**: Lip open area **Bottom**: Radiated pressure.

Figure 3.15 shows the corresponding downward slur preformed by Player B. This figure shows results that are very similar to those seen in the results from Player A. The open area amplitude only decreases slightly before increasing to the second steady state, and the frequency decreases more or less smoothly during the transition. All three amplitude signals show very different characteristics to those of this player performing the upward octave slur; the amplitude is retained through out the transition and the two pressure signals show more erratic behaviour. The instantaneous frequency results of the two pressure signals show more defined steps than was seen for the results of Player A. The frequency of these steps and the difference between them and the expected frequencies of the intermediate resonances can be seen in Table 3.3

The duration of these intermediate frequencies is approximately 10ms, which is significantly less than the time needed to establish a co-operative coupling between the lips and the air column. This set of measurements uses a 4.42m long

Resonant Mode	**Resonant Mode Frequency**	**Player Frequency**	**Difference in Cents**
8	289 Hz	290 Hz	+ 5
7	255 Hz	236 Hz	- 133
6	219 Hz	194 Hz	- 208
5	184 Hz	161 Hz	- 230
4	146 Hz	143 Hz	- 34

Table 3.3: Radiated intermediate resonance frequencies of an octave lip-slur from D_4 to D_3 by Player B. The resonant mode frequency is the expected frequency, the player frequency is the frequency of the steps in the instantaneous frequency. Difference in cents is the difference between the expected and player frequencies.

D horn; for this length of instrument the time for the sound wave to propagate from the lips to the end of the instrument is approximately 10ms. For a co-operative coupling regime to be set up between the lips and the air column, at a particular frequency, the new frequency pressure wave would have to travel the length of the instrument twice - from the lips to the bell end and back again. Once the backward going wave has reached the lips, a standing wave will have been formed within the instrument and if the lips are oscillating at the same frequency the standing wave will act as positive reinforcement for the lips. These, however, are not the conditions present in the case of a downward lip-slur; the lips excite the air column at a frequency of one of the intermediate resonances, for example the 7^{th} resonant mode, and after 10ms the lips move away from this resonance and begin oscillating at a different frequency. This means that as the pressure wave corresponding to the 7^{th} resonance is being (partially) reflected and traveling back towards the lips, a forward going wave of a new frequency, the 6^{th} resonant mode frequency, is beginning to propagate down the instrument towards the bell. Therefore, there is a finite time where there are conflicting frequency pressure waves traveling in opposite directions within the instrument.

It is interesting to hypothesise that these short duration resonances are

'ringing' effects induced by the frequency sweep of the lip oscillations and corresponding excitation at the input of the instrument. The lip opening area frequency decreases relatively smoothly, for both players, between the two played notes, giving a smooth frequency sweep past each intermediate resonance.

We have seen in this section that the behaviour of the lips, pressure signals and corresponding instantaneous frequencies are not consistent between upward and downward lip-slurs. It is not yet clear why players, such as Player A, are able to force their lips into making a smooth transition from a high resonant mode to a lower one, but less able to do so when moving from a low to high resonance, or why it is possible for Player B to jump straight from one resonance to another when slurring upwards but shows very similar characteristics to Player A when slurring downwards.

3.3.4 Slurred transients in different registers

This section presents slurred transients over octave intervals in different registers. Thus far the octave lip-slurs examined on the horn were in the lower end of the instruments range, between the 4^{th} and the 8^{th} resonant modes; this section will explore the similarities and differences between transitions between these modes and the octave above, between the 8^{th} and 16^{th} resonant modes.

As with all brass instruments the input impedance of the horn does not have equal amplitude over all the input impedance peaks. Figure 3.16 shows the input impedance of the Meinl & Lauber/Paxman 'baroque' horn crooked in D used in this set of experiments. A photograph of this horn is shown in Figure 3.17.

The amplitude of input impedance peaks, shown in measurements of brass instruments, are affected by the mouthpiece used; in this work a PHC23a mouthpiece was used, which was chosen as it is a standard medium cup horn mouthpiece. Using this instrument/mouthpiece combination the input impedance envelope is relatively flat over the low-mid frequencies; the resonant modes under investigation here are labeled on the input impedance curve. The amplitude of the 4^{th} and the 8^{th} modes are shown to have only a small difference in amplitude, with the 8^{th} mode being approximately 1 MOhm higher than the 4^{th} mode. However, the 16^{th} mode lies on the other side of the small peak in the amplitude envelope, and has a significantly lower amplitude than the 8^{th} mode.

The experimental setup for this set of experiments differs from the setup

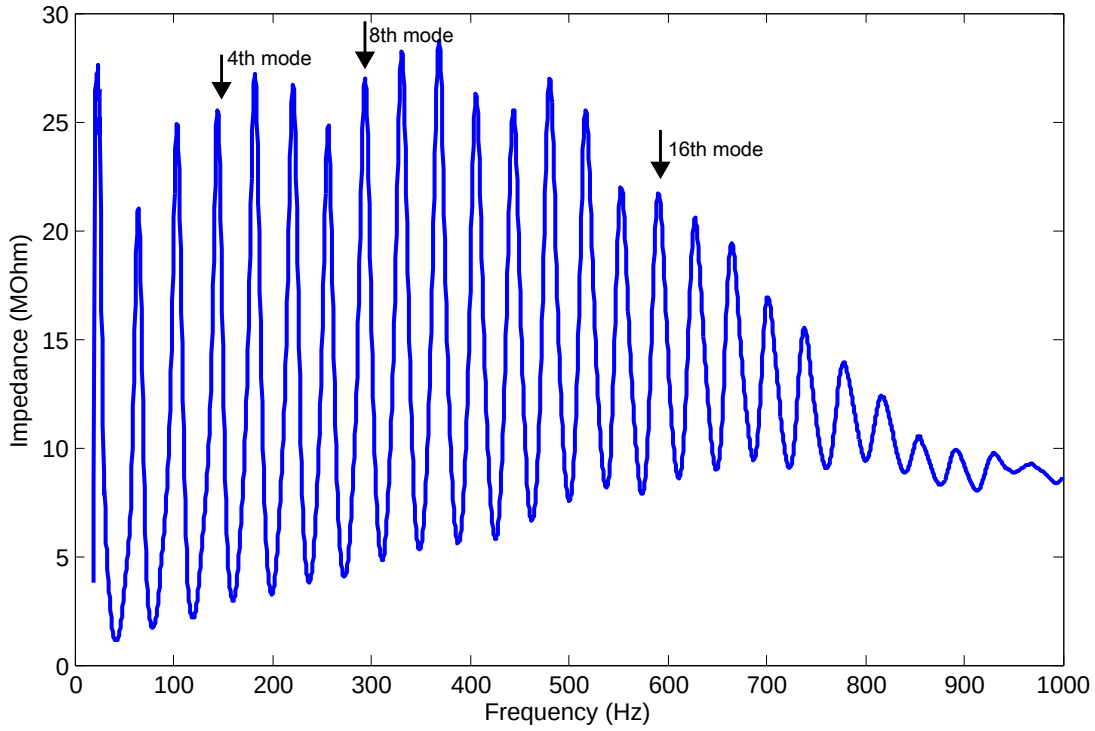

Figure 3.16: Input impedance of the Meinl & Lauber/Paxman 'baroque' horn crooked in D used for this work.

previously described, and is shown in Figure 3.18. This work does not include visualisation of the player's lips and therefore has a more simplified setup. The player is able to hold the instrument in the normal playing position while the pressure is simultaneously measured in the mouthpiece and radiated from the bell. The radiated sound was measured using a 1/2-inch Sennheiser pressure-field microphone placed one bell radius from the bell of the instrument, while the pressure in the mouthpiece was measured using a 1/4-inch Bruël and Kjær 4938 pressure-field microphone. The two pressure signals were simultaneously recorded using an R-09 EDIROL by Roland solid state WAVE/MP3 recorder.

The mouthpiece was modified to accommodate the 1/4-inch microphone, as is shown in Figure 3.19. A hole was bored in the mouthpiece cup to allow the microphone to fit into the wall of the mouthpiece cup by means of a small brass coupler. The microphone diaphragm was then flush with the inside cup wall.

Figure 3.17: Horn used for the work described in this section, a Meinl & Lauber/Paxman 'baroque' horn modelled after an 18^{th} century instrument by Huschauer, Vienna c.1770

Figure 3.18: Experimental setup for transients experiments, simultaneously recording pressure in the mouthpiece and radiated pressure from the bell of the instrument.

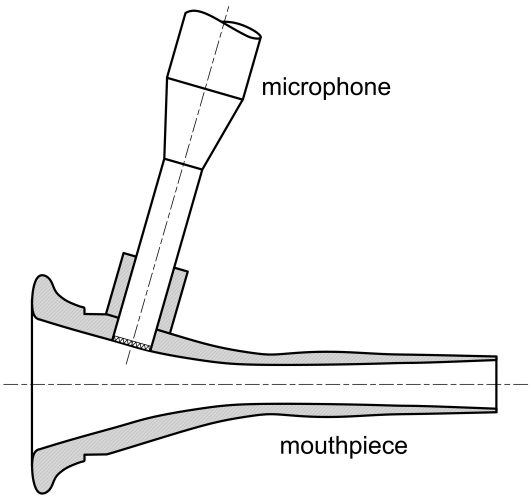

Figure 3.19: Modified mouthpiece to accommodate the 1/4-inch microphone to record the pressure signal within the mouthpiece.

All results shown in this section were performed by Player B. Figures 3.20 and 3.21 show upward and downward octave slurs similar to those presented in Section 3.3.3, between the 4^{th} and the 8^{th} resonant modes which correspond to the notes D_3 and D_4, but in this case on a different horn and performed in a different laboratory session.

The results shown here display similar characteristics to those previously presented for both upward and downward lip-slurs over this octave. The upward slur shows that the instantaneous frequencies for both the mouthpiece and radiated pressure change almost instantaneously from the lower to the higher note. The pressure signals also show similar characteristics to those previously seen on the other horns and the same player. The pressure measured in the mouthpiece shows a significant drop during the transition, to around 0.5kPa, and the radiated pressure amplitude drops to almost zero for around 30ms.

The downward slur results shown in Figure 3.21 also show similar results to those in the previous section. Both the pressure amplitudes for the mouthpiece and radiated pressure show the same slightly erratic behaviour during the transition and do not drop in amplitude to the same extent as the upward transition. The instantaneous frequency results for the mouthpiece pressure again show evidence of steps in the frequency during the transition, which correspond approximately to the intermediate frequencies. This is also true for the radiated pressure, although the steps in the instantaneous frequency are much less defined

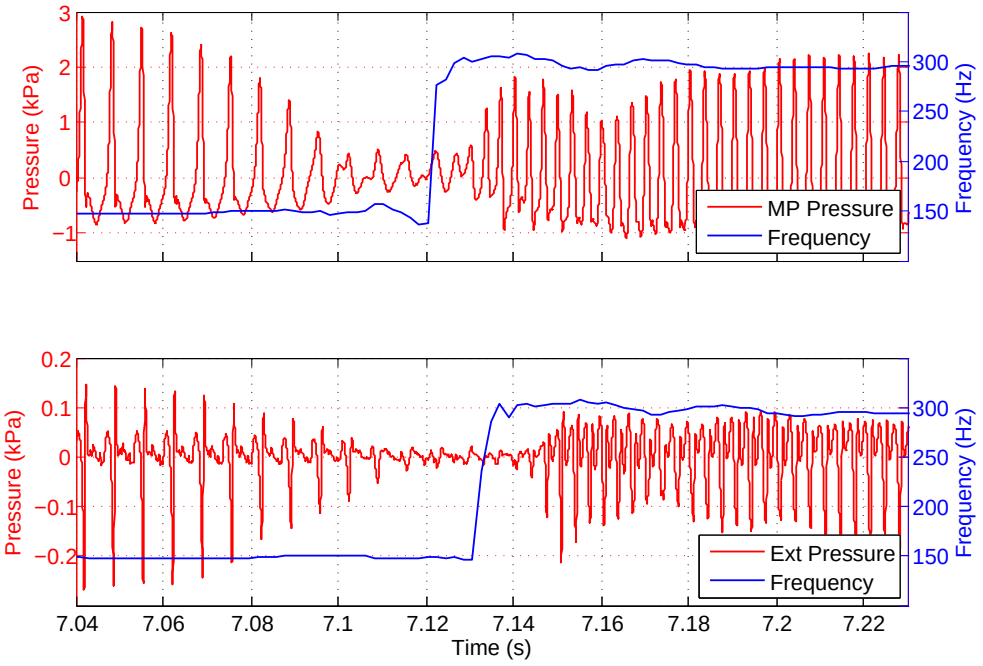

Figure 3.20: Synchronised signals for lip-slur from D_3 to D_4 by Player B, on the 'baroque' horn by Meinl & Lauber/Paxman. **Top**: Mouthpiece pressure **Bottom**: Radiated pressure.

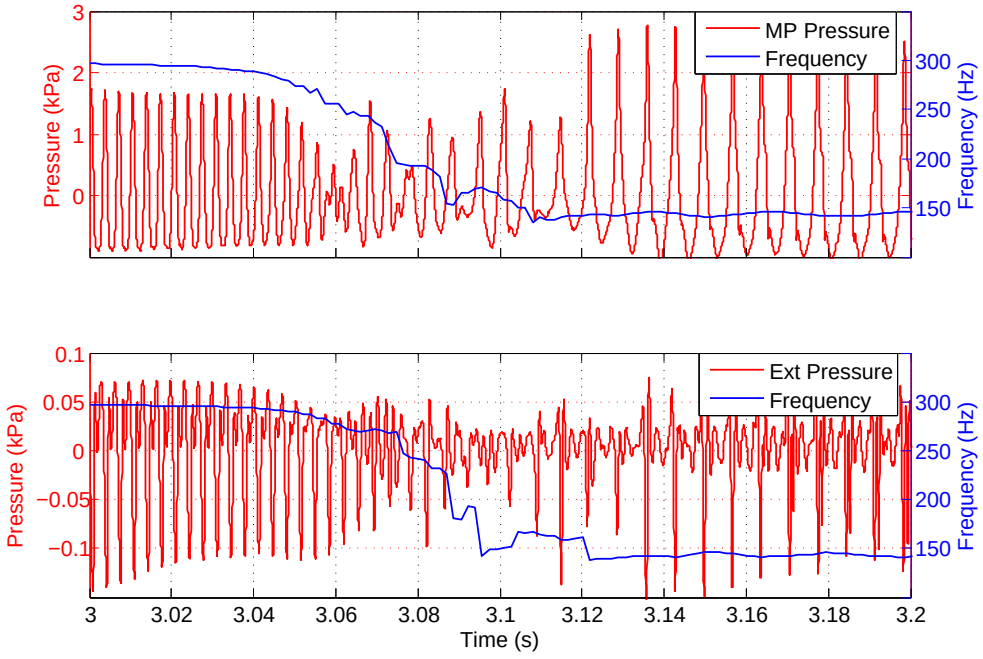

Figure 3.21: Synchronised signals for lip-slur from D_4 to D_3 by Player B, on the 'baroque' horn by Meinl & Lauber/Paxman. **Top**: Mouthpiece pressure **Bottom**: Radiated pressure.

than those seen on the modern Conn horn in Section 3.3.3.

Resonant Mode	**Resonant Mode Frequency**	**Player Frequency**	**Difference in Cents**
8	294 Hz	296 Hz	+ 12
7	256 Hz	241 Hz	- 104
6	220 Hz	191 Hz	- 243
5	182 Hz	162 Hz	- 200
4	144 Hz	142 Hz	- 24

Table 3.4: Radiated intermediate resonance frequencies of an octave lip-slur from D_4 to D_3 by Player B. The resonant mode frequency is the expected frequency, the player frequency is the frequency of the steps in the instantaneous frequency. Difference in cents is the difference between the expected and player frequencies.

Table 3.4 shows the difference in frequency between the expected resonances and the intermediate instantaneous frequency steps. The 6^{th} resonant mode shows the largest difference at 243 cents flat, which is more than seen in the previous section on the modern horn by Conn.

Figures 3.22 and 3.23 show the results for Player B performing upward and downward lip-slurs between the 8^{th} and the 16^{th} resonant modes, which correspond to the notes D_4 and D_5. This lip-slur is an octave higher than those previously discussed and spans the mid to high range of normal playing on the horn. It is clear that there is not the same difference in characteristics between the upward and downward lip-slurs in this register; the upward slur does not show the same almost instantaneous frequency transition between the two notes, as in the lower octave, but instead shows behaviour very similar to that of the downward slur. There are seven clear intermediate peaks shown in both the upward and downward frequency results which is in line with the number of resonant modes between the played notes of D_4 and D_5. The difference between the expected frequencies and those seen in the results shown here are presented in Tables 3.5 and 3.6. As with the lower register all the intermediate resonances are

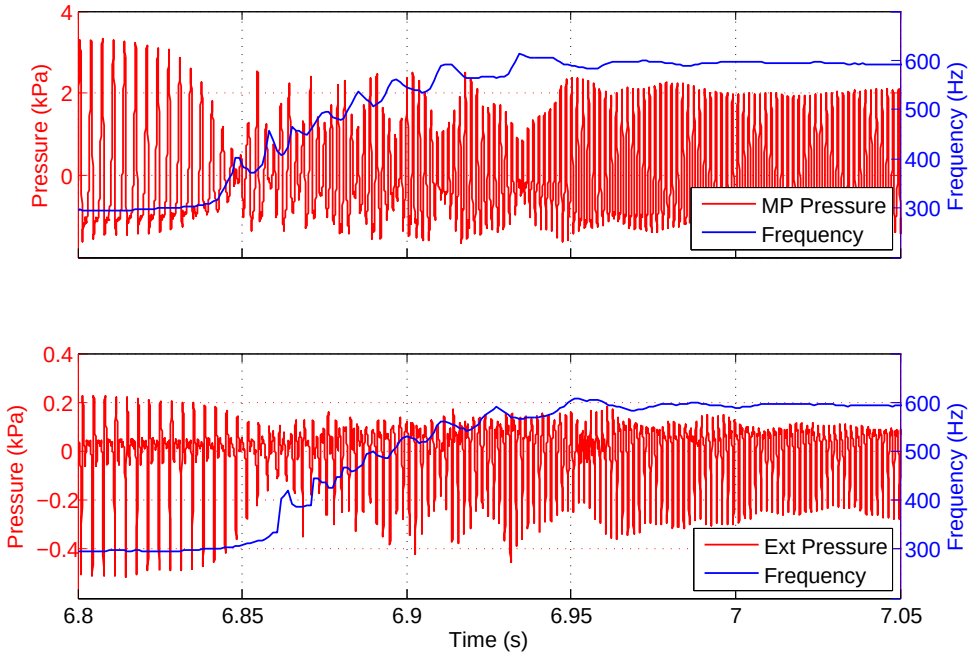

Figure 3.22: Synchronised signals for lip-slur from D_4 to D_5 by Player B, on the 'baroque' horn by Meinl & Lauber/Paxman. **Top**: Mouthpiece pressure **Bottom**: Radiated pressure.

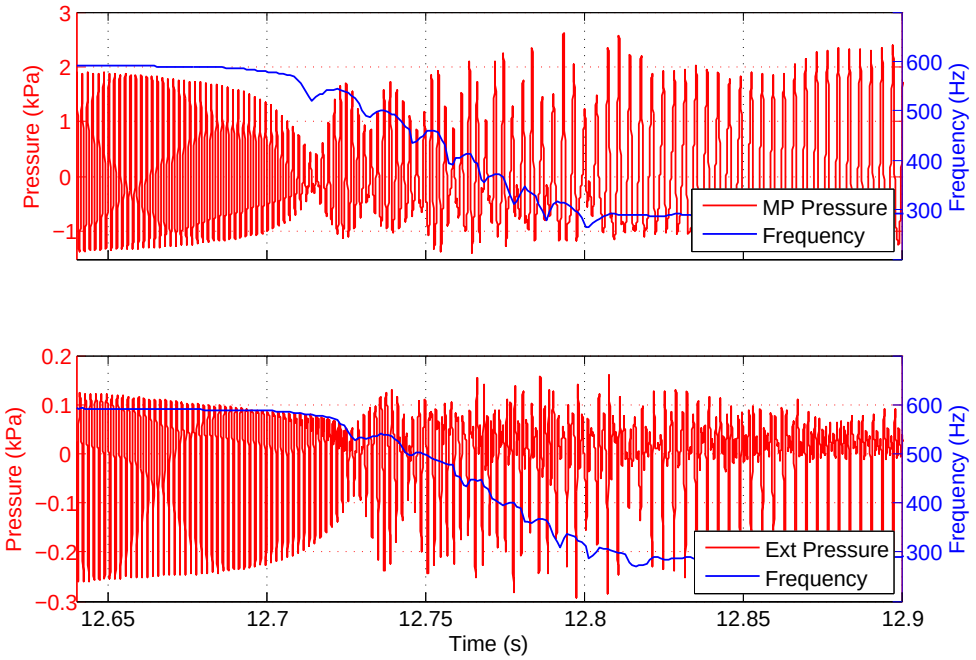

Figure 3.23: Synchronised signals for lip-slur from D_5 to D_4 by Player B, on the 'baroque' horn by Meinl & Lauber/Paxman. **Top**: Mouthpiece pressure **Bottom**: Radiated pressure.

flat in comparison to the expected resonant frequencies, by up to 270 cents in the upward slur and 182 cents in the downward. Although the transition over this range encompasses more intermediate resonances, the transition time for both the upward and downward slurs is no longer than for the lower register transitions, at 100ms.

It has previously been shown that for an upward slur, in the lower register of the horn, the pressure amplitude of the radiated signal dies away to almost zero during the transition, and the mouthpiece pressure also diminishes significantly. The downward slur in the lower octave showed much less of a decrease in both pressure signals during the transition period. In the upper register shown here the pressure amplitude for all the pressure signals show no decrease in amplitude during the transition for both the upward and downward lip-slurs.

The player was not aware of any change in technique when slurring in different registers; the player is again aiming to move as quickly as possible between the two notes and create a smooth sound, while having the sensation of continuously blowing throughout the transition. It is not yet clear why it is possible for players to 'catch' resonances in the upper register when slurring in both directions yet be able to make an almost instantaneous transition upwards in the lower register. It is however interesting to note that these two intervals lie in very different parts of the input impedance curve; the lower octave is over a number of resonances that lie to the left of the peak in the impedance envelope and the upper octave transition lies to the right of this peak and at the point where the resonances decrease significantly in amplitude.

Resonant Mode	**Resonant Mode Frequency**	**Player Frequency**	**Difference in Cents**
8	294 Hz	296 Hz	+ 12
9	330 Hz	386 Hz	- 270
10	368 Hz	425 Hz	- 247
11	406 Hz	460 Hz	- 216
12	443 Hz	485 Hz	- 155
13	480 Hz	520 Hz	- 138
14	516 Hz	542 Hz	- 84
15	552 Hz	568 Hz	- 47
16	590 Hz	595 Hz	- 13

Table 3.5: Radiated intermediate resonance frequencies of an octave lip-slur from D_4 to D_5 by Player B. The resonant mode frequency is the expected frequency, the player frequency is the frequency of the steps in the instantaneous frequency. Difference in cents is the difference between the expected and player frequencies.

Resonant Mode	**Resonant Mode Frequency**	**Player Frequency**	**Difference in Cents**
16	590 Hz	589 Hz	- 2
15	552 Hz	539 Hz	- 41
14	516 Hz	500 Hz	- 54
13	480 Hz	446 Hz	- 126
12	443 Hz	400 Hz	- 175
11	406 Hz	367 Hz	- 174
10	368 Hz	331 Hz	- 182
9	330 Hz	303 Hz	- 147
8	294 Hz	288 Hz	- 34

Table 3.6: Radiated intermediate resonance frequencies of an octave lip-slur from D_5 to D_4 by Player B. The resonant mode frequency is the expected frequency, the player frequency is the frequency of the steps in the instantaneous frequency. Difference in cents is the difference between the expected and player frequencies.

3.4 Forced oscillation input - Experimental technique

Accomplished brass instrument players are very adept at manipulating their lips to produce the best results from the instrument and compensate for inadequacies of the particular instrument. These often subconscious corrections that the player can achieve make it difficult to study the system as independent mechanical components that are coupled together. One way in which we can eliminate the player's unknowing adjustments to the system is to use a forced oscillation input to the instrument. In using a forced oscillation system it can be assumed that this excitation source is independent of feedback from the instrument itself, unlike the player's lips which are subject to reinforcement from the standing wave within the instrument. This set of experiments were carried out to investigate to what extent the results already discussed, are effects of ringing of resonances from a forced oscillation, opposed to the dependance on the interaction with the player's lips.

3.4.1 Instruments

Three different brass instruments were used in the forced oscillation experiments; the horn used for a number of the experiments described in the previous section - the Meinl & Lauber/Paxman 'baroque' horn, a Smith-Watkins trumpet, and a King tenor trombone; these instruments were chosen as they have significantly different lengths of tubing and bore profiles.

3.4.2 Experimental setup

The forced oscillation driving force was produced by means of a JBL compression driver loudspeaker coupled to the instrument. The loudspeaker was coupled to the mouthpiece of the instrument using a plastic coupler that is able to house a 106B PCB Piezotronics dynamic pressure transducer to measure the pressure at the mouthpiece entrance. The radiated pressure was measured using a Bruël and Kjær 4938 pressure-field microphone placed in the plane of the bell of the instrument. The experimental setup with the horn in place is shown in Figure 3.24.

Figure 3.24: Photograph of horn experimental setup for forced oscillation experiments.

The input signal used was a linear sine sweep mimicking a slurred transient performed by a player. The signal begins with a steady frequency before sweeping over a specified time period to a second steady frequency. The sweep time used was either 50ms or 100ms; the time was chosen for each slur as the closest to the transition time taken in the player results. The frequency range in which the sweep covered was determined by the resonant modes of the instrument, as to have a slur between two exact resonant modes. For example, in the horn, the resonant frequencies of the 4^{th} and 8^{th} modes were found to be 165Hz and 315Hz respectively. Both the input and output microphone pressure signals were recorded using a Marantz digital solid state recording device.

The results will be presented as in Sections 3.3.2, 3.3.3 and 3.3.4 and use the same instantaneous frequency analysis methods.

3.5 Forced oscillation input - Results

The trumpet and trombone sections will show the forced oscillation results and the horn section will show the forced oscillation results with the corresponding player results, performed by Player B, as previously discussed in Section 3.3.4.

3.5.1 Trumpet results

The trumpet results presented here in Figures 3.25 and 3.26 are forced oscillation slurs between the 4^{th} and the 8^{th} resonant modes of the trumpet, which corresponds to the notes $B\flat_4$ and $B\flat_5$. This interval is in the mid to high range of the trumpet's normal playing range. The results show the pressure signals recorded at the mouthpiece entrance and radiated from the bell of the instrument, and for both the upward and downward transitions the sweep time used was 100ms. As expected, because of the nature of the excitation signal, the instantaneous frequency signal at the mouthpiece increases steadily between the two resonant mode frequencies. The frequency of the radiated pressure shows a much less smooth transition, there are a number of peaks in the frequency but no clear steps/plateaus. However, in the downward slur there is some indication of the frequency flattening around the times of 1.4s, 1.42s, and 1.45s; this effect is only very slight and only present in the downward slur. If this could be classed as an intermediate frequency effect it would be in line with the horn results, in that it seems to be easier for the players to catch the intermediate resonant modes in a downward slur.

3.5.2 Trombone results

The trombone results are between the 3^{rd} and the 6^{th} resonant modes which correspond to the notes F_3 and F_4; this octave interval is in the mid range of the trombone. Again the frequency of the mouthpiece pressure signals move smoothly between the two notes, and the radiated pressure frequency shows the similarly varying results as seen with the trumpet. There is no sign of intermediate resonance frequencies during the transition but it is interesting to note that, both in the upward and downward transitions, the frequency takes a relatively large number of cycles before it settles on the second note.

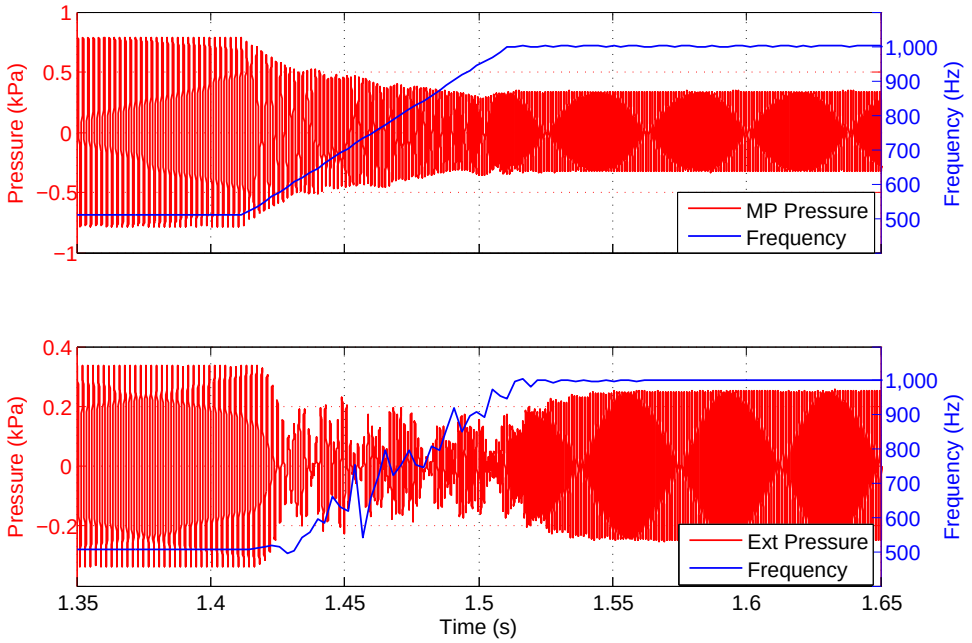

Figure 3.25: Forced oscillation slur from B♭$_4$ to B♭$_5$, on the Smith Watkins trumpet with loudspeaker excitation source. **Top**: Mouthpiece pressure signal. **Bottom**: Radiated pressure signal. Loudspeaker transition time of 100ms.

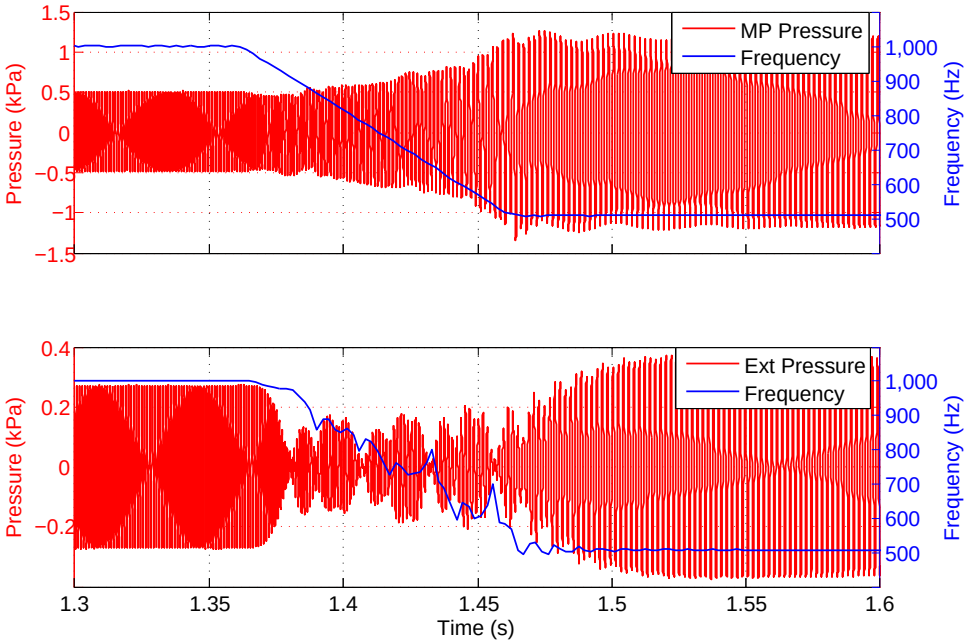

Figure 3.26: Forced oscillation slur from B♭$_5$ to B♭$_4$, on the Smith Watkins trumpet with loudspeaker excitation source. **Top**: Mouthpiece pressure signal. **Bottom**: Radiated pressure signal. Loudspeaker transition time of 100ms.

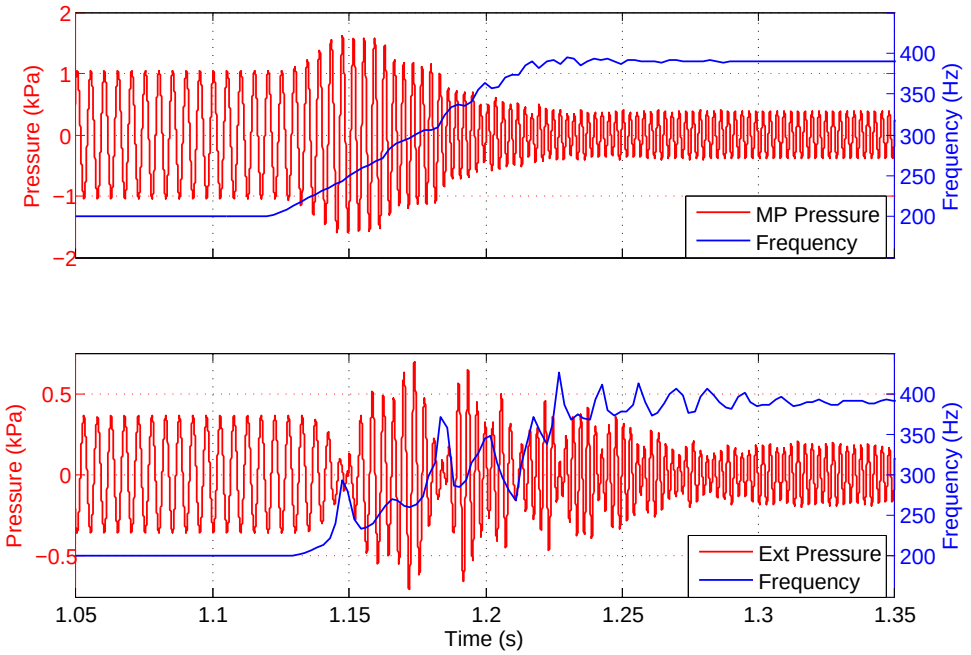

Figure 3.27: Forced oscillation slur from F_3 to F_4, on the medium bore trombone by King with loudspeaker excitation source. **Top**: Mouthpiece pressure signal. **Bottom**: Radiated pressure signal. Loudspeaker transition time of 100ms.

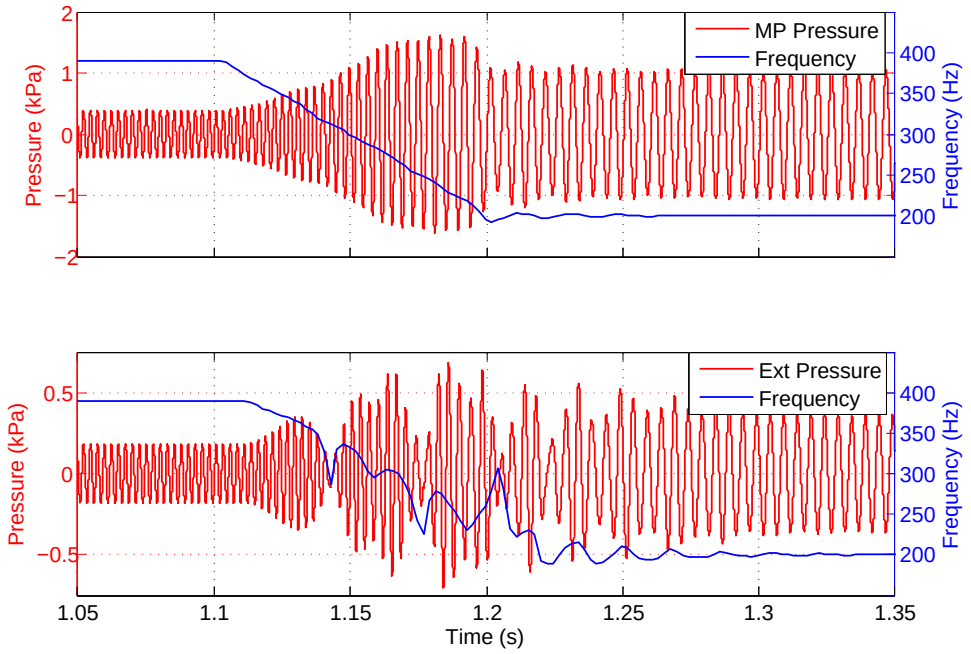

Figure 3.28: Forced oscillation slur from F_4 to F_3, on the medium bore trombone by King with loudspeaker excitation source. **Top**: Mouthpiece pressure signal. **Bottom**: Radiated pressure signal. Loudspeaker transition time of 100ms.

3.5.3 Horn results

In the case of the horn, the forced oscillation results are compared directly with the corresponding player results. Figure 3.29 shows the upward results in the lower register, between the 4^{th} and 8^{th} resonant modes, where the instantaneous frequency of the player results moves suddenly between the two notes; it is for this reason that the forced oscillation sweep time was set at 50ms. The forced oscillation frequency results do not show the same straight transition between the two resonant modes, but instead show an unsteady frequency transition that shows evidence of intermediate frequencies, demonstrating that even at this very fast transition speed there is still some 'ringing' effect of the intermediate resonances that can be seen in the small peaks/shoulders.

Figure 3.30 shows the corresponding downward slur over this range with the forced oscillation sweep time set at 100ms as the player results show a longer transition time than for the upward transition. Both the player and forced oscillation results show an uneven decrease in frequency between the two notes. The large peak in the loudspeaker instantaneous frequency at around 1.25s can be said to be a consequence of the analysis program and not reliable; bearing this in mind there is still evidence of intermediate frequency peaks during the transition as seen in the player results. However, the intermediate frequencies are not as clear as have been previously seen in the higher register player results. This downward, loudspeaker slurred result does have a much closer frequency transition to the player result than the corresponding upward result where the player manages to change the frequency almost instantaneously.

Figures 3.31 and 3.32 show the upward and downward results for the horn measurements over the upper register octave range between the 8^{th} and 16^{th} resonant modes of the instrument; notes D_4 and D_5. It can be seen from the results that the forced oscillation instantaneous frequency shows well defined intermediate peaks for both slurs. When you have the real situation of a musician playing the instrument there is feedback that returns to the player's lips from the resonances of the instrument, which could make it easier for the player to 'latch' onto the intermediate resonances. It is interesting to note that the influence of the resonances on the instantaneous frequency of the radiated sound in these figures are not strongly dependant on this feedback as the loudspeaker cannot be effected by the returning pressure wave. It is assumed that the loudspeaker is

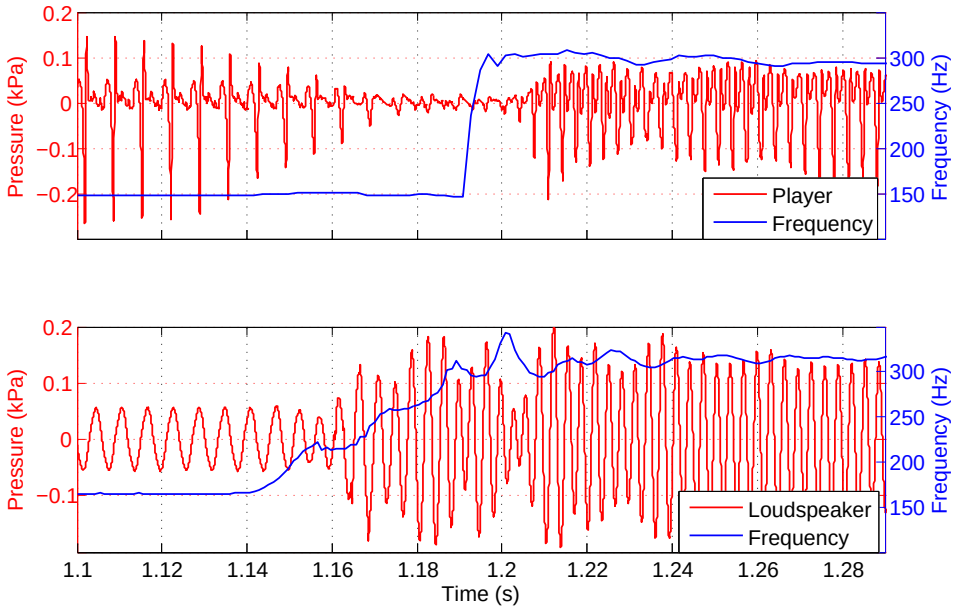

Figure 3.29: Lip-slur from D_3 to D_4, on the 'baroque' horn by Meinl & Lauber/Paxman, showing the radiated pressure signals. **Top**: Player test by Player B. **Bottom**: Loudspeaker test. Loudspeaker transition time of 50ms.

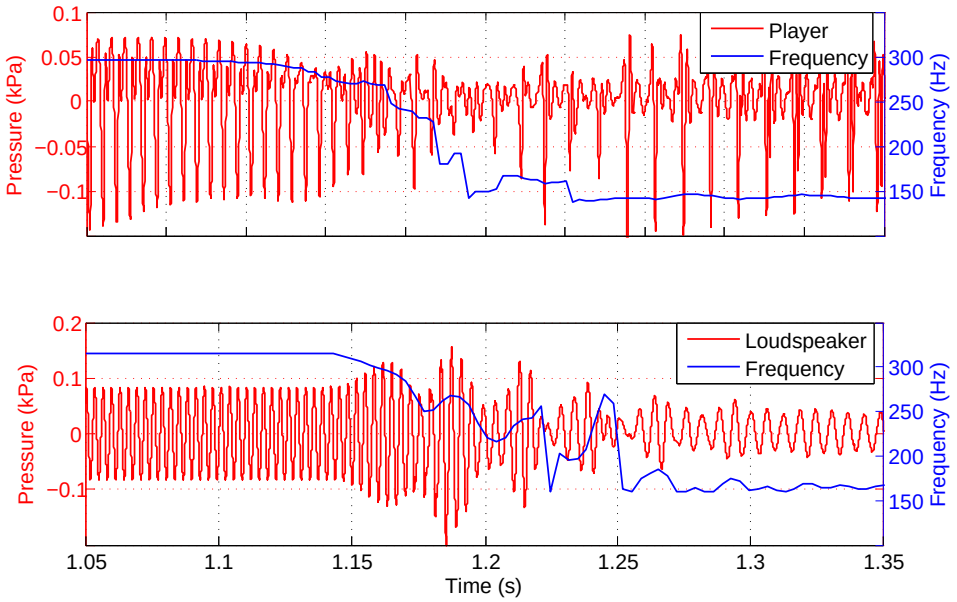

Figure 3.30: Lip-slur from D_4 to D_3, on the 'baroque' horn by Meinl & Lauber/Paxman, showing the radiated pressure signals. **Top**: Player test by Player B. **Bottom**: Loudspeaker test. Loudspeaker transition time of 100ms.

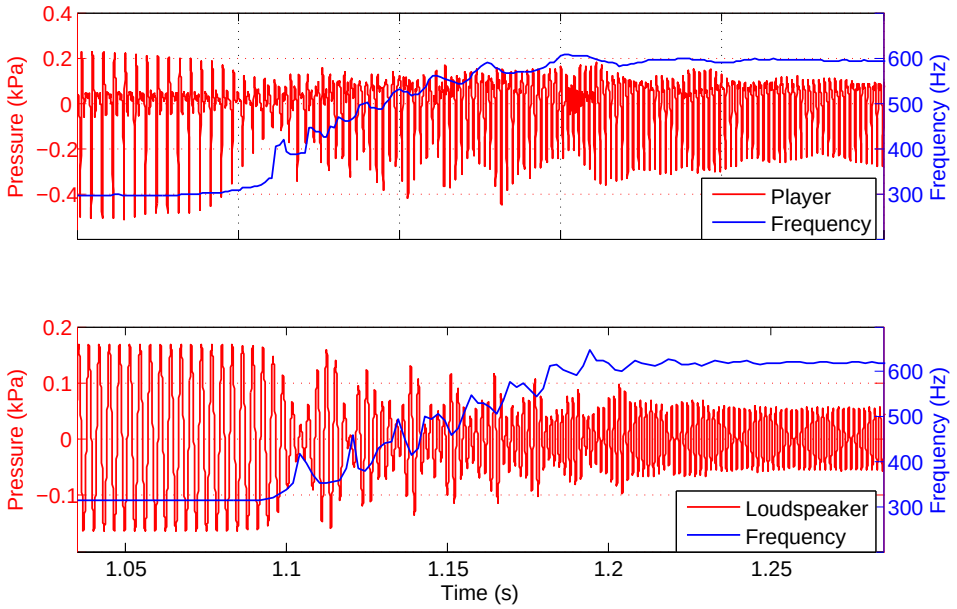

Figure 3.31: Lip-slur from D_4 to D_5, on the 'baroque' horn by Meinl & Lauber/Paxman, showing the radiated pressure signals. **Top**: Player test by Player B. **Bottom**: Loudspeaker test. Loudspeaker transition time of 100ms.

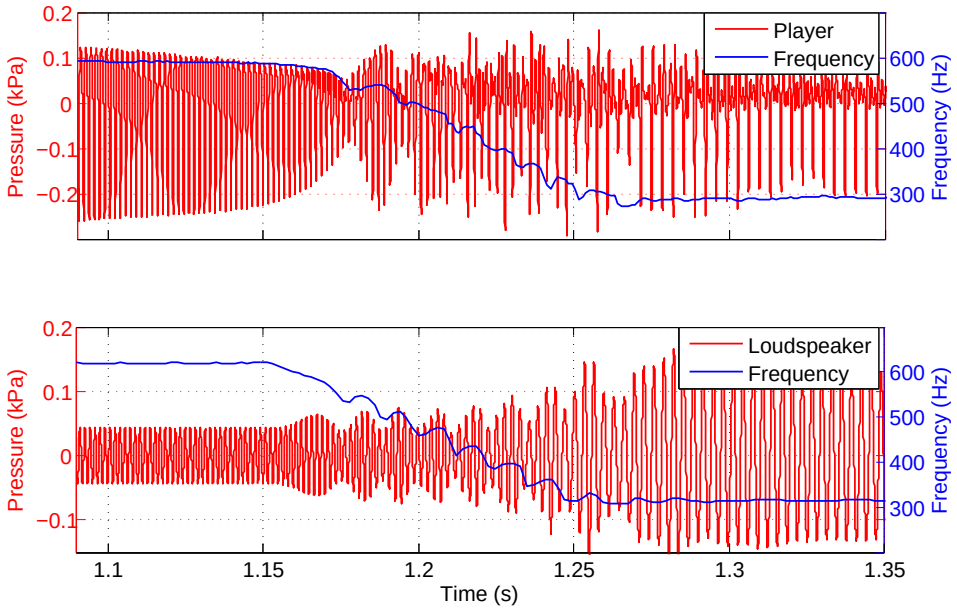

Figure 3.32: Lip-slur from D_5 to D_4, on the 'baroque' horn by Meinl & Lauber/Paxman, showing the radiated pressure signals. **Top**: Player test by Player B. **Bottom**: Loudspeaker test. Loudspeaker transition time of 100ms.

decoupled from the resonating air column in the instrument, and that the input frequency will be unaffected by the resonances of the instrument. It can, however, be seen from these results that there is a 'ringing' effect of the intermediate resonances which is producing the peaks in the frequency as the input sine wave sweeps past these resonances. The radiated pressure that is recorded is showing a mixture of the input signal that has traveled through the instrument, and been partially radiated, and the intermediate resonances that are 'ringing' within the instrument.

These slurred transient results, with both the player and loudspeaker excitation sources, will be compared with a theoretical computational model in Chapter 4.

3.6 Conclusions

This chapter has discussed two separate experimental approaches to the study of slurred transients on brass instruments. A number of different instruments were used, along with players who employ different techniques when slurring between notes.

3.6.1 Visualisation of the lips

High speed photography of the lips, synchronised with pressure signals from inside the mouthpiece and radiated from the bell of the instrument has been successful in visualising the lips under playing conditions. The pressure signals and instantaneous frequency of all experimental data have been analysed.

Typical characteristics of slurred transients

It was shown that, in horn playing, the player's approach to lip-slurring does affect both the pressure and instantaneous frequency results. Presented and discussed were slurs over an upward octave and perfect fourth interval, in the lower register of the horn. It was seen that slurs, by both players, range in transition time between 70-100ms. The results from the player who uses the quick jump between notes showed that there was indeed a quick frequency transition from the first note in both pressure signals and lip opening area. This quick transition did not jump

straight to the second note immediately but jumped up some way before leveling out more slowly onto the second note. It was also seen that the radiated pressure dies away to almost nothing during the transition. When the slurring technique used was that of attempting to catch the intermediate resonances, very different results were seen. There was a significant pressure amplitude seen throughout the transition in both mouthpiece and radiated signals, and all instantaneous frequency results showed an erratic transition.

Upward and downward slurred transients

This section showed that the characteristics of upward and downward octave slurs in the lower register of the horn are significantly different. Players who are able to jump straight from the lower note to the higher one are not able to produce the same frequency transition during a downward slur. The downward slurs for both players, with different techniques, show marked steps in the instantaneous frequency. These steps have been related to the intermediate resonances and it was found that they are all flat in comparison, by up to more than two semitones. It is yet unclear why players are able to produce a smooth frequency transition during an upward slur but show signs of intermediate resonances during a downward slur.

Slurred transients in different registers

When investigating slurred octave transitions in the upper register of the horn it was found that both techniques showed similar results; for both upward and downward slurs there are clear intermediate peaks corresponding to the number of intermediate resonances. Again the frequency of these are all flat compared to the resonant modes of the instrument, by up to two and a half semitones.

3.6.2 Forced oscillation

The forced oscillation experiments allow the instrument to be excited in a similar, but less complex, way as by a human player and it is assumed that the loudspeaker is decoupled from the system. The trumpet and trombone results showed that, when excited by a forced linear sine sweep, there were no discernable intermediate resonances shown in the radiated pressure signals. The horn, however, showed

significantly different results. When compared with player results, in the lower register, it was seen that there were signs of intermediate resonances ringing in some way, in both the upward and downward slurred transitions. This is in line with the player results for the downward slur but not the upward, as Player B shows a smooth jump in frequency between the two notes. The upward forced oscillation result has shown that even at transition speeds of 50ms there is still some ringing effect seen in the frequency transition. In the upper register of the horn the forced oscillation results showed remarkably similar instantaneous frequency results to those of the human player, with a number of very distinct peaks corresponding to the number of intermediate resonances, both in the upward and downward cases. These results show that the ringing of the intermediate resonances is not due to the coupling of the system as the loudspeaker is taken to be decoupled from the instrument. It is unsurprising in some ways, as we know that the short time these resonances are seen to 'ring' for is much too short for the lips of the player to have received constructive reinforcement from any intermediate resonances.

Chapter 4

Computational modelling of slurred transients

This chapter will introduce the one dimensional finite difference computational model used to investigate transients in brass instruments. Two different input parameter approaches will be explored; the first results section will present results from linear sine sweep input data, whereas the second results section will show results using simplified player pressure and frequency input data. The results here will be compared with the experimental player and forced oscillation results presented in Chapter 3.

4.1 Introduction

In the study of playing characteristics of brass instruments, tests with human players are invaluable but it is often interesting, and necessary, to compare these results with those gained through computational methods. A good computational model, which produces results that replicate human player data, can give a fuller insight into the mechanics of the system and allow changes to the system to be made quickly and easily; for example the bore profile of an instrument can be altered easily using a computational approach when it is prohibitive to alter the physical instrument.

The model used in this work was developed by Stefan Bilbao at the University of Edinburgh and is detailed in [Bilbao 11], along with the detailed numerical synthesis theory in [Bilbao 09]; the model uses a simple finite difference time

domain (FDTD) method and includes acoustic radiation and viscothermal losses in the latter use of it.

4.2 Webster's equation and acoustic tube modelling

A standard lossless model of one-dimensional linear wave propagation in an acoustic tube [Morse 68] can be derived from the linearised fluid dynamic equations of conservation of mass and momentum:

$$\frac{S}{\rho c^2}\, p_t = -u_x \qquad \frac{\rho}{S}\, u_t = -p_x \qquad t \geq 0, x \in [0, L] \tag{4.1}$$

where $u(x,t)$ and $p(x,t)$ are the volume velocity and pressure respectively at any point x and at time t and subscripts t and x refer to time and space differentiation, respectively. Density and wave speed are ρ and c respectively, *S(x)* is the cross-sectional area of the tube (more precisely, the area of an isophase surface of a propagating wavefront [Helie 03]) at position x, and L is the length of the tube. See Figure 4.1.

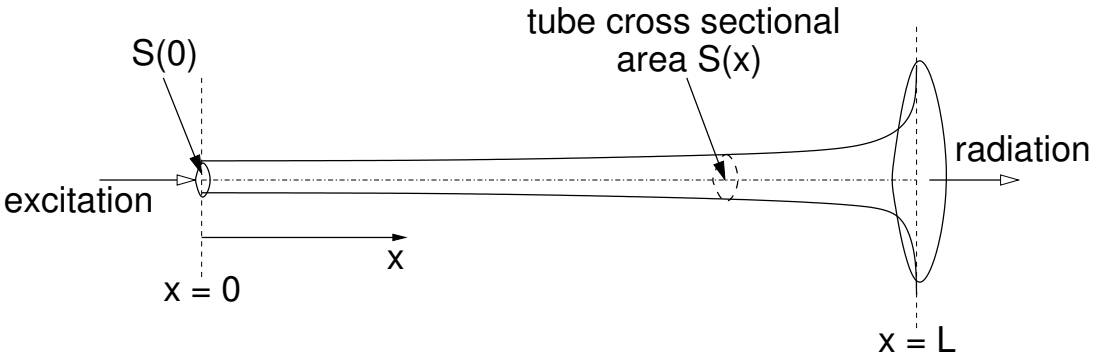

Figure 4.1: Schematic of the one dimensional horn model, with excitation at the mouthpiece and radiated sound from the bell.

From this first-order system a single second-order system is often derived and referred to as Webster's equation [Webster 19]:

$$S\Psi_{tt} = c^2 (S\Psi_x)_x \tag{4.2}$$

where $\Psi(x,t)$ is a velocity potential, and where $p = \rho\Psi_t$, $u = -S\Psi_x$. As well as serving as a basic tool in wind instrument modelling, this equation is the starting point for a number of speech synthesis algorithms [Rabiner 78], such as the Kelly-Lochbaum model [Kelly 62]. There are many assumptions which lead to this model; these include, linearity, losslessness, slow spatial variation in *S(x)* and smallness of radial dimensions relative to wavelengths. It should be noted that the simulation program works with dimensionless variables.

At the radiating end of the tube, a standard approximation to an unflanged tube end is employed [Atig 04, Rabiner 78]. The model of the lips is a standard oscillator model subject to a nonlinear pressure/flow relationship (Bernoulli's Law) [Cullen 00a]. The dynamics of the lips can be represented by the following:

$$\frac{d^2H}{dt^2} + \frac{\omega_L}{Q_L}\frac{dH}{dt} + \omega_L^2 H = \frac{-\Delta p S_e}{m_L} \tag{4.3}$$

where $H(t)$ is the distance between the lips at time t, ω_L is the natural angular frequency of the lips, Q_L is the quality factor of the lips, m_L is the effective mass of the system and is equal to $m/2$ (where m is the mass of each lip) and S_e is the effective surface area of the lips. The pressure difference across the lips is defined as $\Delta p = P_m - P$ where P_m is the overpressure in the mouth and P is the pressure in the mouthpiece. The nonlinear way in which the pressure difference across the lips and the particle velocity in the mouthpiece, U, are related is described by the Bernoulli relation:

$$P_m - P = \frac{1}{2}\rho U^2 \tag{4.4}$$

Using the version of Webster's equation shown in Equation 4.2 the viscothermal losses within the instrument are not modelled; this is a very important effect, especially in portions of the bore of small radius (the throat). The version of the model not including these losses is used for the player input results presented in Section 4.3.3. The results in Sections 4.3.1 and 4.3.2, however, were produced using a version of the model which does include viscothermal losses. The inclusion of viscothermal losses is difficult to model properly using a time domain model, and most acoustic tube loss models are based on an impedance description in the frequency domain [Keefe 84, Causse 84], with the exception of [Amir 95a, Amir 95b] which uses a time domain model concerning

short cylindrical or conical sections. The model used in this work transforms this frequency domain impedance description to a discrete space-time approximation which introduces extra fractional derivative terms into Equation 4.2, which then becomes the Webster-Lokshin equation [Haddar 03].

4.2.1 A simple finite difference scheme

Suppose that Ψ_l^n is a grid function, defined for integer l and n, representing an approximation to $\Psi(x,t)$ at $x = lh$, and $t = nk$, where k is a time step, and where h is a grid spacing; $f_s = 1/k$ is the sample rate. Figure 4.2 shows graphically the grid function used in the finite difference scheme. A simple finite difference scheme for Webster's equation can be written as [Bilbao 09]:

$$\begin{aligned}\Psi_l^{n+1} = \frac{\lambda^2(S_{l+1}+S_l)}{2[S]_l}\Psi_{l+1}^n + \frac{\lambda^2(S_l+S_{l-1})}{2[S]_l}\Psi_{l-1}^n + \\ \left(2 - \frac{\lambda^2(S_{l+1}+2S_l+S_{l-1})}{2[S]_l}\right)\Psi_l^n - \Psi_l^{n-1}\end{aligned} \tag{4.5}$$

where $\lambda = ck/h$, and S_l is a grid function which consists of sampled values of the continuous function $S(x)$ at locations $x = lh$, where $[S]_l$ is an approximation to the continuous function $S(x)$ [Bilbao 09], and $[S]_l = \frac{1}{4}[S_{l-1} + 2S_l + S_{l+1}]$. There is also a stability condition that dictates that $\lambda \leq 1$, and should be chosen as close to 1 as possible.

Again this is the lossless case, and the fractional derivative terms introduced to Webster's equation must also be dealt with in the finite difference scheme and the approach taken is that of discrete time approximation of the fractional derivative terms, as detailed in [Bilbao 11, Mignot 09].

The pressure used for analysis here was extracted at the radiating end of the instrument. This could be an area of possible concern as the experimental results use radiated pressure as measured at a distance of one bell radius from the end of the tube, in the radiation field. However, because the model uses an isophase surface of the propagating wavefront, the actual final point in the simulation will be calculated at some distance, possibly of the order of one bell radius, outside the physical plane of the bell, and because of this it is not entirely unrelated to the experimental measurement point used.

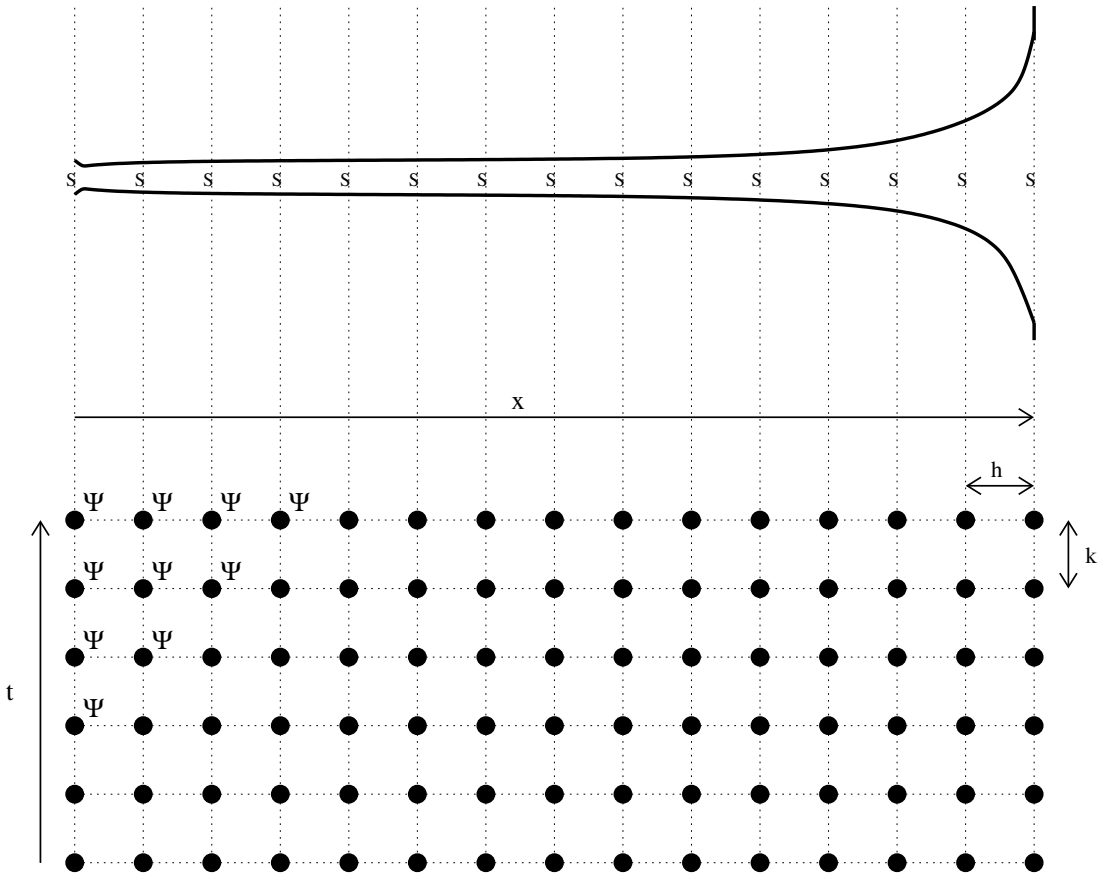

Figure 4.2: Profile of an acoustic tube and finite difference grid, where each point on the grid represents Ψ_l^n, the grid function, h is a grid spacing, k is a time step and S represents the location in the acoustic tube.

Sources of possible error within the computational model include:

- Lack of viscothermal losses in some results
- Location of radiated sound readout
- Correct lip model parameters

4.2.2 Model input parameters

The input parameters needed for the model are mainly taken from experimental data and include the bore profile of the instrument together with information about the reed (i.e. the player's lips). The reed information required includes the reed area, mass and resonant frequency, and also information about the pressure

in the oral cavity of the player. Values for the mass, damping, surface area and quality factor of the lips were estimated to allow the lip model to oscillate, with an attempt to calculate the mass and surface area values from experimental images of the lips.

Many of these parameters are time dependent and for this reason the instantaneous resonant frequency of the lips and the blowing pressure in the player's mouth are based on the experimental work presented in Chapter 3 for the model using the player input data. Examples of the instantaneous frequency during upward and downward slurs between the notes D_3 and D_4 are shown in Figure 4.3, together with the resonant frequency of the reed. The model presented here assumes that the lips of the player act as an 'outward-swinging door' as described in [Fletcher 99a]. The blowing pressure recorded in the player's mouth during a slur between D_3 to D_4 are shown in Figure 4.4, together with the simplified pressure profiles used as the input to the model.

In the case of the forced oscillation results, as discussed in Sections 4.3.1 and 4.3.2, the lossy instrument model is not coupled to the lip model but has a similar excitation method as used in the loudspeaker forced oscillation tests. The excitation signal used was a simple sine sweep which began with a period of steady frequency at the first resonant mode frequency and then swept linearly, over a specified time period, to the steady frequency of the second resonant mode in the transition. The results presented in Section 4.3.3 however, use the complete non-lossy simulation including lip model with the input parameters discussed above for mouth pressure and resonant lip frequency.

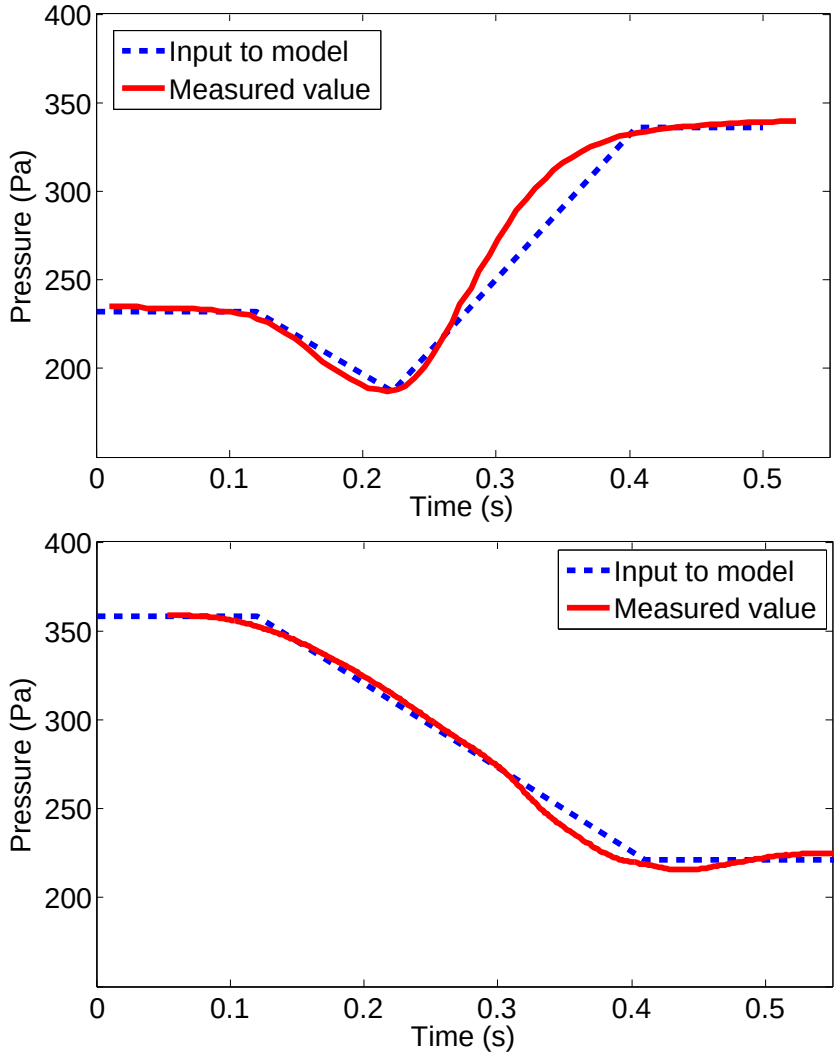

Figure 4.3: Pressure histories measured in the players mouth together with the simplified profile used as input to the model. **Top**: Horn upward slur from D_3 to D_4, transition time 30ms. **Bottom**: Horn downward slur from D_4 to D_3, transition time 30ms.

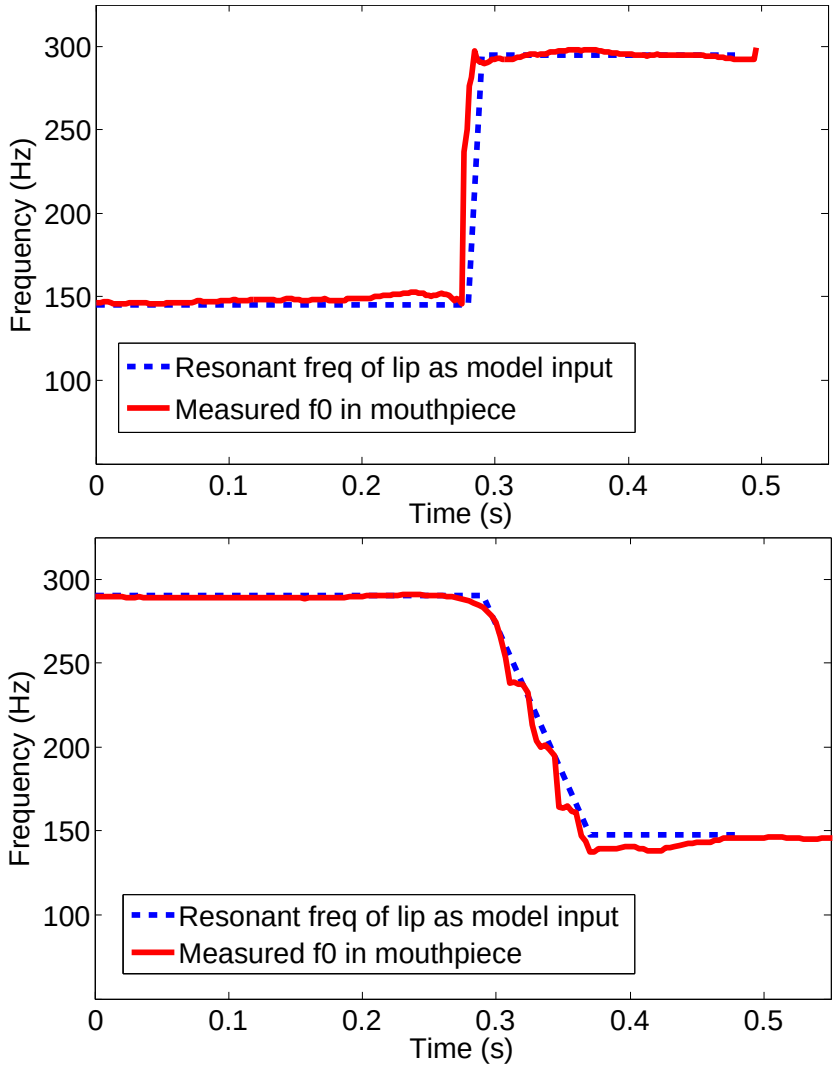

Figure 4.4: Instantaneous frequency of the pressure signal measured in the mouthpiece together with the resonant frequency of the lips used as input to the model **Top**: Horn upward slur from D_3 to D_4, transition time instantaneous i.e. within one cycle of the lips. **Bottom**: Horn downward slur from D_4 to D_3, transition time 8ms.

4.3 Results

4.3.1 Forced oscillation input - horn

All results presented in this section are concerning the Meinl & Lauber/Paxman baroque horn as played by Player B, the player who approaches lip-slurs with the technique in which the first note is stopped and the second started as quickly and smoothly as possible without attempting to catch the intermediate resonances. Figure 4.5 shows the results for an upward octave slur between the 4^{th} and the 8^{th} resonant modes, which corresponds to the notes D_3 and D_4. The player and loudspeaker results are those which have been discussed in detail in Chapter 3. Both the loudspeaker and the model input sine sweep signals were set to have a transition time of 50ms as the player data has a very short transition time.

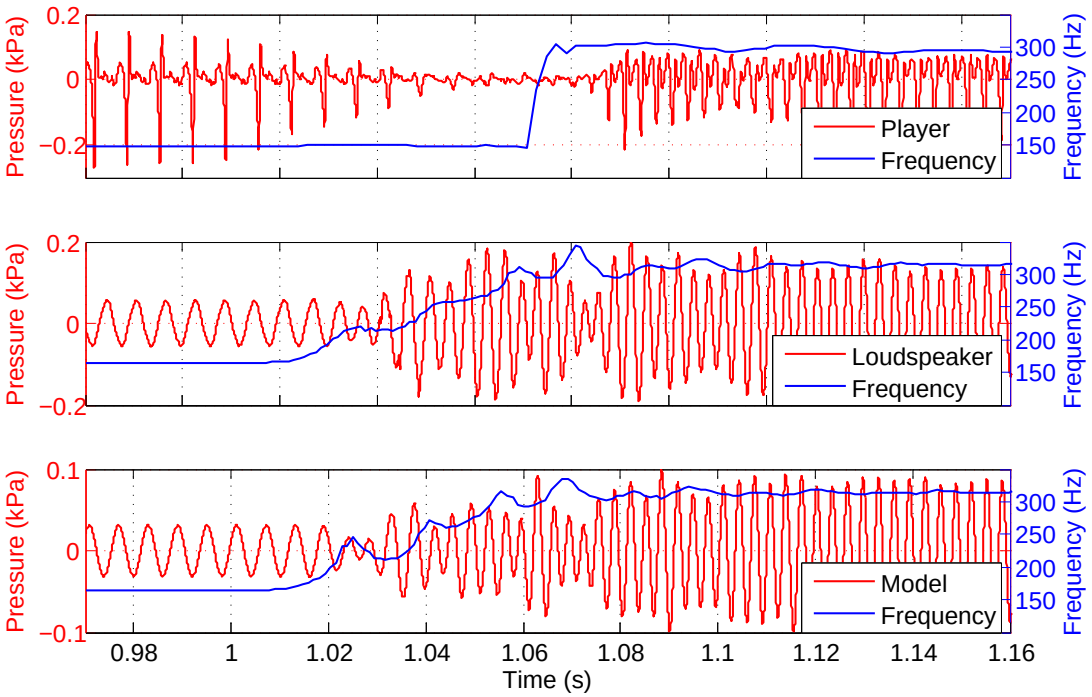

Figure 4.5: Lip-slur from D_3 to D_4, on the 'baroque' horn by Meinl & Lauber/Paxman, showing the radiated pressure signals. **Top**: Played slur. **Middle**: Loudspeaker forced oscillation **Bottom**: Modelled forced oscillation including losses. The loudspeaker test and model were set to have the transition take place over 50ms.

The instantaneous frequency of both the loudspeaker and modelled results do not replicate the quick smooth transition that is seen in the player results.

However, with a forced oscillation input being used as the excitation source in the model the results show very similar characteristics to the loudspeaker forced oscillation results; this is reassuring as it shows the model can replicate the frequency change in the radiated pressure shown in the real instrument, when using a similar excitation source that is not a human player. As with the loudspeaker results the modelled results show intermediate peaks in the instantaneous frequency; these are more pronounced in the model results. The model is showing that even at short transition speeds of 50ms, when there is feedback from the excitation source, there is some possible 'ringing' of the intermediate resonances in an upward slurred transition.

The corresponding downward slur results between the 8^{th} and the 4^{th} resonant modes are shown in Figure 4.6. In this case and all following results the loudspeaker and model input sine sweep transition times were set at 100ms.

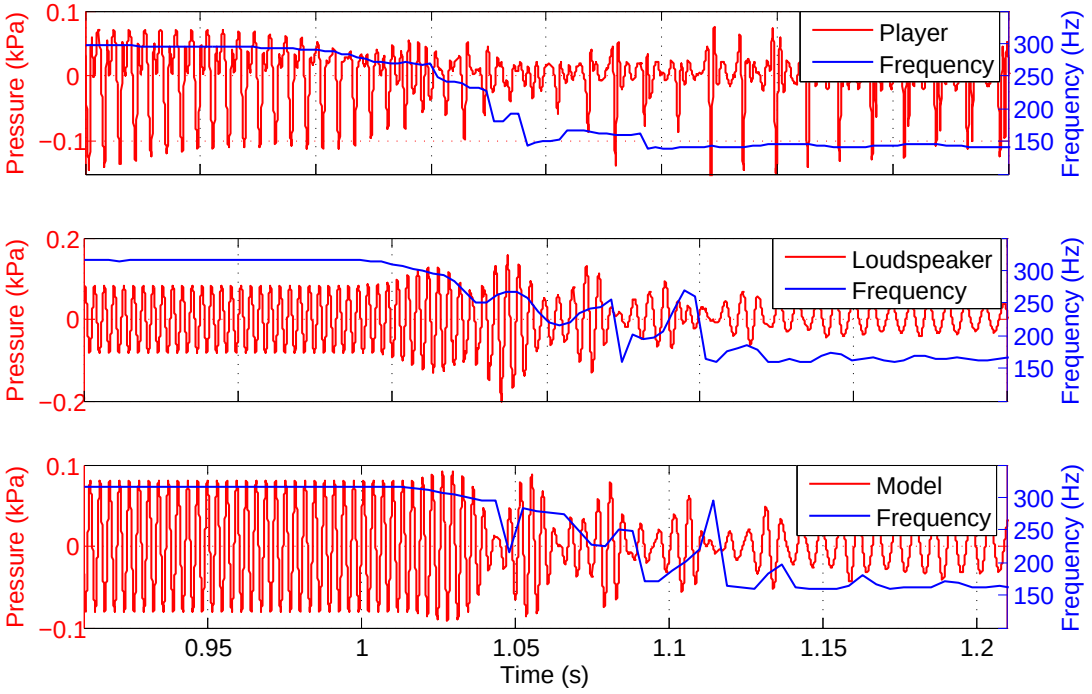

Figure 4.6: Lip-slur from D_4 to D_3, on the 'baroque' horn by Meinl & Lauber/Paxman, showing the radiated pressure signals. **Top**: Played slur. **Middle**: Loudspeaker forced oscillation **Bottom**: Modelled forced oscillation including losses. The loudspeaker test and model were set to have the transition take place over 100ms.

The results in the previous chapter have shown that in the lower register of the horn the characteristics of upward and downward slurs are very different. It was also shown in the previous chapter that the loudspeaker test results have closer instantaneous frequency characteristics in the downward slur than the upward; this is also true of the modelled results. The model results show an uneven decrease in frequency between the two notes, with evidence of intermediate frequency steps within the uneven transition. Again the modelled results do have peaks and troughs in similar places as in the loudspeaker test results.

As in Chapter 3 the octave between the 8^{th} and the 16^{th} resonant modes, in the upper register, has been explored. Figure 4.7 shows the upward slurred results between the notes D_4 and D_5.

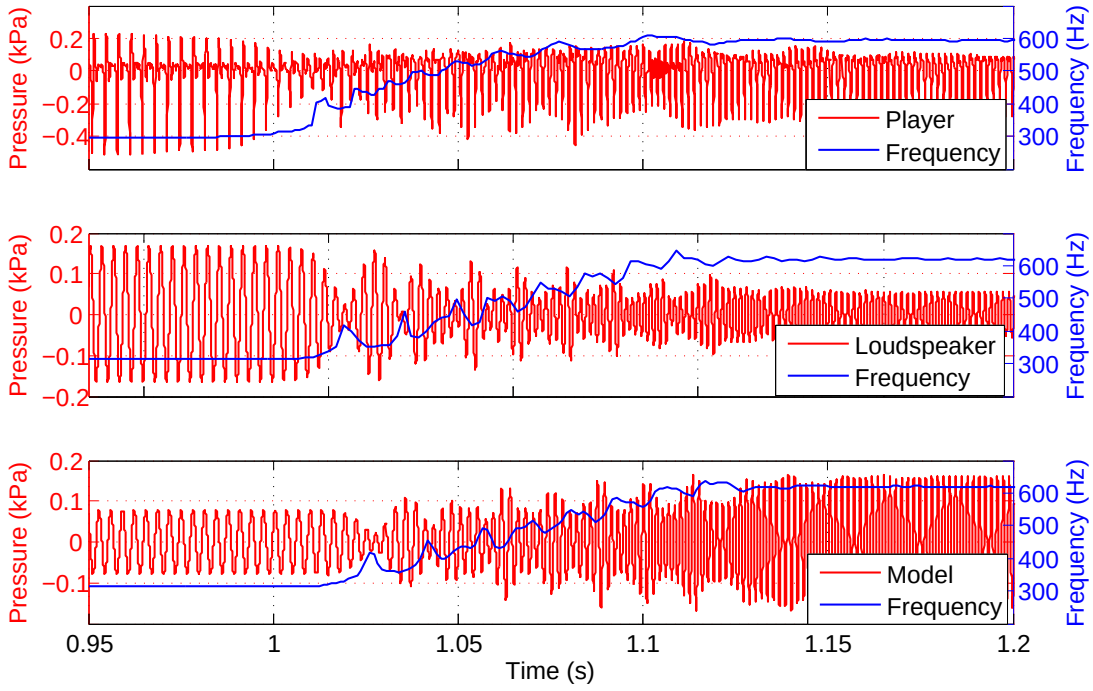

Figure 4.7: Lip-slur from D_4 to D_5, on the 'baroque' horn by Meinl & Lauber/Paxman, showing the radiated pressure signals. **Top**: Played slur. **Middle**: Loudspeaker forced oscillation **Bottom**: Modelled forced oscillation including losses. The loudspeaker test and model were set to have the transition take place over 100ms.

For this higher register upward transition it can be seen that the player, loudspeaker and model results show significantly similar instantaneous frequency results; there are a number of distinct peaks and troughs in each result which

correspond to the number of intermediate resonant modes between the 8^{th} and the 16^{th} mode frequencies. The intermediate peaks are more clearly defined in the loudspeaker and model results than in the player test. The player test pressure amplitude shows slight variation in amplitude during the transition, with a slight increase in amplitude several times during the transition. This variation in pressure amplitude is more clearly seen in the loudspeaker and model tests; there are a corresponding number of amplitude increases as intermediate resonances which could further indicate that there is a ringing effect of each resonance as the frequency sweeps over them.

Figure 4.8 shows the corresponding downward slur from the note D_5 to D_4.

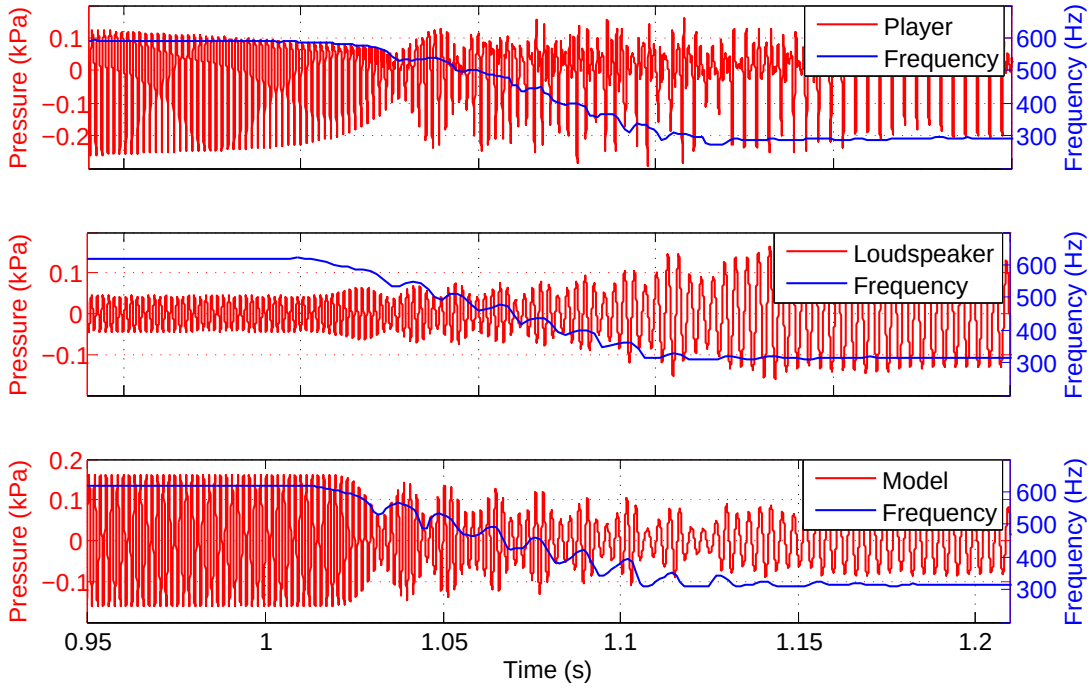

Figure 4.8: Lip-slur from D_5 to D_4, on the 'baroque' horn by Meinl & Lauber/Paxman, showing the radiated pressure signals. **Top**: Played slur. **Middle**: Loudspeaker forced oscillation **Bottom**: Modelled forced oscillation including losses. The loudspeaker test and model were set to have the transition take place over 100ms.

The downward slur in the upper register shown here shows very similar results to that of the corresponding upward slur; all three results show very similar characteristics, with the intermediate peaks and troughs being more well defined in the loudspeaker and model results, and the two forced oscillation results

showing strikingly similar frequency characteristics.

4.3.2 Forced oscillation input - trumpet

This modelling work uses the Smith-Watkins trumpet and compares forced oscillation results with those already presented in Chapter 3. Figures 4.9 and 4.10 show the results of the loudspeaker test and the model results of upward and downward octave transitions between the 4^{th} and the 8^{th} resonant modes of the trumpet, which corresponds to the notes B$\flat_4$ to B$\flat_5$ respectively.

It can be seen in both the upward and downward trumpet slurs that the modelled results compare favourably with the loudspeaker test results and show similar characteristics. It is interesting to note again that in the upward slur there is no evidence of any discernable intermediate resonant frequencies, in either the loudspeaker or the modelled results, during the transition and yet a large number of small peaks and troughs in the frequency results. The downward slur shows much of the same results but with careful inspection there is slight indication of three intermediate steps in the frequency which could correspond to the 7^{th}, 6^{th} and 5^{th} resonant modes of the instrument. The model results have verified that this slight evidence is not solely present in the loudspeaker trumpet test results.

These results broadly show that in the absence of a lip model, when the system is forced to oscillate with a simple linear sine sweep, the computational model replicates very closely the experimental results for both the horn and the trumpet. In this set of the results the model used includes the viscothermal loss model.

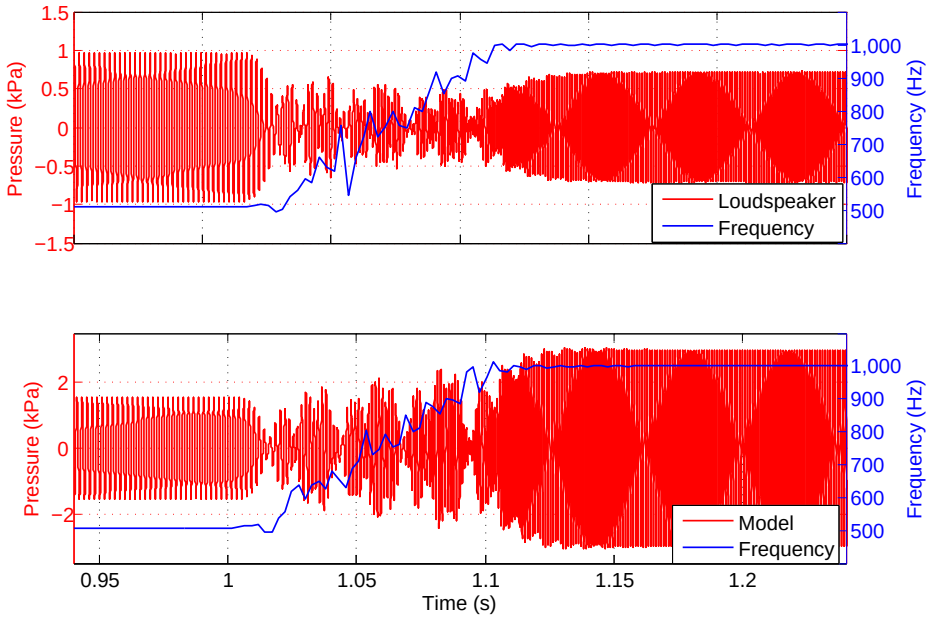

Figure 4.9: Lip-slur from B♭$_4$ to B♭$_5$, on the Smith Watkins trumpet, showing the radiated pressure signals. **Top**: Loudspeaker forced oscillation **Bottom**: Modelled forced oscillation including losses. The loudspeaker test and model were set to have the transition take place over 100ms.

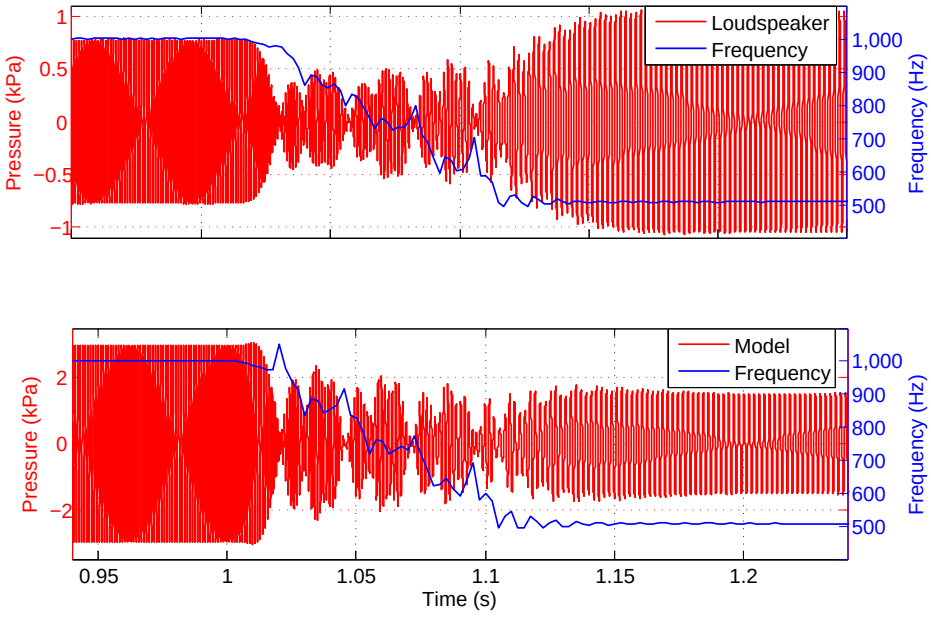

Figure 4.10: Lip-slur from B♭$_5$ to B♭$_4$, on the Smith Watkins trumpet, showing the radiated pressure signals. **Top**: Loudspeaker forced oscillation **Bottom**: Modelled forced oscillation including losses. The loudspeaker test and model were set to have the transition take place over 100ms.

4.3.3 Player pressure input

The results presented in this section were performed by Player B on the modern wide bore horn by Conn, with the player data having been previously discussed in Chapter 3. Figures 4.11 and 4.12 show respectively upward and downward lip-slurs between the 4^{th} and 8^{th} resonant modes of the horn, which correspond to the notes D_3 and D_4. The modelled results shown here have been calculated using the lossless computational model.

As discussed previously, the upward player test results show the pressure signal having a very small amplitude during the transition and a sharp change in frequency between the initial and final sounded notes. Unlike the player pressure signal, the modelled results show a significant pressure amplitude throughout the transition. A possible cause of this increased amplitude signal could be the lack of viscothermal losses in the model, causing there to be less dampening as the wave propagates through the instrument. As the resonant frequency of the lips increases, between the initial and final notes, the intermediate resonances will be excited in some way as the frequency sweeps past each in turn; it could be the case in the model that these intermediate resonances ring on for several cycles after they have been excited and hence create the larger pressure amplitude during the transition, again because there are no viscothermal losses modelled within the instrument. However, if this were fully the case it would be assumed that the instantaneous frequency result from the model output would show some signs of intermediate resonances ringing. The two peaks seen in the modelled results between 1.05s and 1.10s are not considered to be reliable as the pressure signal is very complex and aperiodic at this point meaning that the frequency analysis program has difficulty in ascertaining the correct fundamental frequency. However, the model does show a smooth and direct transition between the two notes as with the results of the human player.

The downward slur results show that for both the player and model results there is a similar level of pressure amplitude shown during the transition. The instantaneous frequency shows similar behaviour to that seen in the modelled upward slur, there is a quick and relatively smooth frequency transition between the two notes; the dip in the frequency seen around 1.12s is again thought to be unreliable. There are no intermediate frequency steps seen in the modelled results like those seen in the player results, this could be partially down to the

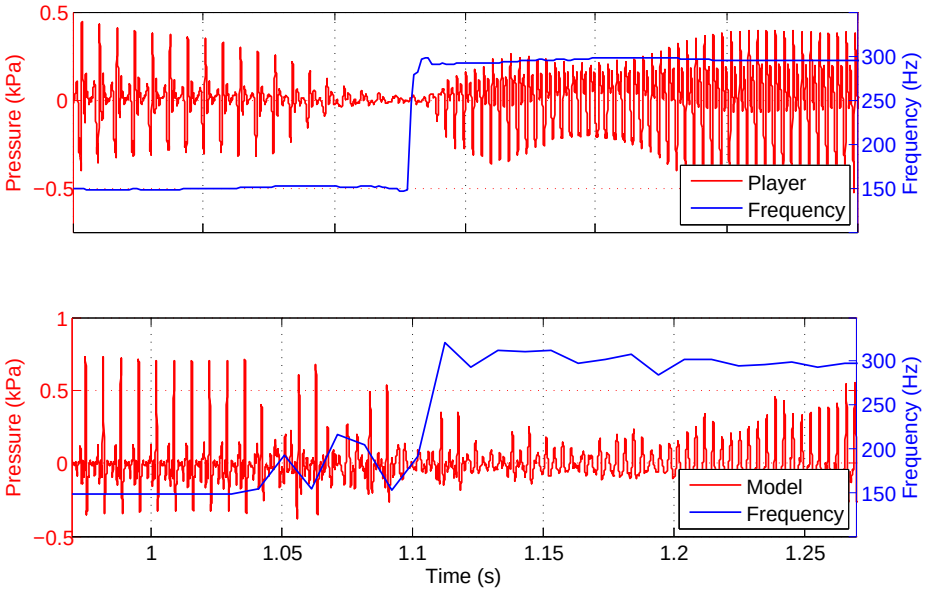

Figure 4.11: Lip-slur from D_3 to D_4, on the wide bore horn by Conn, showing the radiated pressure signals. **Top**: Player test **Bottom**: Modelled results excluding losses.

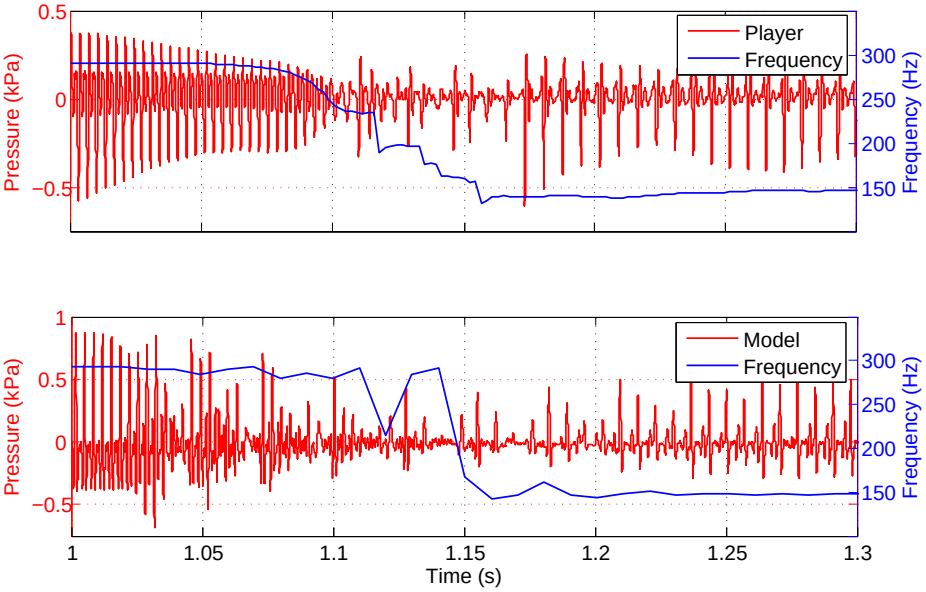

Figure 4.12: Lip-slur from D_4 to D_3, on the wide bore horn by Conn, showing the radiated pressure signals. **Top**: Player test **Bottom**: Modelled results excluding losses.

model input frequency sweep. In the player results presented in Chapter 3 the mouthpiece pressure signal showed significant steps in the frequency; a simplified version of this was used as the input to the model which resulted in the resonant frequency of the lips sweeping linearly between the two notes.

4.4 Conclusions

A simple one dimensional, finite difference, time domain computational model has been presented and used to model slurred transitions on both the horn and trumpet; in the case of the horn these results have been compared with player data which was presented in Chapter 3.

When excited by a linear sine sweep between two notes, and not involving a lip model, the simulation showed strikingly comparable results to the experimental forced oscillation results; both the pressure and frequency signals showed very similar characteristics during the transition to the comparable experimental results. It has already been shown that in the upper register of the horn the forced oscillation results compare much more favourably with the player results, as is true for the model results shown here. These results show that the behaviour within the instrument, when not concerned with the complex lip model, is modelled well.

When the model uses simplified player data as an input, incorporates the lip model but does not include viscothermal losses, the results are not quite as favourable when compared with the player results. Although the sound output does sound convincing to the listener, the pressure amplitude and instantaneous frequency do not show as similar characteristics, to the player results, as possible; this could be for a number of reasons. The lack of viscothermal losses is thought to be a major factor as these are important. It is not clear yet if the point at which the radiated sound readout is taken is of major importance but could be a contributing factor. Lastly, the lip model parameters are many, and difficult to define, which could also contribute to the less similar results. However, a new time domain model has been implemented with encouraging first results of such transients.

Chapter 5

Extreme high notes

This chapter will explore the high register of the trumpet, where specialist high note players can sound notes above the normal playing range. Using a human player the motion of the player's lips will be examined, with the use of high speed filming of the lips under playing conditions. The transfer function between the mouthpiece and radiation field of the trumpet will also be examined with the excitation being produced by a forced oscillation source.

5.1 Introduction

The extreme high notes under consideration here are mostly used in jazz trumpet playing, and generally only possible for highly skilled players. There is much controversy among players about why and how these notes are able to be sounded above the expected range. One theory is that the lips of the player are vibrating at a sub-frequency of the perceived note, and because these notes are only possible at high dynamic levels that the second harmonic is becoming dominant. Some players believe that nothing peculiar is happening when playing these high notes, and that it is simply a progression from the normal playing range that only skilled players can achieve. The book "A new approach to altissimo trumpet playing" [Lynch 84] suggests practise methods for achieving extreme high notes, which include embouchure control, pressure control, air flow control, playing position and even the player's attitude towards these notes.

Instrument manufacturers are not oblivious to the fact that players want to know how to play these notes and if certain instruments are more likely to

produce these notes. Smith Watkins trumpets are known for having a set of interchangeable lead pipes that make the instrument better suited to different types of playing [SmithWatkins 13]. With the correct instrument, leadpipe and mouthpiece combination a Smith Watkins trumpet is said to be easier to sound extreme high notes on, as with other specific instruments.

In general, low frequencies reflect strongly from the open end of a trumpet and it is this process which is responsible for the formation of resonances and anti-resonances, depending on whether the reflection is in phase or out of phase, with the forward going wave, for the frequencies under consideration. When the player buzzes the lips close to the frequency of one of the input impedance peaks it can create a strong standing wave. Should the lips be buzzed at a frequency half way between peaks a convincing note will not be produced, but rather the note is likely to change during the initial transient into a note at one of the nearby peak frequencies. Players sometimes refer to the frequencies or pitches where they can play notes as 'slots'.

It is the cutoff frequency of an instrument that dictates the frequency above which the sound is radiated freely to the environment, and not reflected back down the instrument to produce resonances [Fletcher 98]. In brass instruments the cutoff frequency is primarily determined by the mouth radius. In a simple model the frequency for which $ka = 2$, where $k = \omega/c$, gives the cutoff frequency as:

$$\omega = 2c/a \tag{5.1}$$

where a is the radius of the horn mouth and c is the speed of sound in air [Fletcher 98]. In the more complex real case the cutoff frequency also depends on the shape and flare rate of the bell [Benade 74]. This explains why the number of strong input impedance peaks in brass instruments is limited. Very high notes on brass instruments are therefore expected to involve very little of the energy input to the mouthpiece being reflected back from the bell. This in turn implies that any note can be sounded by the lips, but only weakly. There will be a region in between the two extremes in which highly skilled players playing carefully designed instruments can play extremely high notes in spite of linear acoustics predicting a very small level of reflection of energy from the bell.

5.2 Instrument and mouthpiece combination

The trumpet used for this study was a modern instrument by Smith Watkins, and was coupled with a commercially available Kelly 'screamer' mouthpiece, a very shallow cup mouthpiece, injection moulded from an undyed polycarbonate. This combination of instrument and mouthpiece is typical of that used by trumpet players who specialise in playing in the highest register of the instrument. The acoustic input impedance of this instrument and mouthpiece combination is shown in Figure 5.1, as measured using the commercially available Brass Instrument Analysis System [BIAS 13]. This figure shows a notional cut-off frequency at around the 12^{th} resonant mode (corresponding to the note F_6). Close inspection of the impedance curve above this frequency reveals that there are small resonances at the frequencies we would expect for the upper modes, but that these are much less well defined. It is not clear if these small peaks are sufficient for an experienced player to identify as useful 'slots', of if there are other effects which provide slots for extreme high notes. The 16^{th} resonant mode (corresponding to the note C_7) is known by trumpeters as a 'super C', this is because it is at the upper limit of the trumpet range and therefore not as easy to play as notes in the lower registers; it is even possible to play some notes higher than this 'super C'. Such notes are most commonly used in jazz playing and can normally only be achieved by very skilled players.

5.3 Transfer function

In this study the transfer function is used to compare the pressure signal measured at the mouthpiece entrance and the pressure signal radiated from the bell of the trumpet, in the frequency range of interest. Here we measure the effective transfer function which is defined as:

$$T_{eff} = p(out)_{rms}/p(in)_{rms} \tag{5.2}$$

where $p(out)_{rms}$ is the RMS pressure measured in the radiation field, and $p(in)_{rms}$ is the RMS pressure measured at the mouthpiece entrance. A full explanation of theory surrounding the transfer function is presented in Chapter 2, Sections 2.5.6 and 2.5.7.

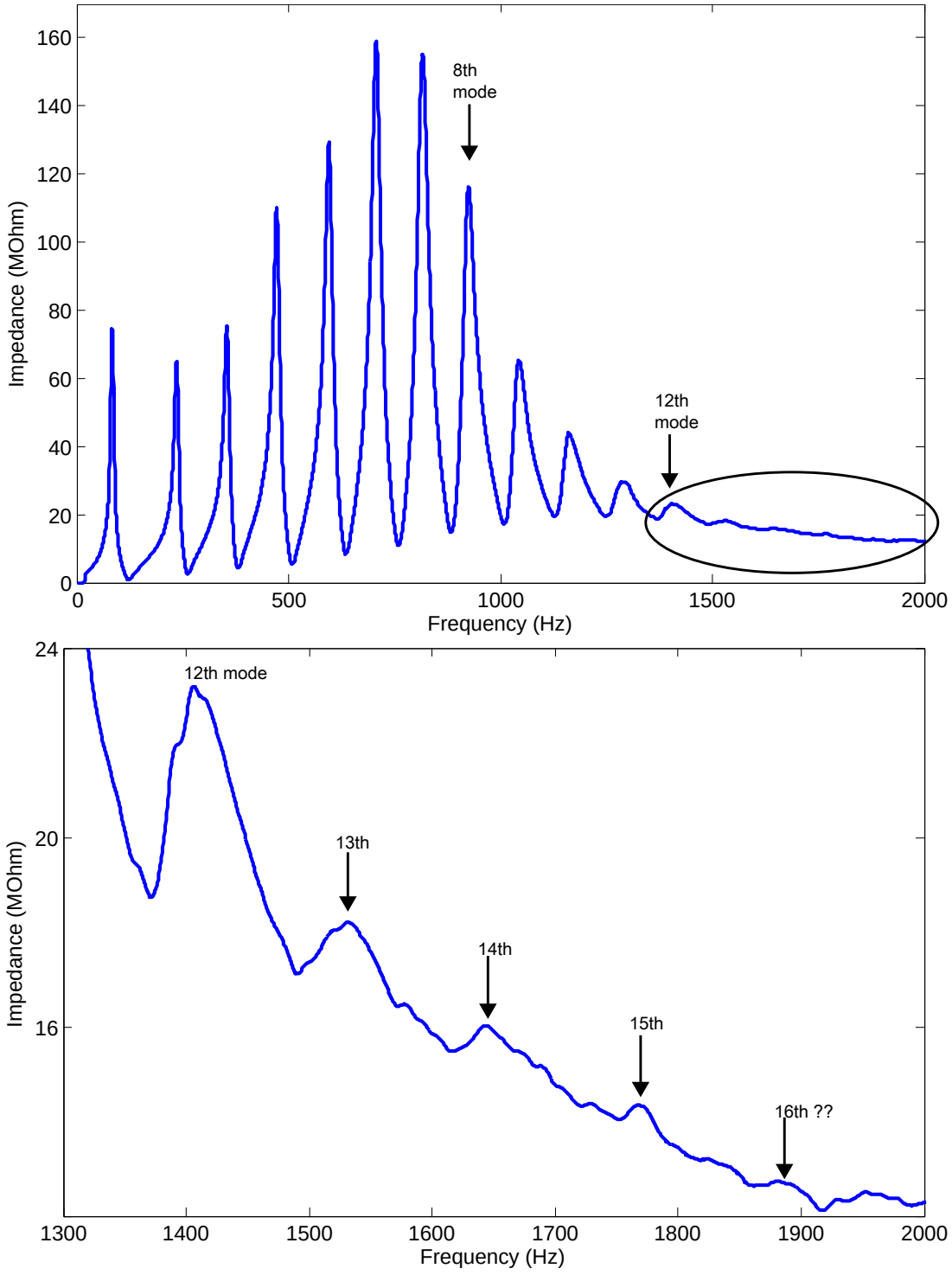

Figure 5.1: Input impedance of Smith Watkins trumpet and Kelly 'screamer' mouthpiece combination as used by specialist high register players.**Top**: Full input impedance **Bottom**: Zoomed section of input impedance from the top figure, showing small peaks/ shoulders at the frequencies of the upper resonant modes.

5.3.1 Experimental technique

The transfer function setup was driven by a JBL 2446H horn loudspeaker driver. The input signal was a 10s linear sine sweep, sweeping over the frequencies 900Hz to 2500Hz. The input pressure was measured using a PCB 106B microphone which was located in a cylindrical coupler that allowed the mouthpiece to be connected to the loudspeaker driver. The radiated pressure was measured on axis, at a distance of one bell diameter from the bell end, by a Bruël and Kjær 4192 pressure-field microphone. Recordings of the microphone signals were made at a sample rate of 51.2kHz, giving a frequency resolution of 0.1Hz, using a Labview [National Instruments 13] program, written and developed by Adam Apostoli at the University of Edinburgh. The resulting pressure signals were split into sections of 1000 samples for analysis, and the transfer function calculated in MATLAB. The transfer function of each section of the sweep was calculated by taking the ratio of the root mean square (RMS) pressures in the radiation field and at the mouthpiece. A photograph of the experimental setup can be seen in Figure 5.2.

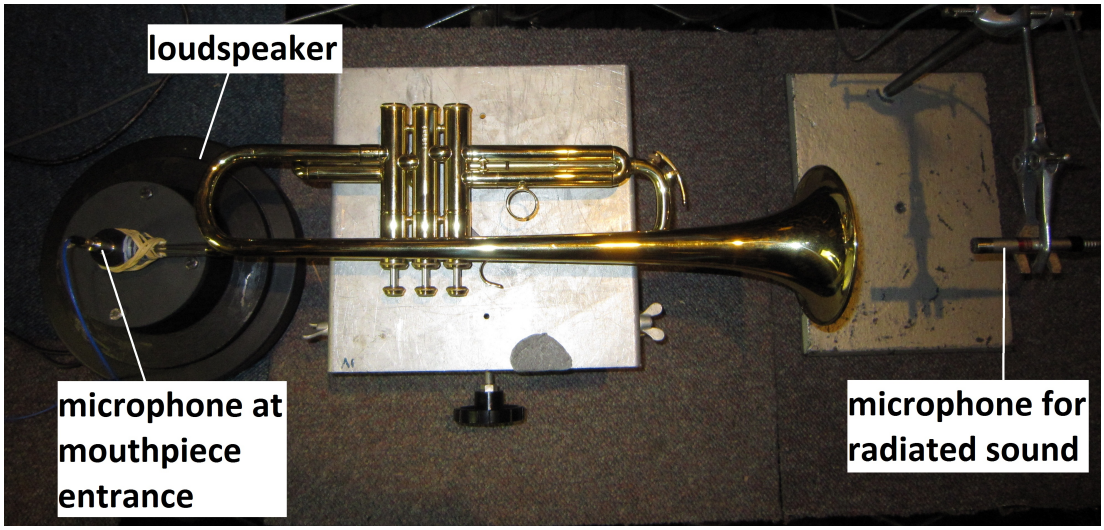

Figure 5.2: Photograph of trumpet transfer function experimental setup, showing microphones measuring the pressure at the mouthpiece and outside the bell.

5.3.2 Results

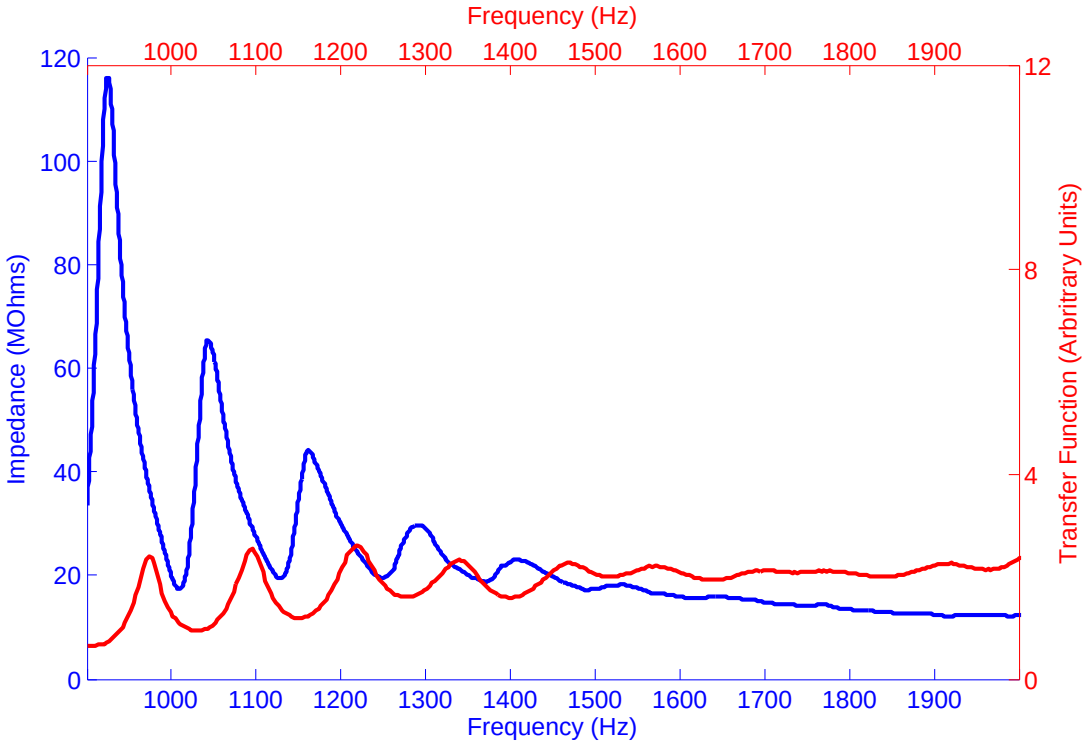

Figure 5.3: Transfer function between mouthpiece and radiation field and input impedance for trumpet and mouthpiece combination used by specialist high register players.

We would expect the dips in the transfer function curve to approximately match the peaks in the input impedance; this is because the ratio of the radiated pressure, to the pressure at the mouthpiece entrance, will be smallest when the forward going wave is reflected strongly at the end of the instrument, and this is the situation that correspond to peaks in the input impedance. Figure 5.3 shows the transfer function and input impedance curves plotted together. The frequency of the transfer function dips are slightly lower than the frequency of the peaks in the input impedance curve. We can attribute this reduction in frequency to the effects of the microphone cavity which effectively increases the volume of the mouthpiece, and possibly temperature differences between measurements. When examining the input impedance in Section 5.3.1 it was seen that there was a notional cut-off frequency around the 12^{th} resonant mode; this can also be seen in the transfer function results but to a lesser extent. The dips in the transfer

function that can be seen corresponding to the 13^{th}, 14^{th}, 15^{th}, 16^{th} and 17^{th} resonant modes are more significant than the corresponding peaks in the input impedance.

Figure 5.4 shows the transfer function results for the trumpet as presented in Figure 5.3, and show the ratio of the RMS pressure signal in the radiation field and the RMS pressure measured at the mouthpiece entrance, in the loudspeaker coupler. Because of the nature of the transfer function the dips observed in the curve, marked by arrows in the figure, correspond to the resonances of the instrument. Therefore, it can be seen that the transfer function curve confirms that there are weak resonances at least up to the 17^{th} mode with this trumpet and mouthpiece combination.

5.4 Visualisation of the lips

To gain a better understanding of the mechanics of the player's lips when playing in this high register, a high speed video camera was used to focus on the lips through a transparent mouthpiece. As mentioned at the beginning of this chapter, one theory is that the lips could be vibrating at a different frequency from the playing frequency that is perceived. Through visualisation of the player's lips the frequency at which they are oscillating can be measured quantitatively.

5.4.1 Experimental technique

These experiments were carried out by a professional freelance trumpeter who specialises in very high note jazz playing.

The mouthpiece used was the same as for the transfer function experiments, a transparent Kelly 'screamer' mouthpiece. To allow better optical access to the player's lips some material was machined away from the outside of the mouthpiece cup, this made the cup walls significantly thinner and so reduced optical distortion. A photograph of the modified mouthpiece is shown in Figure 5.5. The brass microphone coupler can also be seen in this photograph, located in the mouthpiece backbore.

The experimental setup is shown in Figure 5.6. The setup is similar to that described in Section 3.2.2; a high speed camera (Vision Research Inc. Phantom v4.1 camera), set to take 10,000 frames per second and was focused on the player's

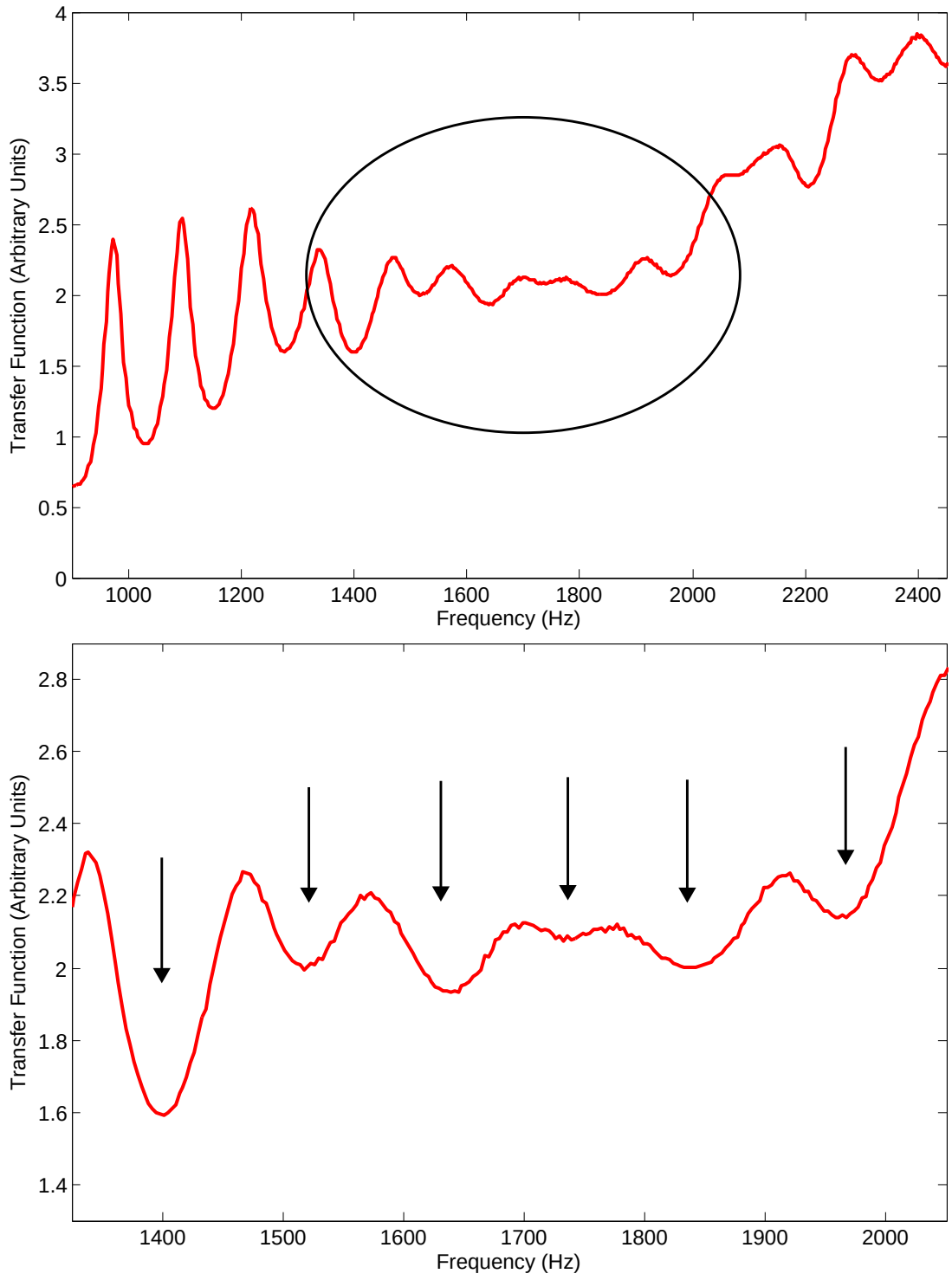

Figure 5.4: Transfer function between mouthpiece and radiation field for trumpet and mouthpiece combination used by specialist high register players. **Top**: Full transfer function **Bottom**: Zoomed section of transfer function from the top figure, showing dips at the frequencies of the upper resonant modes.

Figure 5.5: Transparent Kelly 'screamer' mouthpiece used for visualisation of the lips, the outside of the mouthpiece cup has had some material machined away to make the wall of the cup thinner to allow better optical access.

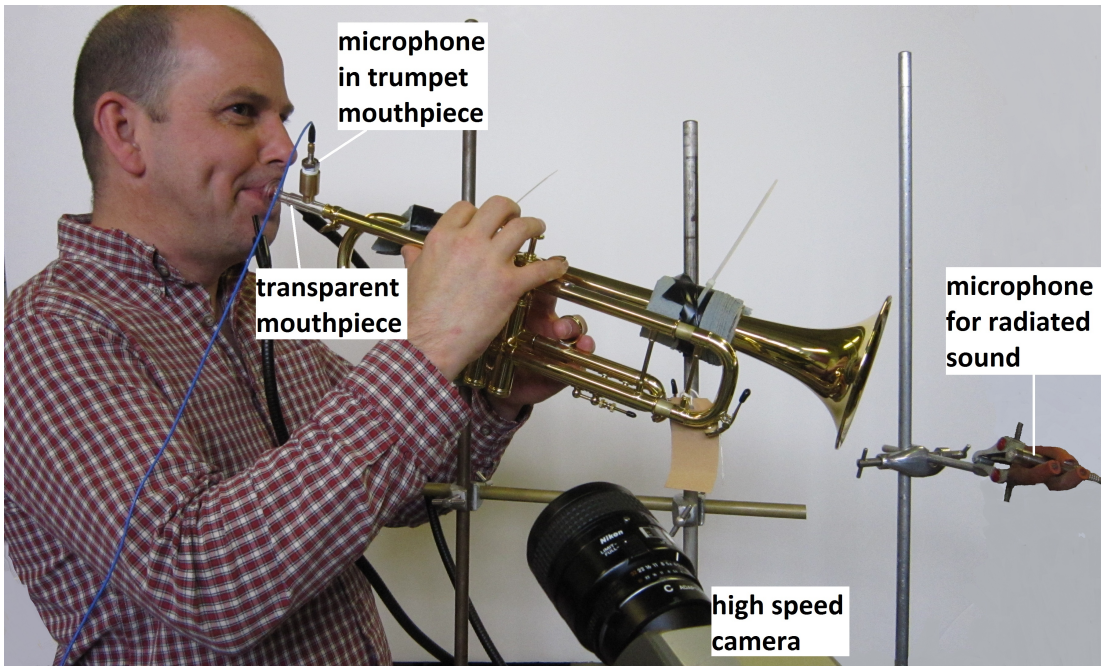

Figure 5.6: Photograph of experimental setup for high speed filming of the player's lips, showing microphones in the mouthpiece and outside the bell.

lips. Necessary additional illumination was provided by a fibre optic 'cold' light source. A 106B PCB Piezotronics dynamic pressure transducer was used to measure the pressure in the backbore of the mouthpiece. The radiated sound from the bell was measured using a Bruël and Kjær 4192 pressure-field microphone, located one bell diameter from the plane of the bell of the trumpet. Signals from both transducers were fed to a Bruël and Kjær PULSE system for data acquisition and synchronisation with the high speed video data.

Each frame from the high speed film was 'binarised' such that the open area of the lips can be identified and isolated from the rest of the image. Despite the inevitable image distortion resulting from a combination of refraction through the wall of the mouthpiece together with the indirect camera angle, a pixel count of the open area in each frame provided a qualitative assessment of the movement of the lips.

5.4.2 Results

The open area of the player's lips as a function of time, for the 8^{th} and 12^{th} resonant modes, corresponding to the notes $B\flat_5$ and F_6 respectively, can be seen in Figure 5.7. It can be seen clearly from these results that the lips are opening and closing once per cycle and that there are no sub-harmonic or other unusual phenomena occurring for notes played in the high register.

For the 8^{th} resonant mode the time between adjacent peaks in the lip opening area is approximately 1.1ms, which relates to a frequency of $\sim$ 909Hz. The time between adjacent peaks for the 12^{th} resonant mode is approximately 0.75ms, which gives a lip opening frequency of $\sim$ 1333Hz. Both these notes are slightly flat but there is no disputing that the lips are opening and closing periodically at the resonant frequency of the modes being sounded by the player.

There is not a result shown here for the trumpets 'super C' note, which corresponds to a $B\flat_6$, as the player found the experimental setup slightly uncomfortable and was unable to sound notes any higher than are shown here. The results in Figure 5.7 do however show notes in the upper end of the trumpet range.

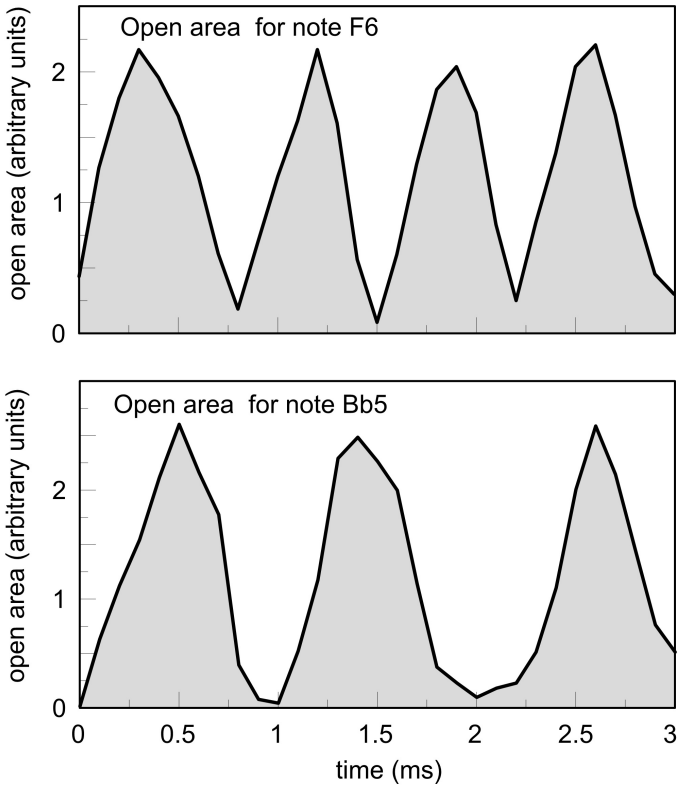

Figure 5.7: Open area as a function of time for the 8^{th} and 12^{th} resonant modes of the trumpet and mouthpiece combination used by specialist high register players.

5.5 Conclusions

This chapter has presented two experimental techniques used to explore the extreme high notes on the trumpet, above the normal playing range. The transfer function measurements have shown that there are distinct dips in the results, which correspond to resonances of the instrument, up to and possibly beyond 2000Hz. The high speed filming of the lips has shown clearly, in the experiments presented here, that the lips do indeed open and close periodically at the expected frequency of the note being sounded. The notes played in this section, however, are not as high as is able to be played on the trumpet, but does imply that the situation would be similar at a slightly higher frequency.

Chapter 6

Cylindrical tubes as a simple brass instrument

This chapter will explore the relative significance of the effects of nonlinear wave steepening and viscothermal wall losses in brass instruments using the simplified case of cylindrical tubes. Using a forced oscillation input and cylindrical tubes of varying diameter, comparable to those of many orchestral brass instruments, experimental results will be compared with those produced using a computational simulation based on weakly nonlinear propagation theory.

6.1 Introduction

The bore profile of a brass instrument is one of the major factors in determining the playing characteristics of a particular instrument. Different instruments that are pitched in the same sounding key can have very different characteristic timbres and this is mainly due to the differences in bore profile [Gilbert 07, Myers 07]. The different timbres of these instruments can be less apparent at low dynamic levels, with instruments in the same sounding key sounding similar. When played at higher dynamic levels, energy is transferred into the upper harmonics which leads to a 'brassy' sound. The spectral enrichment is caused as the pressure wave travels along the instrument bore and nonlinear wave steepening occurs because of the high dynamic levels, which alters the harmonic content of the sound [Beauchamp 80, Beauchamp 82, Hirschberg 96]. However, the extent of spectral enrichment can vary with bore profile, hence causing instruments to

have significantly different characteristic timbres. Instruments, such as trumpets and trombones, which have a large proportion of cylindrical tubing, show more spectral enrichment than instruments such as euphoniums and flugelhorns, whose bore profile expands steadily throughout a significant proportion of the tubing.

Nonlinear wave steepening is not the only factor affecting the harmonic content in brass instruments while being played. Viscothermal losses in the boundary layer at the tube wall act to dissipate energy at all frequencies but are frequency dependent, and therefore act to dissipate the high frequency energy more than the low frequencies. This means that the high frequency components resulting from the nonlinear wave steepening will lose more energy because of the viscothermal losses. Although the boundary layer thickness is typically very small it will have a different effect in different diameter tubes. The viscothermal wall losses are likely to have a larger effect in small diameter tubes than in larger diameter tubes because the boundary layer occupies a larger percentage of the internal area of the tube [Fletcher 98]. The theory surrounding this topic is discussed in Chapter 2, Section 2.5

6.2 Experimental Method

The experimental approach taken in this study was to use a specifically chosen set of cylindrical tubes, whose lengths and diameters are typical of those found in trombones. To these tubes a sine wave of fixed frequency and varying amplitude was injected; and with the use of internal microphones and an external microphone, the way in which the transfer function and spectral centroid vary as the amplitude is increased was explored.

6.2.1 Cylindrical Tubes

All tests were carried out in an anechoic chamber. Five cylindrical tubes were used, each with length 2.96m and with bore diameters 6mm, 8mm, 10mm, 12mm and 14mm. These diameters were chosen as 14mm is a typical slide bore diameter for a modern orchestral tenor trombone, and 10mm slide diameters can be found in some nineteenth-century French trombones. While the 6mm diameter tube is unrealistically narrow for a trombone, it was chosen to explore the effect of viscothermal losses in a tube where they are very significant, see Chapter 2,

Section 2.5.6. All five tubes were stainless steel with a wall thickness of 2mm, manufactured to ASTM A269/A213, and with uniform, semi-polished surface finish on the inside wall. The tubes were divided into 3 sections to accommodate housing for various microphones to allow the pressure of the wave inside the tube to be measured at different points along the tube length. The sectioning of the tubes is shown in the schematic Figure 6.1.

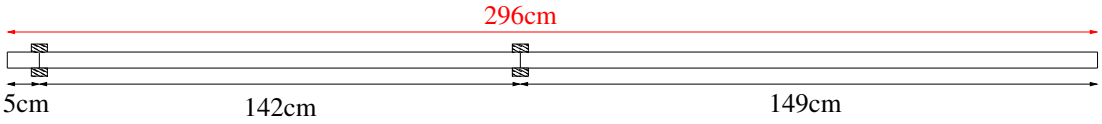

Figure 6.1: Schematic showing the sectioning of all 5 tubes.

6.2.2 Experimental Setup

A 106B PCB Piezotronics dynamic pressure transducer was used to measure the pressure at the entrance to the tube. To measure the pressure within the tube, Bruël and Kjær 4938 1/4-inch pressure-field microphones were used; these were located a short distance from the entrance - 0.05m in, and close to the mid point of the tube - 1.47m in. The radiated sound was measured using a Bruël and Kjær 4145 1-inch free-field microphone at a distance of 0.2m on axis from the exit of the tube.

The experimental setup and placement of the four microphones is shown in Figure 6.2.

The 1/4-inch microphones, measuring the pressure signal within the tube, were housed in brass couplers as shown in Figure 6.3. These couplers allow the microphones to be inserted so that the diaphragm is nominally flush with the inner tube wall and causes as little perturbation to the wall surface as possible. To verify that the acoustic reflections were not significant in the tube due to these couplers, the Brass Instrument Analysis System [BIAS 13] was used to gain an input impulse response which is shown in Figure 6.4. This figure shows that the only reflection in the tube comes from the termination at 2.96m, and that the joints between sections are continuous and do not introduce any other points of reflection.

The tubes were excited by a JBL 2446H compression driver producing a sine wave input signal. The input sine wave pressure amplitude was increased from

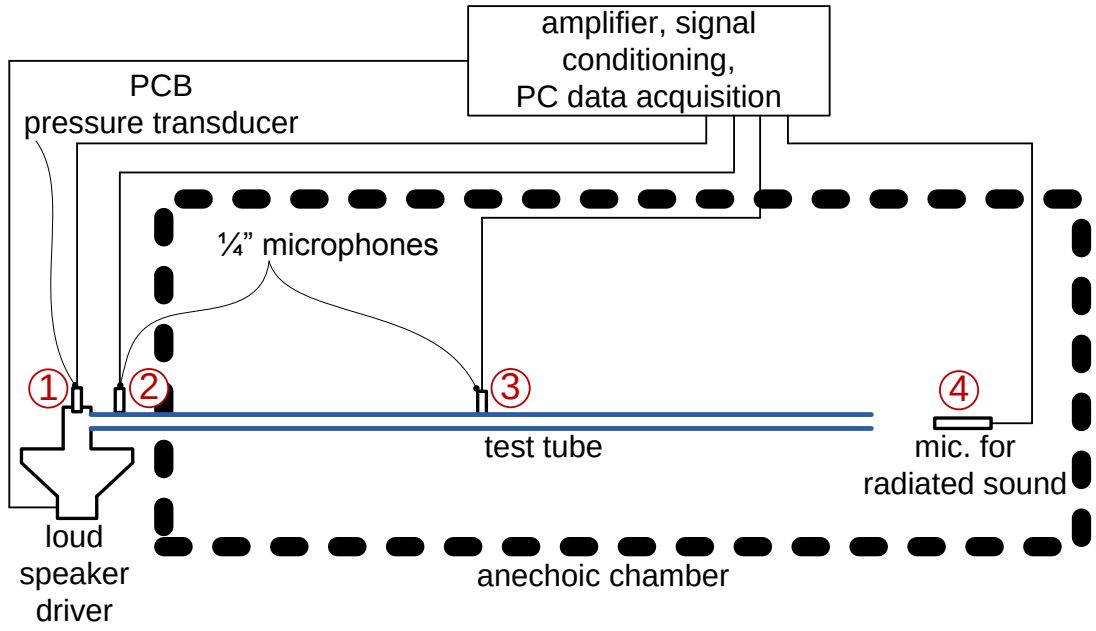

Figure 6.2: Schematic of cylindrical tubes experimental setup. Pressure measured at the four labelled locations 1-4, the distances between microphone positions can be seen in Figure 6.1.

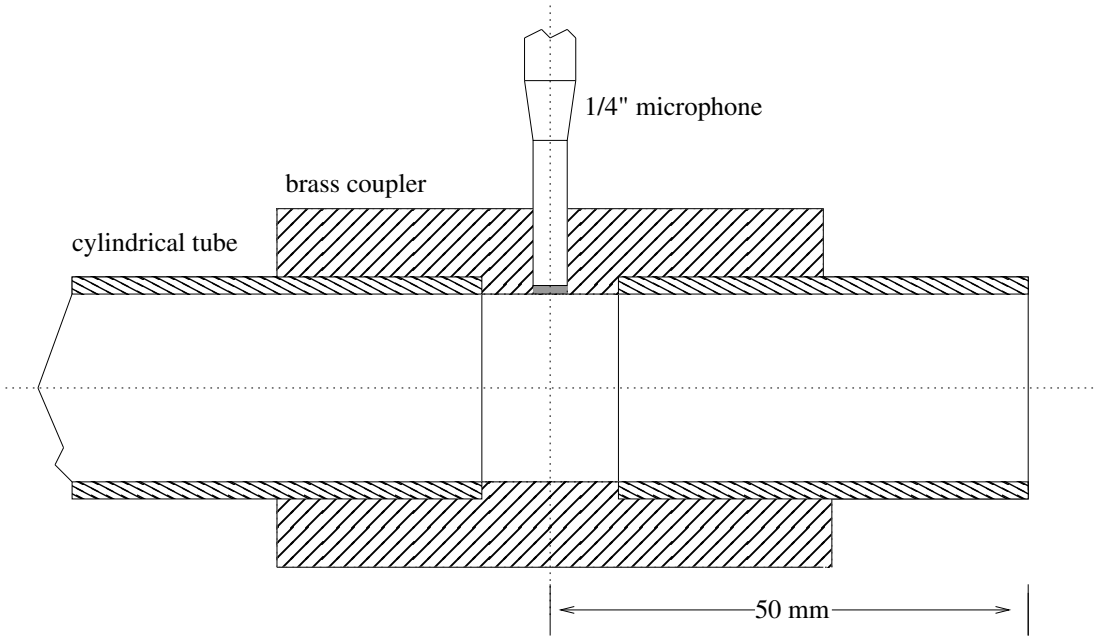

Figure 6.3: Schematic of brass coupler design, housing the 1/4-inch microphones.

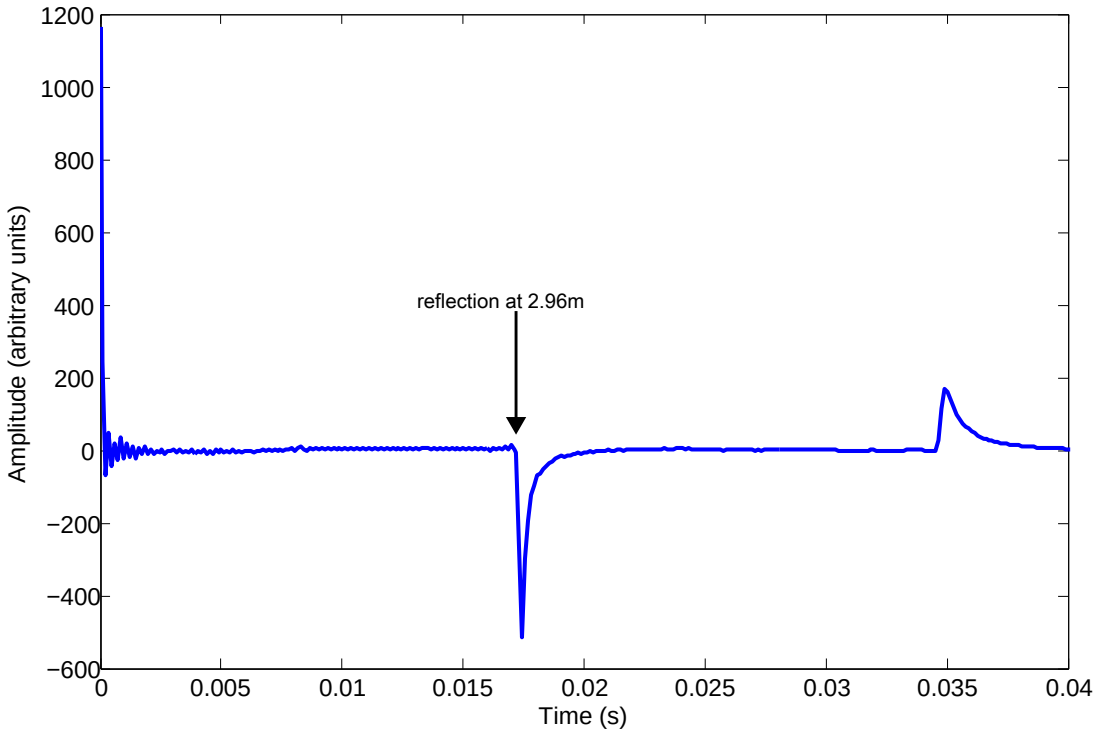

Figure 6.4: Input impulse response curve for the 10mm diameter tube showing a round trip time corresponding to a tube length of 2.96m.

zero to a maximum value, determined by the limit at which distortion by the loudspeaker could be observed in the microphone signal. The sine wave amplitude sweeps were each of 5s duration and the frequency of the sweep was chosen for each tube independently.

6.2.3 Data acquisition

A computer using a Labview [National Instruments 13] program, written and developed by Adam Apostoli at the University of Edinburgh, was used for the creation of the input signal for the loudspeaker and also data acquisition. The program allows the user to determine the type of sweep produced - amplitude or frequency, the sampling frequency, duration of signal, and frequency. The sampling frequency used was 100,000Hz. The four microphone signals were passed through appropriate signal conditioning amplifiers and then taken as inputs to the computer and Labview program which simultaneously recorded the 4 microphone signals.

6.2.4 Choice of frequency of amplitude sweep

The frequency at which the amplitude sweeps were conducted was chosen to correspond to a minima of the transfer function, $T14$ (the ratio between the root mean square [RMS] pressure measured by microphone 4, in the radiated field 20cm from the tube exit on axis, and the RMS pressure measured by microphone 1 at the tube entrance). A minimum in $T14$ occurs when the wave reflected from the open end arrives at the input in phase with the forward going wave and hence lies approximately on a resonant frequency of the tube - the 13^{th} resonant mode was chosen since this was at a pitch which was (just) playable on a trombone, but sufficiently high for the speaker driver to sound at an adequately high dynamic level. The pressure recorded by microphone 1, $P1$, is the sum of the forward and backward going waves at this measurement point. At a resonant mode of the tube, and hence a minimum of $T14$, $P1$ will be approximately twice the pressure amplitude of the forward going waves, P_+. This means that for a given $P1$, there will be a constant P_+ at the input for all of the tubes. If it were the case that the measurement frequency was not tuned to a resonant mode of the individual tubes, and each measurement was conducted at the same frequency it is unlikely that for a given $P1$ the forward and backward going waves will be exactly in phase at the entrance to the tube. When the forward and backward going waves are not in phase at the microphone position it is not known what the pressure amplitude of P_+ is. This of course is not strictly true - both the forward and backward going wave, P_+ and P_- respectively, are subject to the viscothermal losses within the tube and therefore $P1$ will not be exactly twice P_+. However, using a frequency corresponding to a minimum of $T14$ is the closest to this ideal situation as is possible. In the case of comparing the experimental results with the simulation results, it is not critical that the values of P_+ are known as the simulation produces a value of $P1$, i.e. $P1 = P_+ + P_-$, which can be compared directly to the experimental values of $P1$.

Figure 6.5 shows $T14$ over the frequency range 700-800Hz for the 14mm diameter tube with an air temperature of 15 °C. It can be seen here that the minima and maxima are not uniformly 'sharp'; the maxima peaks show a much sharper point than the shallow minima troughs. This reinforces why it is advantageous to use the $T14$ minima frequencies as a small shift from the exact minima will have less of an effect on the $T14$ results than using a frequency that

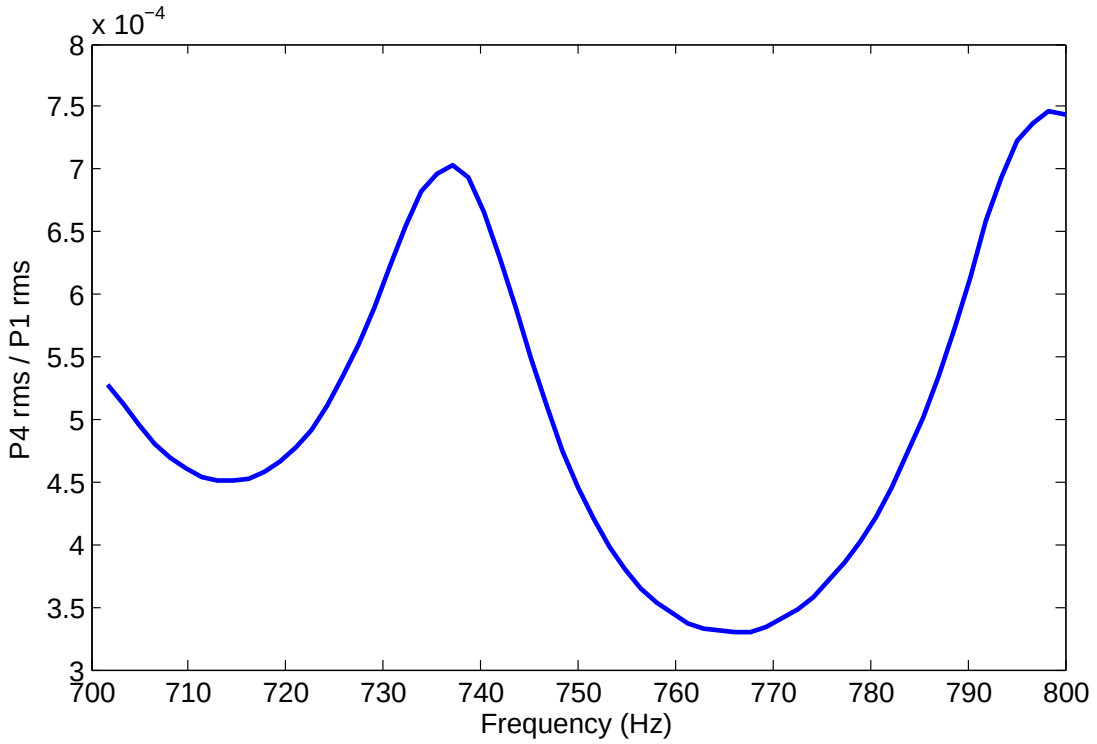

Figure 6.5: Transfer function $T14$ over frequency range 700-800Hz, showing the minima and maxima. 14mm diameter tube, air temperature of 15 °C

is near the maxima or in between the minima and maxima and hence on the steepest part of the curve. The two minima shown in Figure 6.5 correspond to the 12^{th} and 13^{th} resonant modes of the 14mm diameter tube.

Due to the tubes having different end correction conditions the frequency of the 13^{th} resonant mode is slightly different for each tube, as shown in Table 6.1. The corresponding $T14$ maxima frequencies for the maxima preceding the minima frequencies shown in Table 6.1 are shown in Table 6.2. As it is difficult to measure the exact minima frequency for any chosen resonant mode there is an associated error of ±3Hz on the stated minima frequencies.

Tube Diameter	Frequency (Hz)	
	Experiment	Simulation
6mm	762	760
8mm	767	762
10mm	765	764
12mm	770	766
14mm	770	766

Table 6.1: Transfer function $T14$ minima frequencies for all five different diameter tubes, with associated ±3Hz error.

Tube Diameter	Frequency (Hz)	
	Experiment	Simulation
6mm	734	734
8mm	738	738
10mm	737	740
12mm	742	740
14mm	742	740

Table 6.2: Transfer function $T14$ maxima frequencies for all five different diameter tubes, with associated ±3Hz error.

6.2.5 Tube Entrance Conditions

Figure 6.6 shows the plastic coupler design that was used to couple the tubes to the loudspeaker, along with housing the PCB microphone for measuring the pressure signal at the entrance to the tube. It was assumed that the plastic coupler connected to the loudspeaker has little effect on the input signal and to verify this a small experiment was carried out.

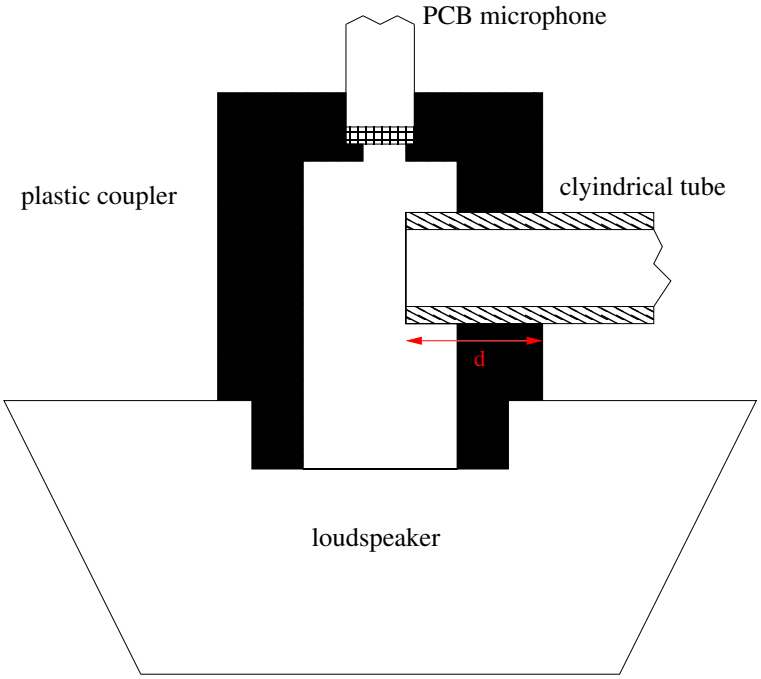

Figure 6.6: Schematic of plastic loudspeaker coupler design, housing the PCB microphone at the tube entrance. Insertion depth shown as d.

The 4cm section of tubing at the beginning of the tube can have a varied insertion depth into the plastic coupler - this insertion depth was maintained, as much as was possible, throughout all experiments but for verification the effect of different insertions was investigated. By measuring the distance between the outside of the plastic coupler and the beginning of the brass coupler, while the 4cm section was inserted, the length of the tube section that was inside the plastic coupler was calculated and this was the insertion depth denoted henceforth.

Figure 6.7 shows results for the 14mm diameter tube of the RMS pressure signals as recorded by microphone 1, in the plastic coupler at the entrance to the tube, at a chosen of amplitude of 782Hz which corresponds to neither a minima or maxima of $T14$. The RMS pressure signals, at this point, differ in amplitude

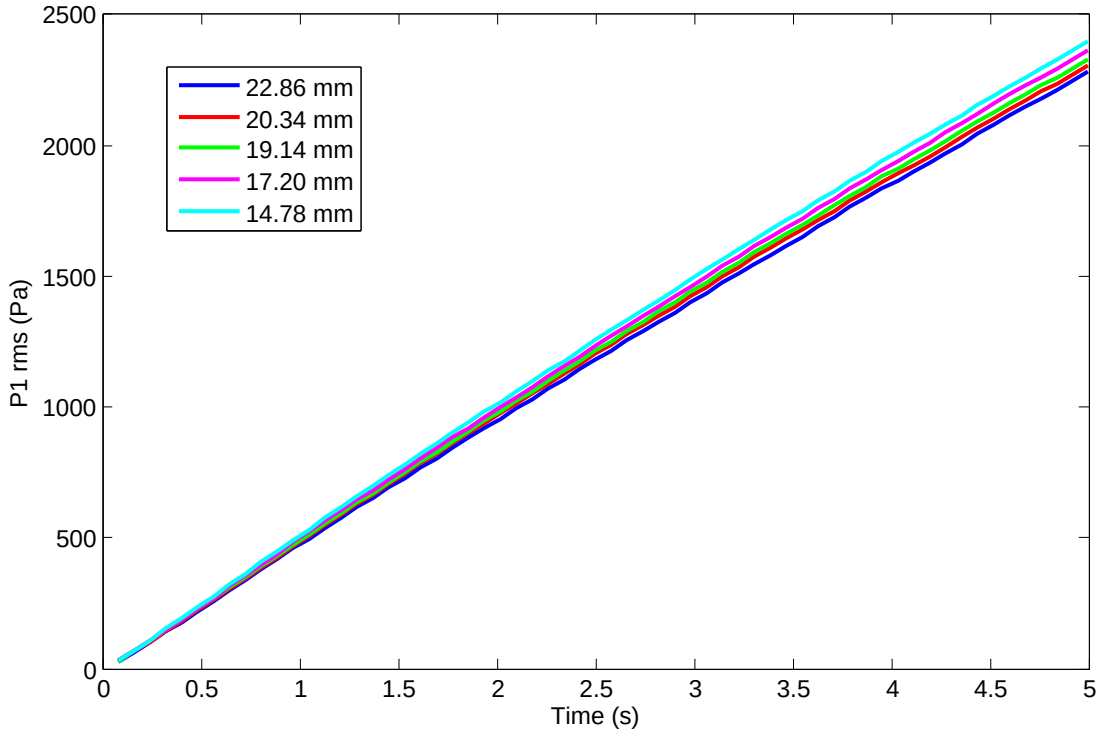

Figure 6.7: 14mm diameter tube $P1$ RMS during an amplitude sweep at 782Hz. Different insertions depths of the tube into the loudspeaker coupler.

only very slightly with insertion depth and show an increase as the insertion depth becomes smaller.

If there was no change in RMS pressure amplitude between microphones 1 and 2 we would see that the ratio of these two signals, $T12$, would be equal to 1. The transfer function results between microphones 1 and 2, $T12$, are shown in Figure 6.8. It can be seen that for varying insertion depths $T12$ has little variation, at only around 1% difference. The absolute values of $T12$ are between approximately 0.973 and 0.990, showing that the RMS pressure measured at microphone 2 is only very slightly lower than that measured at microphone 1 for all insertion depths and hence that the use of the plastic coupler does not make a large difference to the pressure signal entering the tube.

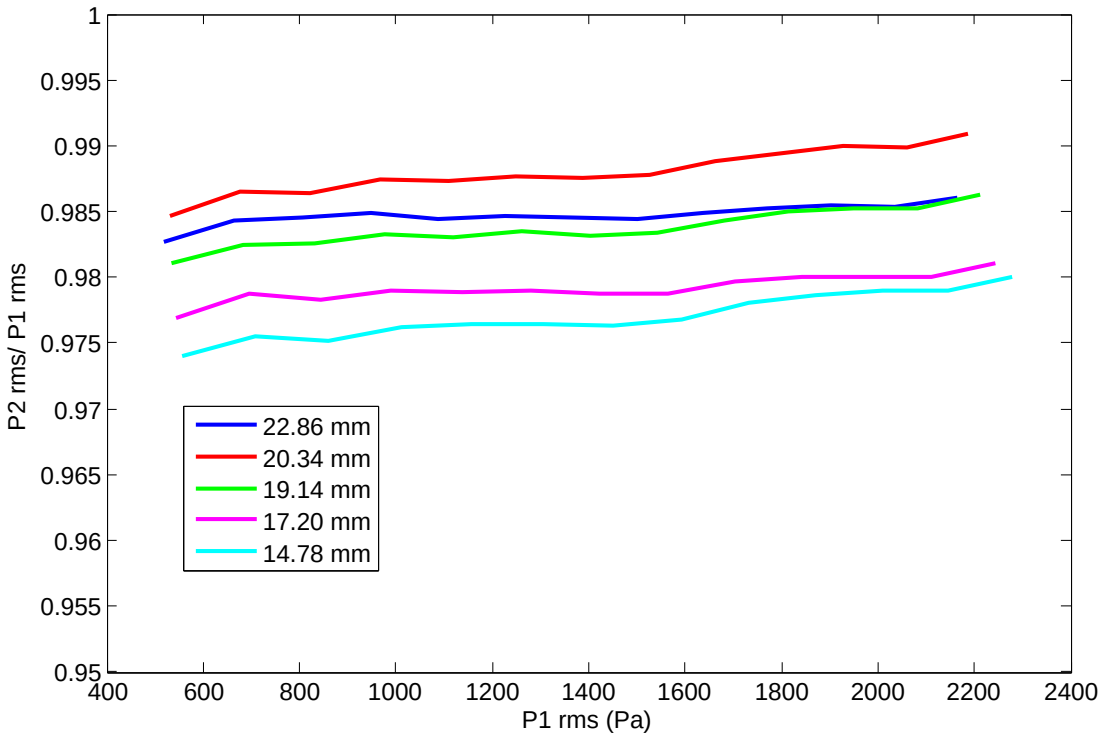

Figure 6.8: 14mm diameter tube transfer function $T12$ during an amplitude sweep at 782Hz. Different insertion depths of the tube into the loudspeaker coupler.

6.2.6 Radiation Conditions

It is reassuring to find that the loudspeaker coupler has little effect on the input signal of the system but this is not the case with all the variable factors in the experimental setup. It was found that the orientation of microphone 4, the microphone placed in the radiation field 20cm from the termination of the tube, had a larger effect on the results gained from the setup. Figure 6.9 shows the difference in the $T14$ results, for the 14mm diameter tube with the radiated microphone on axis and approximately 10 degrees off axis, as being around 6% higher when the microphone is off axis. It was endeavored for the placement of this microphone to be kept as constant as possible between measurements, in terms of both distance from the termination of the tube and angle, so that it remained on axis at all times.

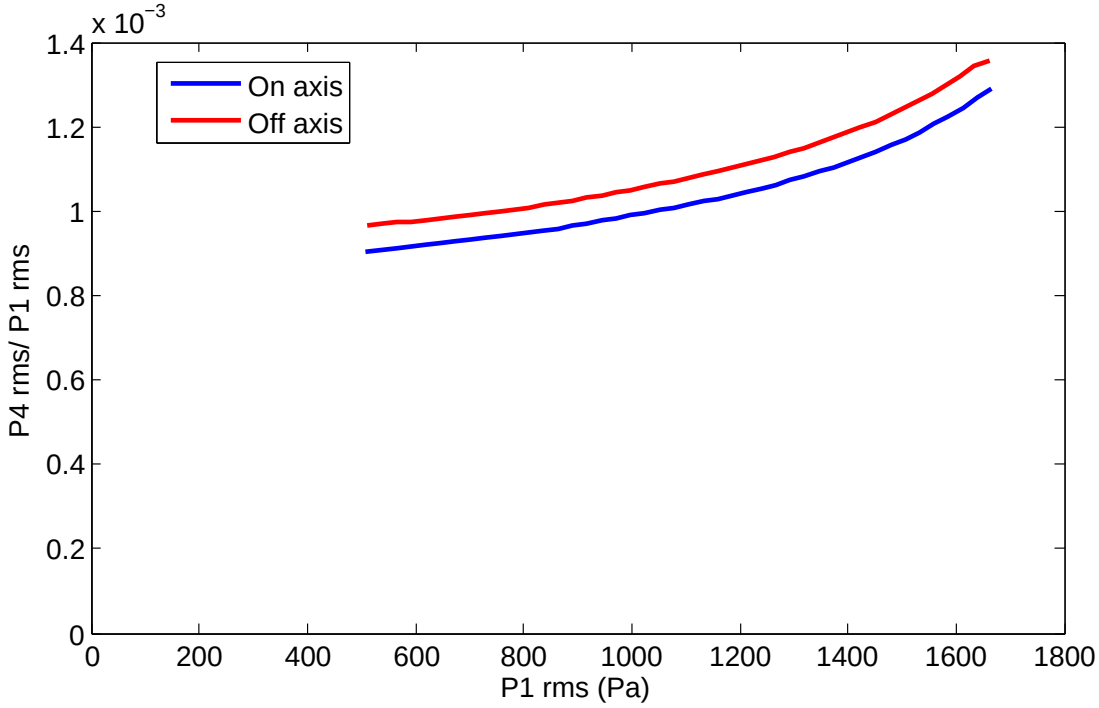

Figure 6.9: 14mm diameter tube transfer function $T14$ during an amplitude sweep at 760Hz. Radiated microphone 4 on axis and 10 degrees off axis.

6.2.7 Temperature Effects

The air temperature in the anechoic chamber was also found to be a vital factor in gaining consistency between measurements. To investigate the quantitative effects of temperature on the measured transfer function, a series of measurements were carried out at a range of ambient temperatures. In order to carry out measurements at a consistent temperature, standard lamps containing high wattage bulbs were used to increase the air temperature gradually to a chosen value; this was done slowly to ensure the temperature of the air inside the cylindrical tube was increased as well as the surrounding air. After the experimental setup had been assembled and the tube positioned within the setup, it was left to acclimatise for an hour as the tubes themselves could become very warm after being handled for several minutes. Figure 6.10 shows the effect on $T14$ due to air temperature differences in experimental measurements. The variation in the experimental transfer function at the highest input pressure amplitude is around 10%, with $T14$ having a higher value for the lowest temperature of 15 °C. The variation in $T14$ is relatively small but still significant when aiming

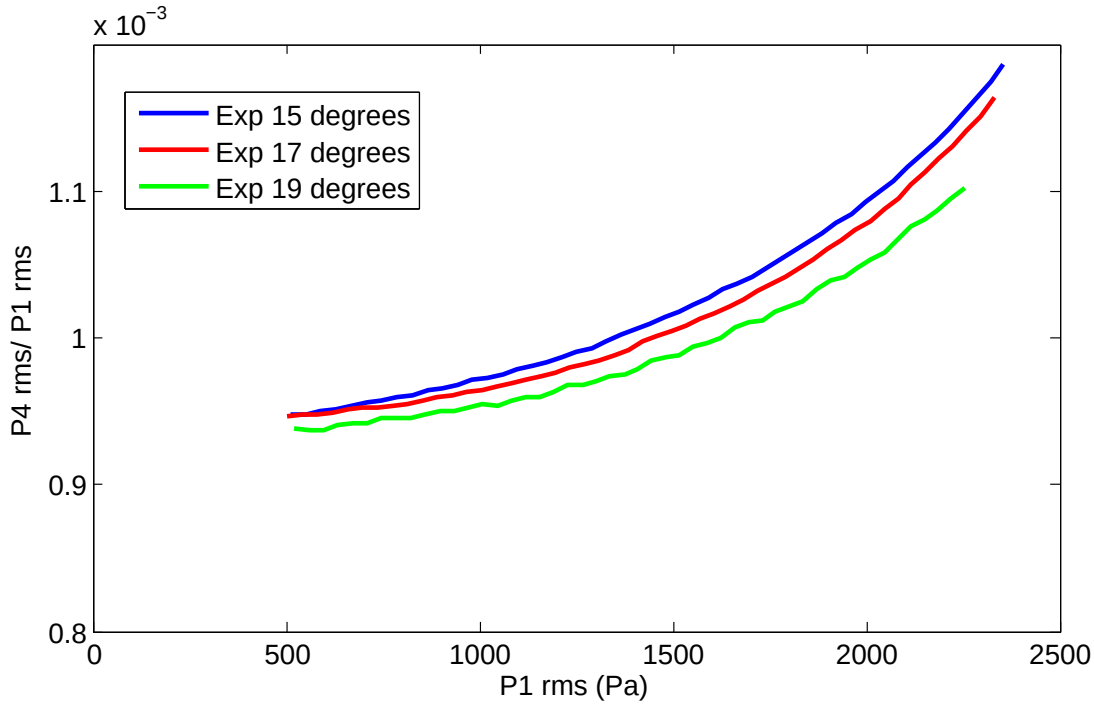

Figure 6.10: 14mm diameter tube transfer function $T14$ during an amplitude sweep at frequencies corresponding to a minima of the transfer function, at varying air temperatures.

to compare experimental results with simulation and hence all experimental measurements were carried out at 15 °C. It is estimated that the error in the temperature for any given measurement is ±0.5 degrees, which will give an approximate percentage error of 1.25% in the transfer function results.

6.2.8 Experimental Errors

It has been shown in the previous sections that the experimental setup and technique used for this work can be very sensitive to variable factors; it is for this reason that so much care has been taken in refining the experimental technique, and hence repeatability of the measurements.

In the short quantitative assessment of the variable factors in the experimental setup one of the most significant errors was shown to be the positioning of the microphone in the radiation field. It should be noted that the technique used to gain repeatable alignment of this microphone was simply a sheet of paper rolled lengthways, with a mark indicating 20cm along its length. This sheet of paper

was then inserted into the end of the tube and the microphone aligned on axis, 20cm from the tube termination, using the rolled paper as a guide. The error associated with a 10 degree, off axis, movement of the radiated microphone was found to be 6%; this can hence be taken as the maximum error bound for this work as a 10 degree movement of the microphone would be immediately obvious to the experimentalist.

It can therefore be stated that the experimental error in this work will be significantly less than 6%, with this value being the outermost error bound, and that as the experimental technique was refined it was increasingly easy to ensure repeatability from the given setup.

6.3 Computational Simulation

The numerical simulation used was developed by Joël Gilbert and is detailed in [Gilbert 08b]. It is a frequency-domain numerical model which can be used to model the sound production and brassiness of a brass instrument. This model was not the first of its kind; numerical simulation programs were developed in both the time domain [Msallam 00, Vergez 00] and frequency domain [Thompson 01]; these previous models made some assumptions, such as modelling the wave steepening in only part of the bore or not taking into account the nonlinear wave propagation of the backward going wave. The numerical simulation used here is based on the generalised Burgers' equations relating to weakly nonlinear wave propagation in nonuniform ducts.

Assuming a one dimensional flow, within a nonuniform duct, in a dissipative viscothermal homogeneous fluid and using weakly nonlinear propagation theory, the first-order nonlinear differential twin equations that are the generalised Burgers' equation for the forward and backward going wave are produced:

$$\frac{\partial q_+}{\partial \sigma} - q_+ \frac{\partial q_+}{\partial \theta_+} + q_+ \frac{\partial ln(D(\sigma)/D(0))}{\partial \sigma} = +\frac{1}{\Gamma}\frac{\partial^2 q_+}{\partial \theta_+^2} - \frac{T}{\epsilon}\frac{\partial^{1/2} q_+}{\partial \theta_+^{1/2}} \tag{6.1}$$

$$\frac{\partial q_-}{\partial \sigma} + q_- \frac{\partial q_-}{\partial \theta_-} - q_- \frac{\partial ln(D(\sigma)/D(0))}{\partial \sigma} = -\frac{1}{\Gamma}\frac{\partial^2 q_-}{\partial \theta_-^2} - \frac{T}{\epsilon}\frac{\partial^{1/2} q_-}{\partial \theta_-^{1/2}} \tag{6.2}$$

where Γ, the Gold'berg number, is a measure of how strongly nonlinear effects will accumulate before absorption losses eventually cause the acoustic signal to

decay away [Kinsler 00]. Equations 6.1 and 6.2 use dimensionless variables σ (a slow geometric scale $\sigma = (\gamma+1)/2Mx$, where γ is the specific heat ratio, M a Mach number, and x a dimensionless geometric scale), θ_+ and θ_- (dimensionless delayed time scales), and q_+ and q_- (forward and backward variables). These equations also contain a second term on the right-hand side that is determined by the dimensionless number T/ϵ, which is a measure of the strength of nonlinearity relative to the wall dissipation; this term arises as a consequence of the viscothermal boundary layer attenuation on a plane wave propagating in a duct with rigid walls.

Equations 6.1 and 6.2 have no analytical known solutions, and therefore the solutions calculated numerically in the frequency domain. The traveling wave $q_+(\sigma, \theta)$ is considered:

$$q_+(\sigma, \theta) = \sum_{n=1}^{\infty} [a_n(\sigma) \sin n\theta + b_n(\sigma) \cos n\theta] \tag{6.3}$$

The nonlinear term from the Burgers' Equations, 6.1 and 6.2, becomes a Fourier series which gives the following, for each harmonic component n, when each term of the Fourier series is equalised:

$$\begin{aligned}\frac{\partial a_n}{\partial \sigma} =& n \left(\sum_{p=1}^{n-1} \left(\frac{a_p a_{n-p}}{2} - \frac{b_p b_{n-p}}{2} \right) - \sum_{p=n+1}^{+\infty} (a_{p-n} a_p + b_p b_{p-n}) \right) \\ &+ \frac{1}{\Gamma} n^2 a_n - a_n \left(\frac{\partial ln(D(\sigma)/D(0))}{\partial \sigma} \right) - \frac{T}{\epsilon} \frac{D(0)}{D(\sigma)} \sqrt{\frac{n}{2}} (a_n - bn)\end{aligned} \tag{6.4}$$

$$\begin{aligned}\frac{\partial b_n}{\partial \sigma} =& n \left(\sum_{p=1}^{n-1} \left(\frac{a_p b_{n-p}}{2} + \frac{b_p a_{n-p}}{2} \right) + \sum_{p=n+1}^{+\infty} (b_{p-n} a_p - b_p a_{p-n}) \right) \\ &+ \frac{1}{\Gamma} n^2 b_n - b_n \left(\frac{\partial ln(D(\sigma)/D(0))}{\partial \sigma} \right) - \frac{T}{\epsilon} \frac{D(0)}{D(\sigma)} \sqrt{\frac{n}{2}} (a_n + bn)\end{aligned} \tag{6.5}$$

These equations are solved numerically in the simulation program, using a spatial finite difference method, with the boundary condition $q_+(0, \theta)$, a time

periodic function. The classical Euler method is used at first order, and correction is performed using the Adams Moulton second order method.

A monopole radiation approximation is used to predict the radiation from the output of the tube/instrument. The volume velocity spectrum Q_{out} at the termination of the tube is estimated by multiplying the output acoustic velocity spectrum by the terminating surface area. The radiated pressure, P_{rad}, is calculated using

$$P_{rad} = \frac{\rho}{4\pi r} j\omega Q_{out} e^{-jkr} \tag{6.6}$$

where ρ is the density of air and r is the distance from the end of the tube. This uses the low frequency approximation for a monopole source having a volume strength equal to Q_{out}.

The simulation program requires a simple bore profile as an input, which in the case of a cylindrical tube was simply the length and internal diameter. The program then creates a very accurate bore profile with points at 0.5mm intervals. Two input files were also created with the parameters of the input signal, one corresponding to the conditions at the lowest amplitude of the crescendo, *pp*, and the other corresponding to the conditions at the highest amplitude, *ff*. These files contain the fundamental frequency, number of harmonics, and the pressure amplitude and phase for each harmonic. Other input parameters include temperature and distance to radiated measurement point. The simulation program was set to have measurement points at the same positions as the microphone positions in the experimental setup; in turn the RMS pressure and spectral centroid data is returned at each of these points.

6.4 Transfer Function

The transfer function between the input and the output of an instrument, or tube, has been shown to be a value that is particularly responsive to nonlinear effects, as far back as the work conducted by Beauchamp [Beauchamp 80]. In this section the results of a further exploration of the transfer function at different dynamic levels for the case of a range of simple cylindrical tubes is presented.

6.4.1 Entrance transfer function

$T12$, the transfer function between the microphone at the entrance to the tube and the microphone 5cm from the entrance is shown in Figure 6.11 for the experimental results.

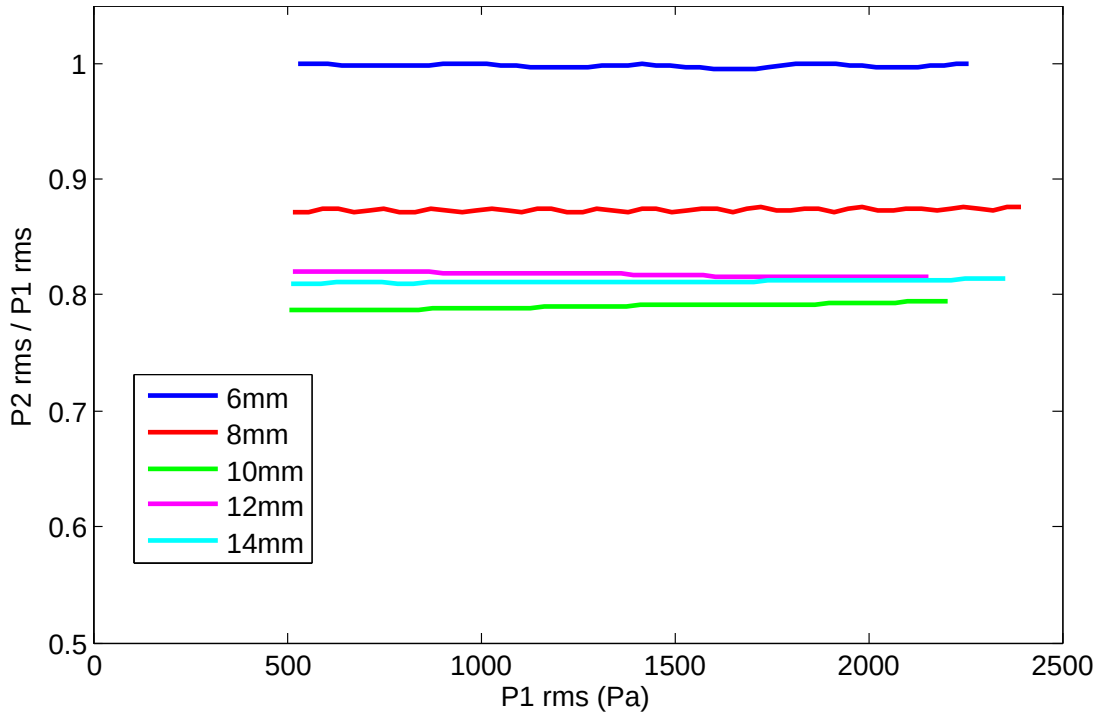

Figure 6.11: Experimental transfer function $T12$ during an amplitude sweep at frequencies corresponding to a minima of the transfer function. Five tubes with diameters 6mm, 8mm, 10mm, 12mm, and 14mm.

This figure shows some interesting details about the five tubes; it can be seen that the 6mm diameter tube has a much higher $T12$ result than the other 4 tubes, implying that the difference in RMS pressure signals for the 6mm tube in the first 5cm is much less than for the other tubes. The value of $T12$ for the 6mm tube is essentially equal to 1 which signifies that the two pressure signals are basically identical. The 8mm diameter tube shows a $T12$ of approximately 0.88, and the 10mm, 12mm, and 14mm results are all around 0.8.

The wavelength, λ, for each tube, at the $T14$ minima frequency, is approximately 44cm and hence $\frac{1}{4}\lambda$ is approximately 11cm. This means that the distance between adjacent nodes and antinodes in the standing wave will be around 11cm. The distance between the microphones that are being considered in the case of

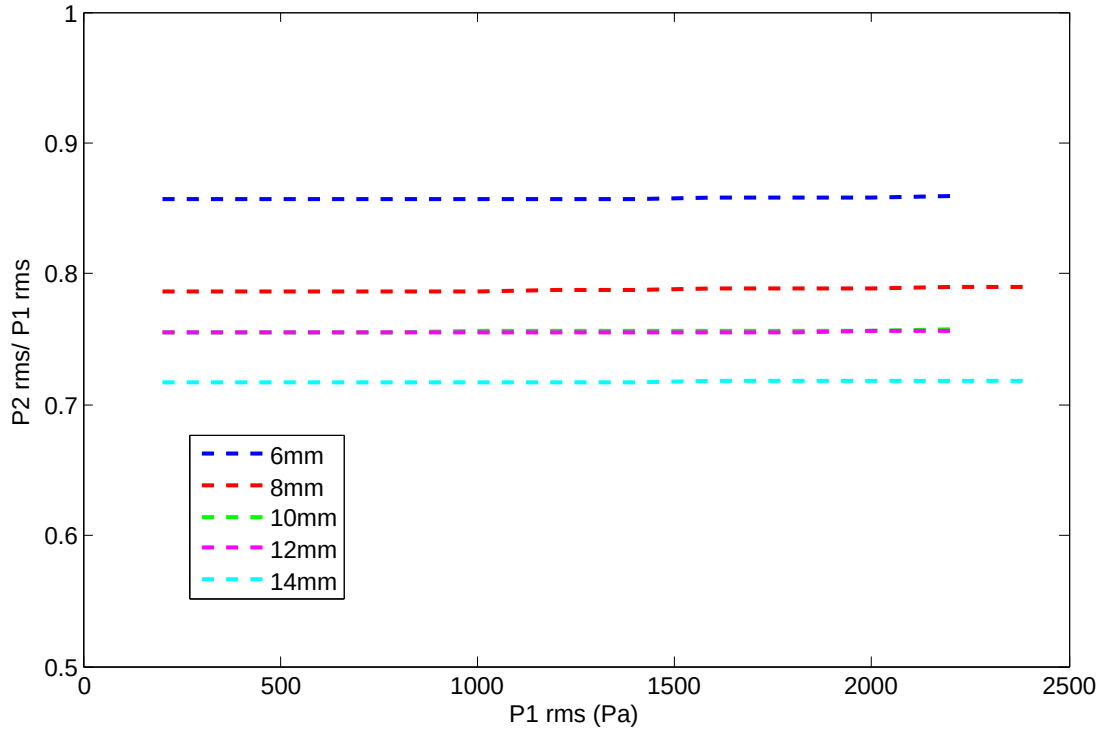

Figure 6.12: Simulated transfer function $T12$ during an amplitude sweep at frequencies corresponding to a minima of the transfer function. Five tubes with diameters 6mm, 8mm, 10mm, 12mm, and 14mm. Noting that the 10mm T12 result lies at exactly the same point as the 12mm result, and hence is not visible on the plot.

$T12$ is roughly half of this $\frac{1}{4}\lambda$ and hence there could be a substantial difference in the absolute pressure amplitude of the standing wave between the two microphone positions. Although the losses are more apparent in the smaller diameter tubes, it is the 6mm diameter tube that shows no decrease in RMS pressure after 5cm. This could be understood as the losses acting on the propagating wave to the extent that the difference between the maximum and minimum (the antinodes and nodes) of the pressure wave is small and therefore over the 5cm distance there may not be a large difference in RMS pressure. Indeed the same effect is seen in the simulated $T12$ results, as shown in Figure 6.12. Although all the transfer function results are lower here than those seen in the experimental results a similar effect can be seen; the 6mm diameter tube shows the highest $T12$ result at around 0.86, the 8mm diameter tube is slightly lower at around 0.79 and the three largest tube diameters are grouped between 0.72 and 0.75.

6.4.2 Radiated transfer function

Figure 6.13 shows experiment and simulation results, for the five tube diameters used, of the transfer function $T14$, between the microphone at the entrance to the tube and the microphone in the radiation field.

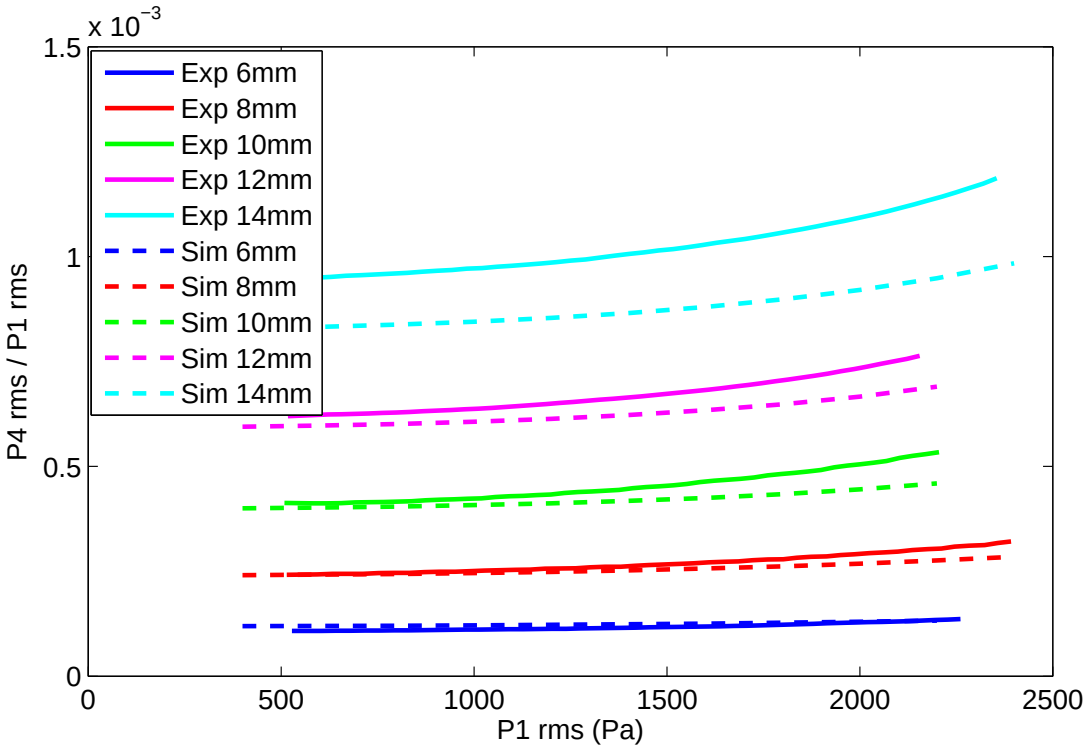

Figure 6.13: Transfer function $T14$ during an amplitude sweep at frequencies corresponding to a minima of the transfer function. Five tubes with diameters 6mm, 8mm, 10mm, 12mm, and 14mm.

There is a clear increase in $T14$ with bore diameter increase from the 6mm to 14mm diameter tubes. This increase with diameter is in line with expectations, as the increase in tube diameter increases the surface area at the end of the tube and hence the volume velocity and associated radiated pressure will be larger. We also know that the viscothermal wall losses become less significant in the larger tubes, and therefore in the smaller diameter tubes there will be more dissipation of energy as the sound wave propagates along the tube before some of this wave is radiated at the end of tube. The smallest diameter tube, 6mm, experiences almost no change in transfer function $T14$ with amplitude, which is what we would expect if we were to assume the viscothermal losses were independent of

amplitude and that there was no nonlinear distortion. As the diameter of the tubes increase, $T14$ increases more with increasing pressure amplitude, with this being most evident for the 14mm diameter tube. This behaviour of $T14$ can be partly understood as a consequence of the nonlinear steepening that has occurred within the tubes and partly because of the smaller viscothermal loss coefficient for the larger diameter tubes. The nonlinear wave steepening means that the radiated pressure wave has more high frequency components and because these high frequency components are more efficiently radiated from the end of the tube. At the highest input pressure amplitudes it can be seen that the experimental results deviate more from the simulation results; because the transfer function is the ratio of two pressure signals this shows that the radiated pressure $P4$ has a smaller value, at the highest amplitudes, in the simulation than in the experiment. The simulation results are qualitatively similar to the experimental results but are not entirely quantitatively similar across all five tubes. The experimental $T14$ results are all larger than the simulated results, with the exception of the 6mm diameter tube, and this discrepancy increases with tube diameter. The quantitative difference between simulation and experiment is most marked for the 14mm diameter tube with the simulation results being around 10% lower than experiment. This difference could perhaps be attributed to the monopole radiation approximation made in the numerical simulation being an oversimplified approximation of the realistic radiation from the tubes.

The monopole radiation model predicts that there is a uniform distribution of sound energy in all directions emanating from the termination of the tube. This approximation is applicable for low frequency components, but as the frequency increases to the point where this approximation ceases to be true, more energy is expected to be concentrated into the central radiation lobe, where microphone 4 is placed.

6.4.3 Internal transfer function

The placement of microphones 2 and 3 within the tube length allowed the evolution of the nonlinear distortion and viscothermal losses to be explored at different points along the wave propagation. The weakly nonlinear propagation theory assumes that there is no local nonlinear interaction between the forward and backward going waves, but that the pressures measured by the microphones

are the sum of these two waves.

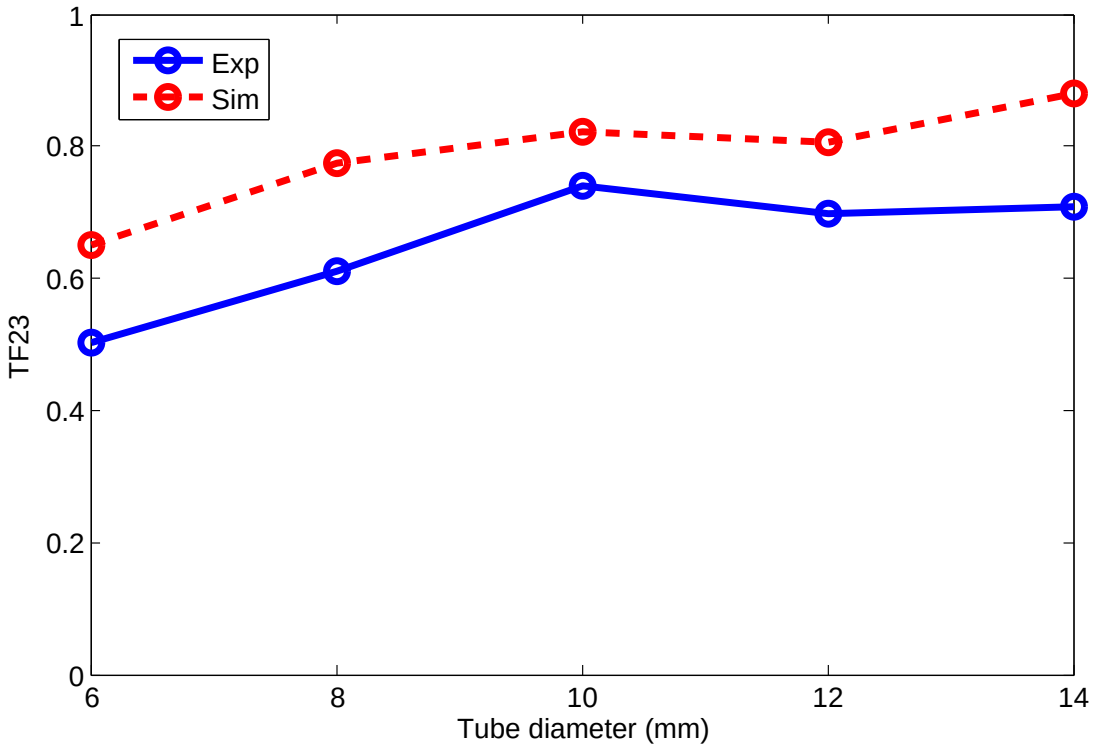

Figure 6.14: Transfer function $T23$ at 1000Pa RMS input pressure at frequencies corresponding to a minima of the transfer function plotted against the five tube diameters 6mm, 8mm, 10mm, 12mm, and 14mm.

Figure 6.14 shows measured and simulated results for $T23$ (the ratio between the RMS pressure measured by microphone 3, roughly in the middle of the tube - 147cm from the tube entrance, and the RMS pressure measured by microphone 2, 5cm from the tube entrance). The $T23$ results are essentially independent of input pressure amplitude so are plotted here against tube diameter. The absolute values of the internal transfer function $T23$ depend on the relative phases of the forward and backward going waves at the microphone position. The evaluation of $T23$ allows us to examine purely the effects of the nonlinear wave steepening and the viscothermal losses without the added complication of the radiation from the end of the tube. So from these results we can see that excluding the slightly crude radiation approximation in the simulation the results are broadly in accord with the experimental results but still between 15-30% higher. This difference between simulation and experiment suggests that the treatment of the losses in

the simulation is not fully in accord with what is observed experimentally; the simulation appears to be under predicting the amount of losses in the system. The trends, with regard to tube diameter, are slightly different between the two curves - the simulation results increase with tube diameter almost steadily, with the exception of the 12mm diameter tube showing a slightly lower value for $T23$. However, the experimental results increase with a peak at the 10mm diameter tube and then decrease slightly with the two largest diameter tubes.

When considering the internal transfer function $T23$, it may be less complex than the case where the radiation field must be taken into account, but a number of effects must still be evaluated. At measurement point 2, 5cm from the entrance of the tube, the pressure wave has already propagated a small distance and will therefore have already been slightly distorted and have been affected by the viscothermal losses. However, we assume that these effects will have had a minimal effect at this point. As the forward going wave propagates further down the tube to measurement point 3, 147cm from the entrance, it will have became distorted due to the nonlinear distortion. The nonlinear distortion acts in such a way to transfer energy into the upper harmonics. The viscothermal losses are however frequency dependent, meaning that they act to diminish the energy of the higher harmonic content more so than the lower frequencies. As the forward going wave propagates further down the tube it will lose energy due to the viscothermal wall losses as it travels. The pressure measured at the measurement points, in both the experiment and simulation, is a summation of the forward and backward going wave pressures at that point. The forward going wave has propagated to the end of the tube and at the termination some fraction of this wave is reflected and becomes the backward going wave. The backward going wave will have already been subject to the viscothermal wall losses as it propagated to the end of the tube as the forward going wave, and hence, will have lost energy. This smaller amplitude backward going wave will be subject to the same wall losses as it propagates back toward the entrance of the tube and hence lose even more energy. It can be seen in Figure 6.15 the effect the losses have on the transfer function $T13$, as predicted by the simulation program.

It is clear that the inclusion of the viscothermal losses has a very significant effect of the pressure amplitude of the propagating wave. In the case where there are no wall losses in the system, and the same extent of nonlinear distortion, $T13$

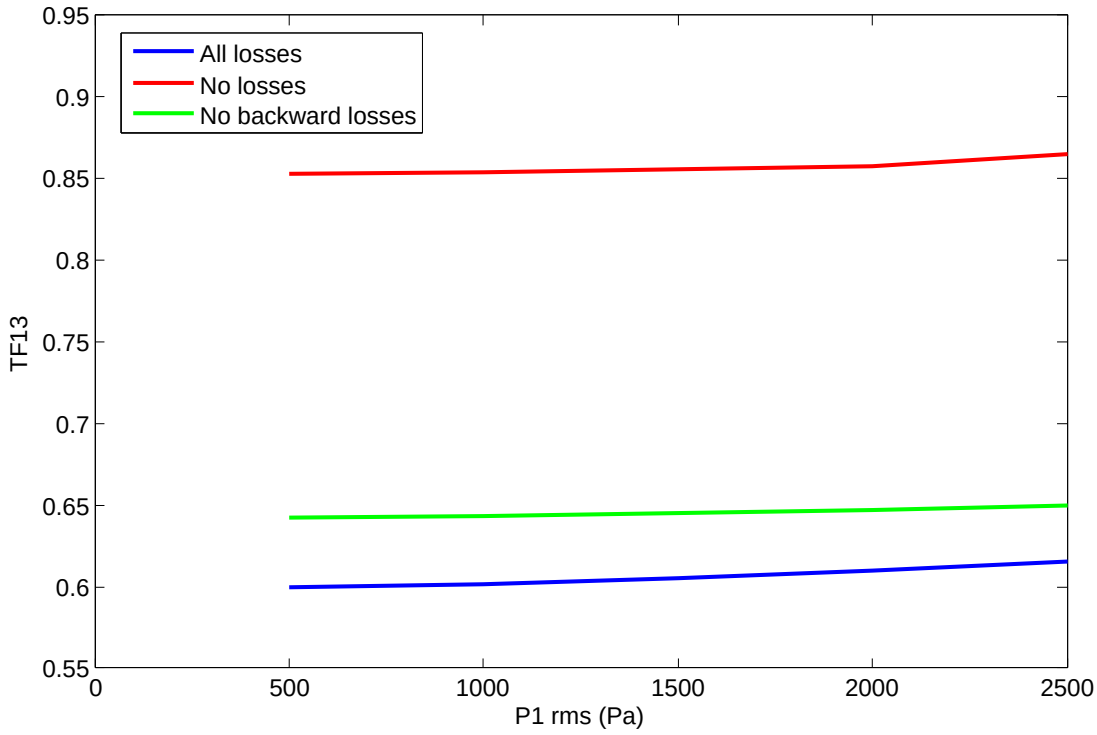

Figure 6.15: Simulated transfer function $T13$ of the 12mm diameter tube showing results including viscothermal losses on both the forward and backward going wave, only the backward going wave and no losses at all.

is approximately 0.85. Whereas, when viscothermal wall losses act on both the forward and backward going wave $T13$ has, unsurprisingly, a much lower value of around 0.6. What is perhaps more interesting is the case where the viscothermal losses are apparent in the forward going wave propagation but neglected from the backward going wave. In this case $T13$ lies around 0.65, showing that the wall losses on the backward going wave have a much smaller effect on the total pressure of the wave than those on the forward going wave, as the pressure amplitude of this wave has already been significantly diminished as it propagated from the tube entrance towards the end of the tube.

6.5 Spectral Centroid

The program used to anaylse the evolution of the measured spectral centroid was developed by Joël Gilbert and is discussed in [Gilbert 07]. The program takes pressure signals from the microphones and splits these signals into overlapping

segments of 4096 samples each. These segments are each analysed with a discrete Fourier transform and the mean value of the instantaneous fundamental frequency and the RMS pressure signals for each are estimated. The spectral centroid (as defined in [Beauchamp 82]) is calculated using Equation 6.7

$$SC = \frac{\sum_n nP_n}{\sum_n P_n} \tag{6.7}$$

where P_n is the amplitude of the n^{th} harmonic of the signal.

6.5.1 Input Signal

It was found in the experimental results for each tube, at the highest amplitudes, that the input signal was not a perfectly sinusoidal signal and that there were very small, 2^{nd} and 3^{rd} harmonic components present - as shown in Figure 6.16 for the 12mm diameter tube. This figure shows the harmonic components as calculated in MATLAB [Mathworks 13] using a fast fourier transform (FFT). Because we are interested in the harmonic content of the signal at the highest amplitude, a section is taken from the end of the signal, this consisted of the last 4096 samples. This section of the signal was re-sampled to a sample rate which was an integer multiple of the frequency of the amplitude sweep, and a rectangular window used. The section of the signal was also zero padded to give a finer frequency resolution in the FFT, this is what produces the side lobes in Figure 6.16.

These small harmonics are inevitable as such a setup as the measured signal is the sum of the forward and backward going waves; the backward going wave returns to the measurement point with a definite degree of nonlinear distortion and hence when added to the forward going wave will result in a slightly distorted pressure wave. The program used to calculate the spectral centroid allows a noise-floor to be defined; all frequency components with amplitude less than this defined value are discounted from the spectral centroid calculation.

The calculation of the spectral centroid is very dependent on distinguishing the harmonics that you wish to identify from the background noise. If too many components are taken into account, it is possible that the calculated spectral centroid will not be valid; it will be taking into account some degree of the background noise and hence changing the final result. Each experimental signal was assessed individually and a value for the noise floor determined for each.

The value chosen was determined by examining the spectrogram produced by the program, and finding the amplitude of smallest harmonic component that was identifiable above the background noise, this was done by inspection.

Although very small in amplitude relative to the first harmonic these higher harmonics do affect the spectral centroid, as can be seen in Figure 6.17 which shows both the far field, $SC4$, and internal, $SC3$, spectral centroid results for the measured data, and the simulation with and without the extra harmonics. In both the internal and far field cases, the spectral centroid at the highest input pressure values are slightly higher for the simulation results which include the extra input harmonics, than the pure sine input simulation results. The phase data for each of the harmonics in the measured data is also included in the simulated results; both the amplitude and phase data should be included to provide as close an input signal to the simulation, as to that used in the experimental setup. The phase information of the input harmonics is important for the simulation; it will determine how the these harmonic components develop with increasing input pressure amplitude and how the resulting waveform in the tube will develop.

At the highest input pressure amplitude values there are a large number of harmonics present in the far field signal. As the pressure wave propagates down the tube it is becoming increasingly distorted and the harmonic content of the signal is changing. It is therefore important that when evaluating the spectral centroid of a signal with a much higher number of high frequency components, all significant components are taken into account. The number of harmonics used in the calculation of the spectral centroid must be chosen both in the simulation program and when analysing the experimental data. Figure 6.18 shows far field spectral centroid, $SC4$, results for both simulation and experiment using the 12mm diameter tube at the $T14$ minimum frequency. The importance of the small amplitude, highest harmonics, on the spectral centroid results can be seen; there is up to a 15% difference, at the highest input pressures, between calculations of the spectral centroid using 10 and 15 harmonics.

15 harmonics were used for all calculations of the spectral centroid for both simulation and measured results, as at this point it was beginning to be difficult to distinguish the harmonic peaks from the noise in the experimental results.

All results hereafter have been calculated taking into account 15 harmonics and have the appropriate extra harmonics in the simulation input signal at the

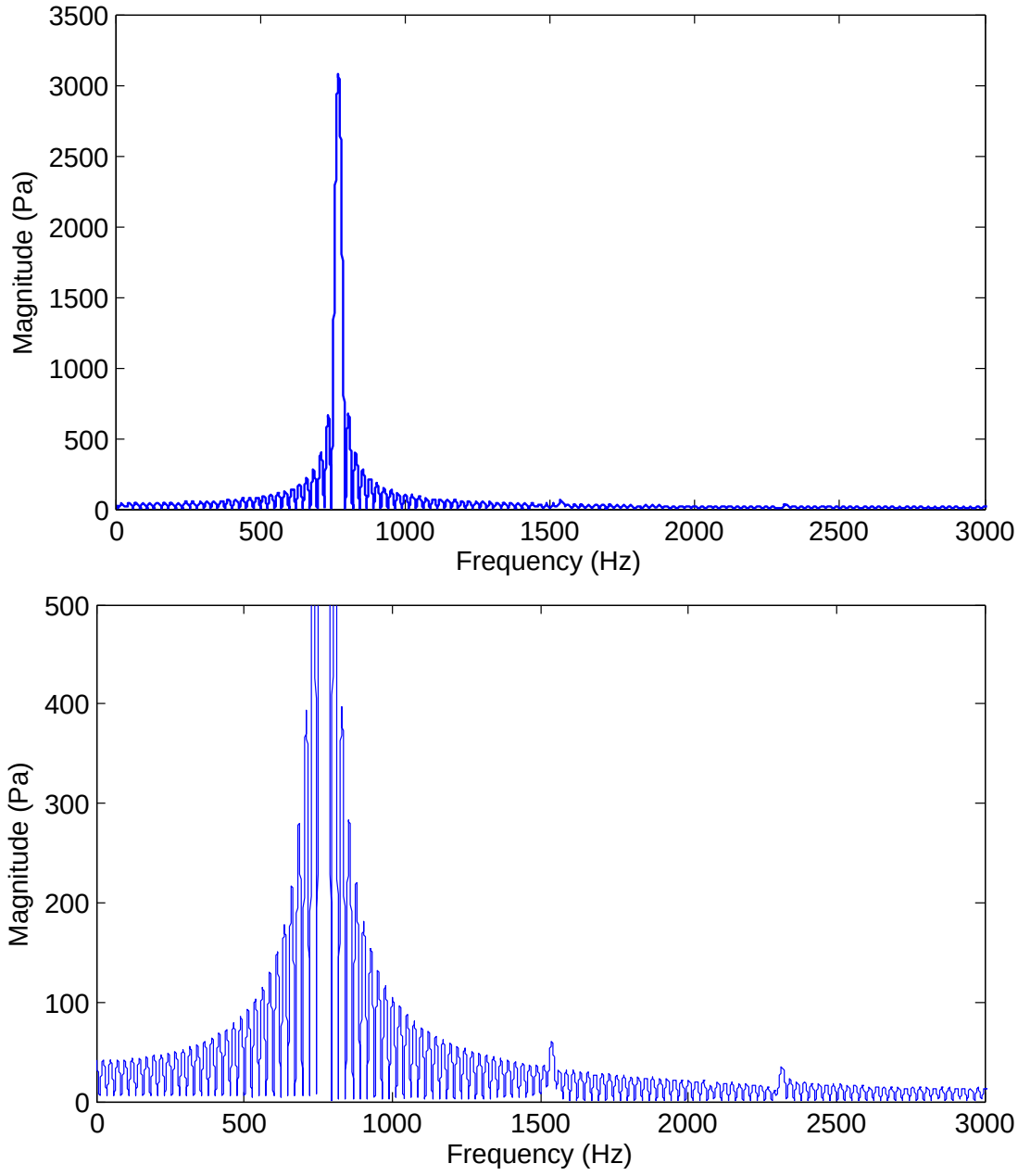

Figure 6.16: 12mm diameter tube measured input signal spectrum at highest input amplitude, showing harmonics above the fundamental. **Bottom**: Zoomed section.

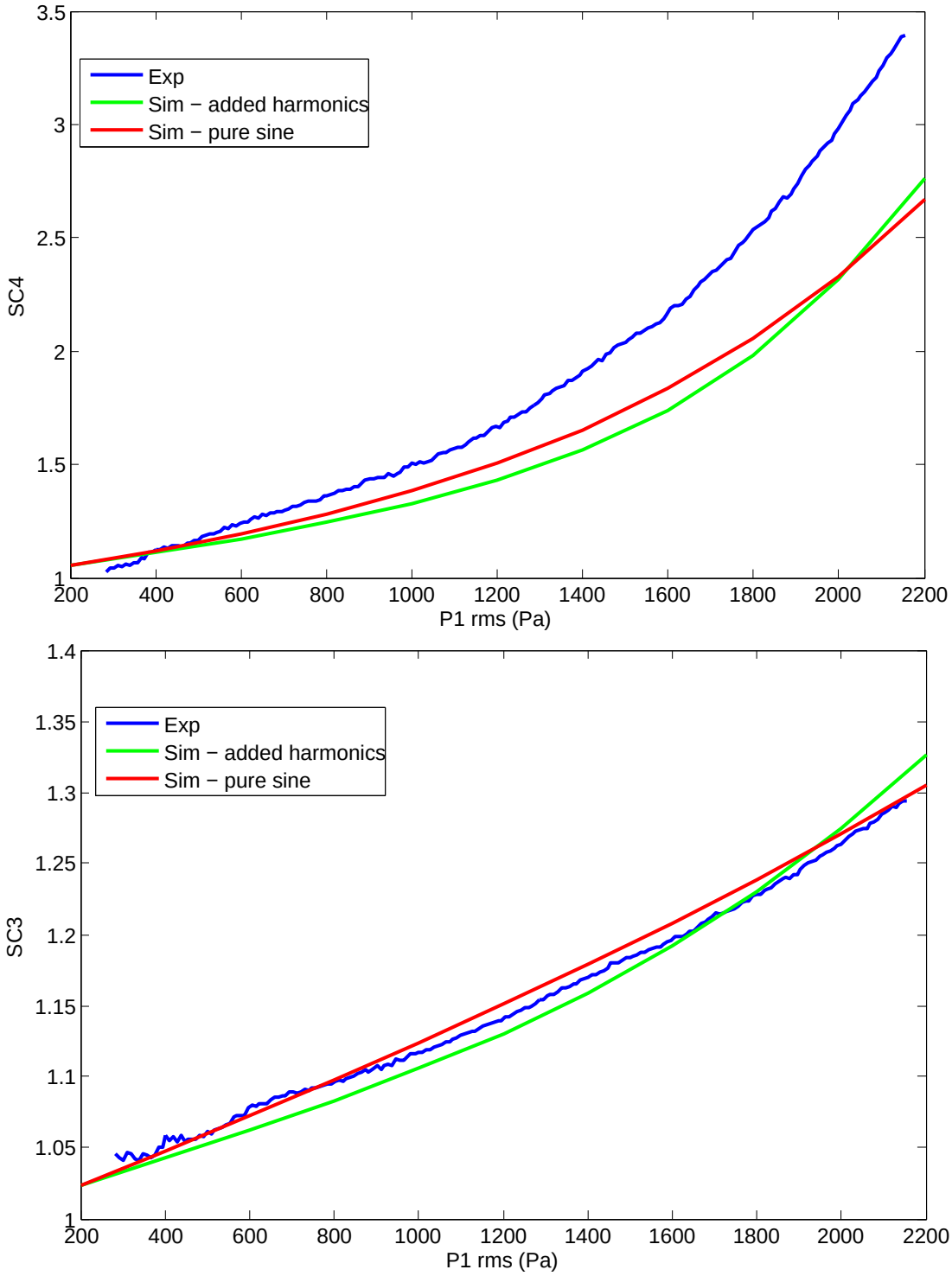

Figure 6.17: 12mm diameter tube spectral centroid during an amplitude sweep at 766Hz. Simulation with and without additional input harmonics. **Top**: Far field **Bottom**: Internal

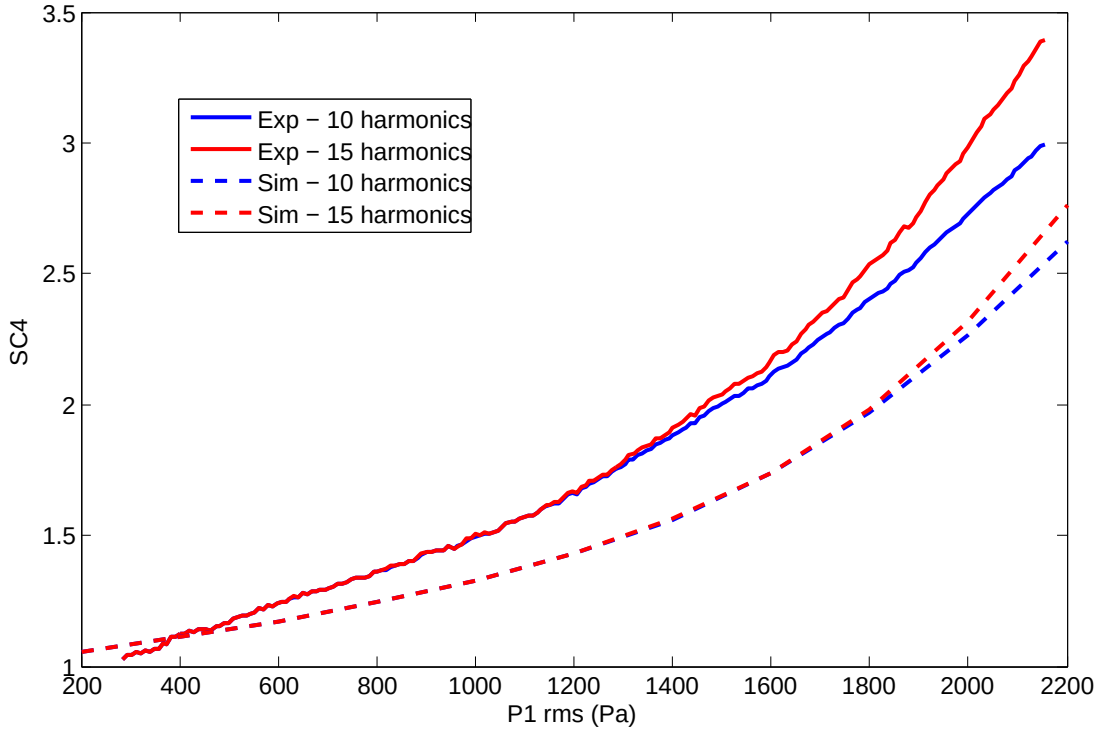

Figure 6.18: 12mm diameter tube far field spectral centroid at 766Hz. Showing experimental and simulation results using 10 and 15 harmonics in the spectral centroid calculation.

highest amplitudes.

6.5.2 Results

The spectral centroid measured in the far field, $SC4$, can be seen in Figure 6.19 for the 10mm diameter tube, which shows both the measured and simulated results. The measured spectral centroid has a maximum value of approximately 3.8 at the highest input pressure amplitude. However, the simulated spectral centroid result has a significantly lower value, of around 2.7, at the highest input pressure value. This result is typical of all the different diameter tubes and the far field spectral centroid, $SC4$, results for each of the tubes can be seen in Appendix B.

Figure 6.20 again shows both the experimental and simulation results at the transfer function minima frequencies for the far field spectral centroid, plotted in such a way as to see the dependence of $SC4$ on tube diameter. It can be seen that the simulated $SC4$ results (bottom section of Figure 6.20) show little

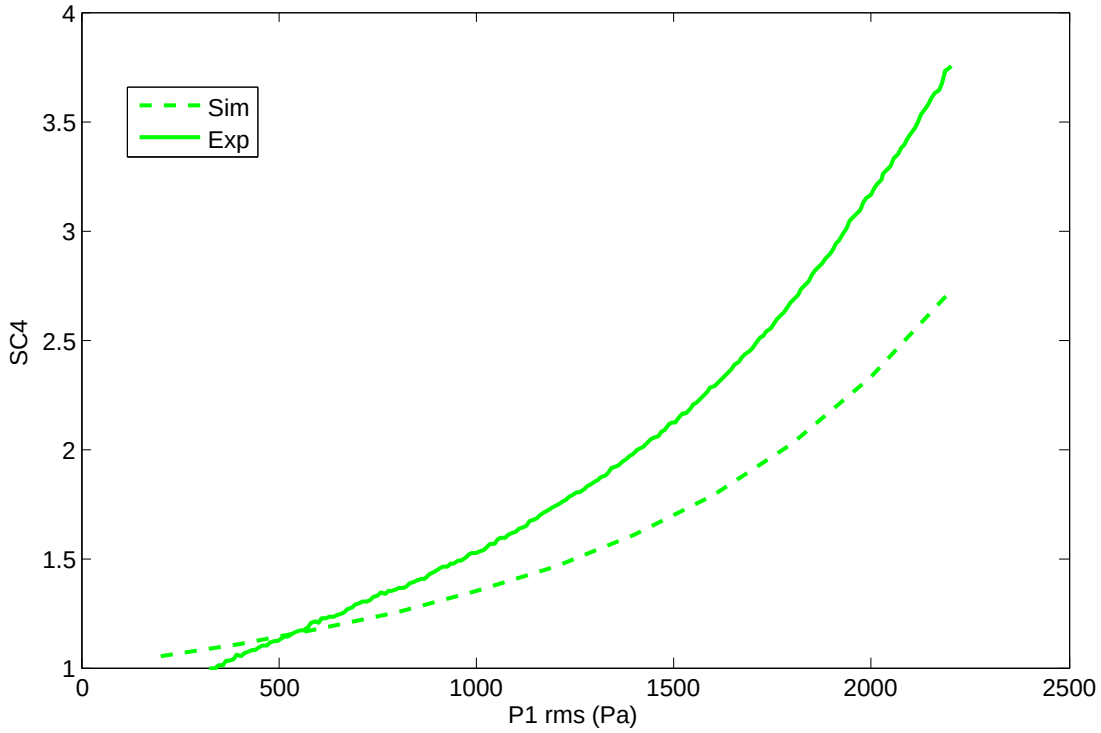

Figure 6.19: Far field spectral centroid of the 10mm diameter tube during an amplitude sweep at frequencies corresponding to a minima of the transfer function, showing experiment and simulation results.

dependence on tube diameter at the highest input pressure amplitudes. However, the measured results show much greater variation with diameter. The measured results show the 10mm diameter tube as having the highest $SC4$ value, and a sharp drop in the spectral centroid for the 8mm diameter. There is also a decrease in $SC4$ for the 12mm and 14mm diameter tubes.

As shown in Figure 6.19 there is a significant difference between measured and simulated results, with absolute values of the simulated spectral centroid being lower by as much as 30%. The difference between simulated and experimental results might be attributed, at least in part, to the fact that for larger tube diameters the assumption of a monopole radiation source at the tube exit becomes less applicable for the higher frequency components. This does not however explain the similar proportion of difference in the smaller diameter tubes.

To eliminate possible effects resulting from the monopole radiation assumption, the spectral centroid near the mid point of the tube (microphone 3) was also investigated and the corresponding 10mm diameter tube results are shown

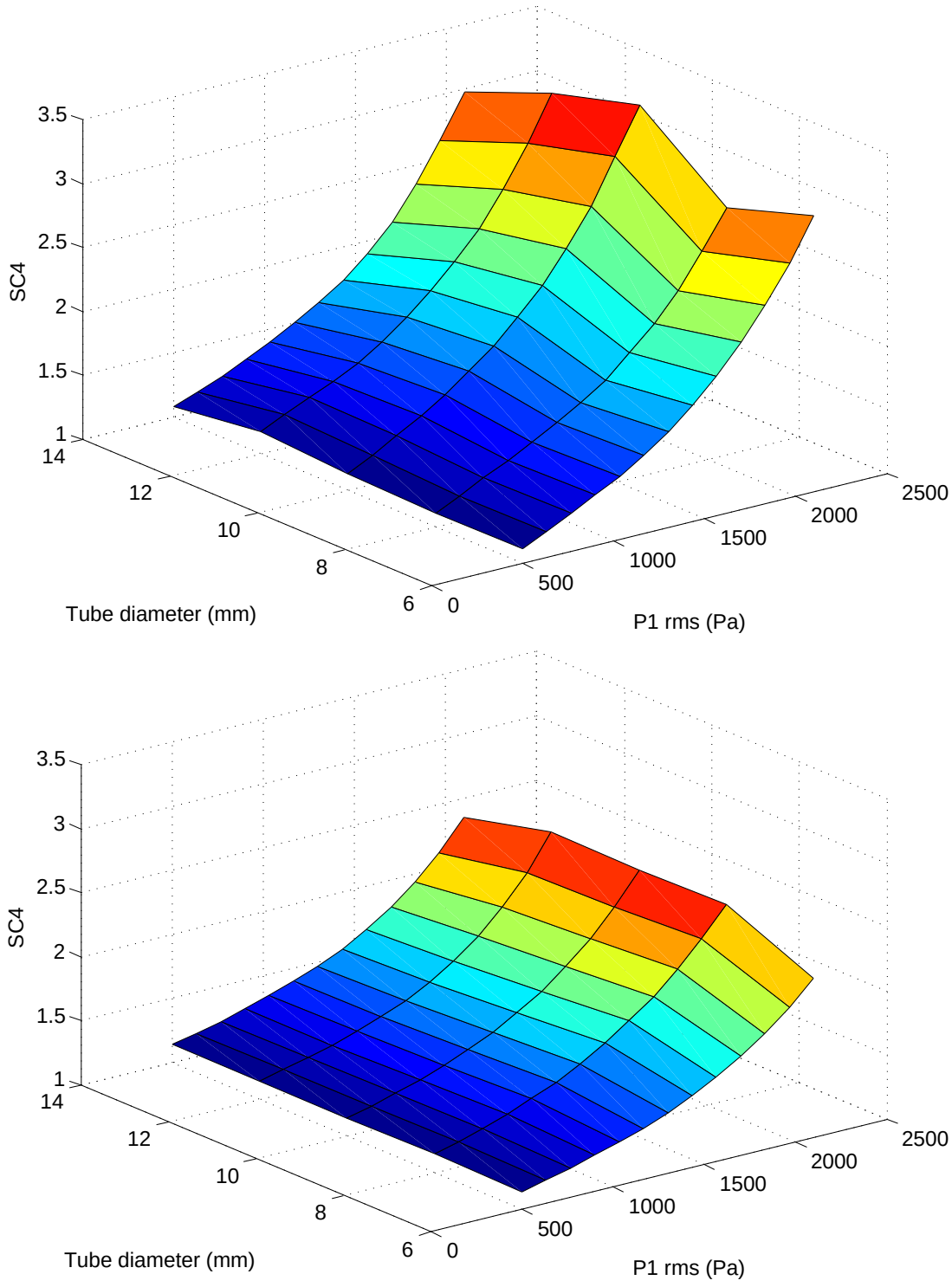

Figure 6.20: Far field spectral centroid of the five tubes (6mm, 8mm, 10mm, 12mm, and 14mm diameter) during an amplitude sweep at frequencies corresponding to a minima of the transfer function. **Top**: Experiment **Bottom**: Simulation

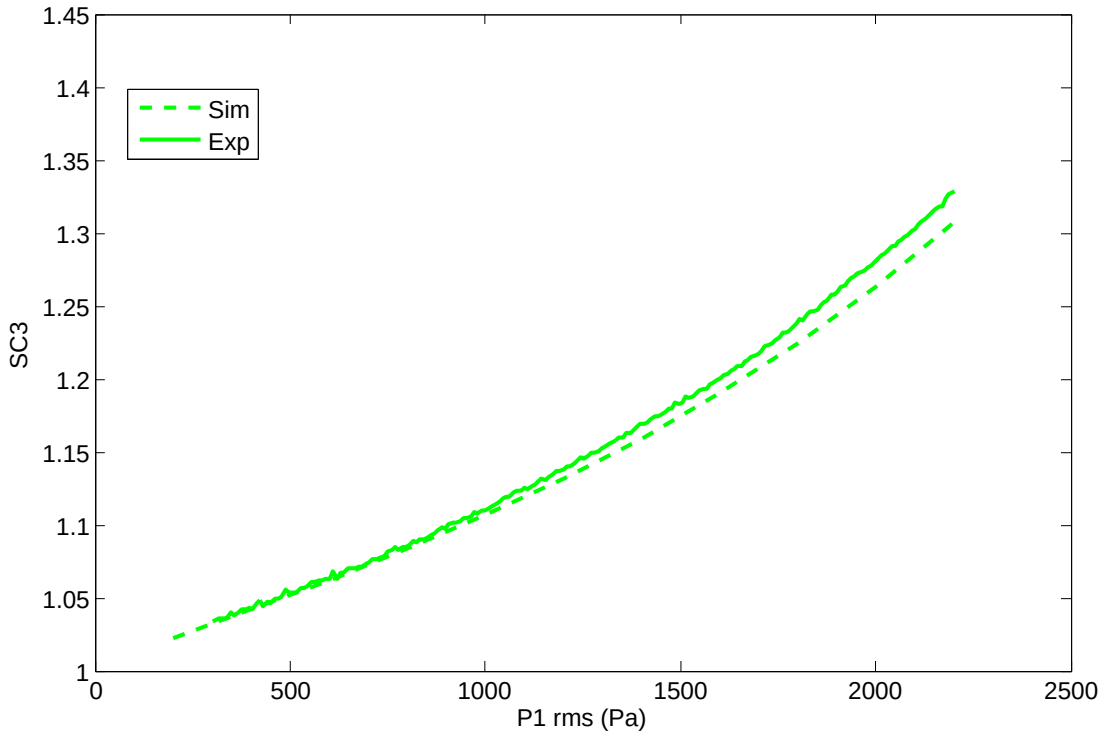

Figure 6.21: Internal spectral centroid of the 10mm diameter tube during an amplitude sweep at frequencies corresponding to a minima of the transfer function, showing experiment and simulation results.

in Figure 6.21. It can be seen here that the measured and simulated $SC3$ results are significantly more consistent than those of $SC4$ that were shown in Figure 6.19. Both the measured and simulated spectral centroid results have a maximum between 1.3 and 1.35 for the highest input pressure amplitudes. Again the results for each individual tube can be seen in Appendix B.

Figure 6.22 shows the dependence of $SC3$ on tube diameter. There is much less variation with diameter for the internal spectral centroid results than the far field. The maximum spectral centroid for all measured and simulated results is shown to be approximately 1.3, except the measured 6mm diameter tube result, which is slightly higher. The 6mm tube did however show slightly anomalous results in the transfer function.

In both Figures 6.20 and 6.22, showing the internal and far field spectral centroid results, there is no discernable trend relating the spectral centroid to tube diameter. This could be attributed to the small phase differences that occur from having tuned the measurement frequencies to be at transfer function minima.

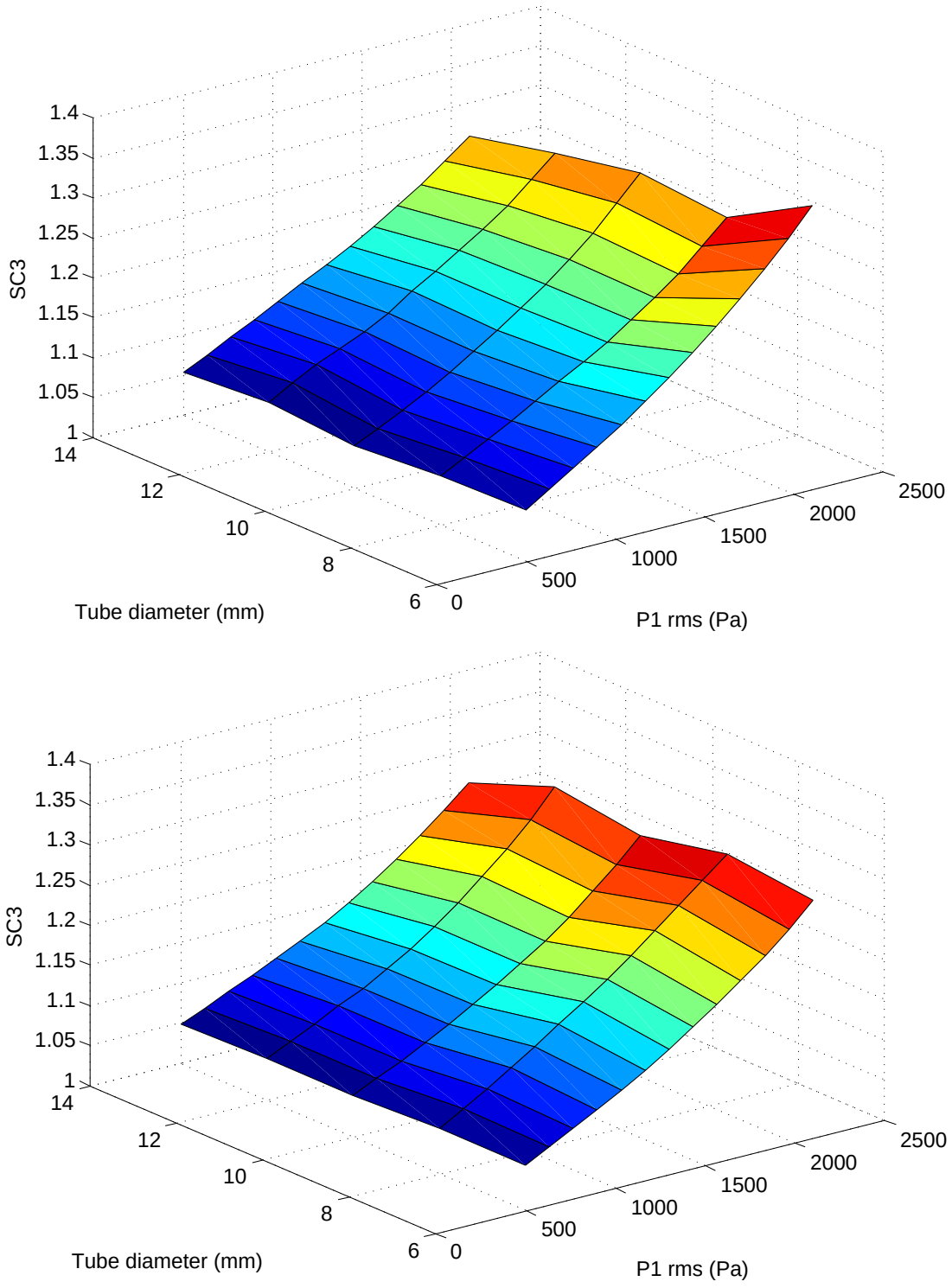

Figure 6.22: Internal spectral centroid of the five tubes (6mm, 8mm, 10mm, 12mm, and 14mm diameter) during an amplitude sweep at frequencies corresponding to a minima of the transfer function. **Top**: Experiment **Bottom**: Simulation

To eliminate these possible phase differences simulations were carried out using a pure sinusoidal input signal at a constant frequency of 764Hz. A larger range of tube diameters than measured experimentally was chosen to explore the overall effect on spectral centroid of varying diameter. Figure 6.23 shows simulated results of the spectral centroid calculated in the radiation field, 20cm from the tube exit on axis, assuming monopole radiation.

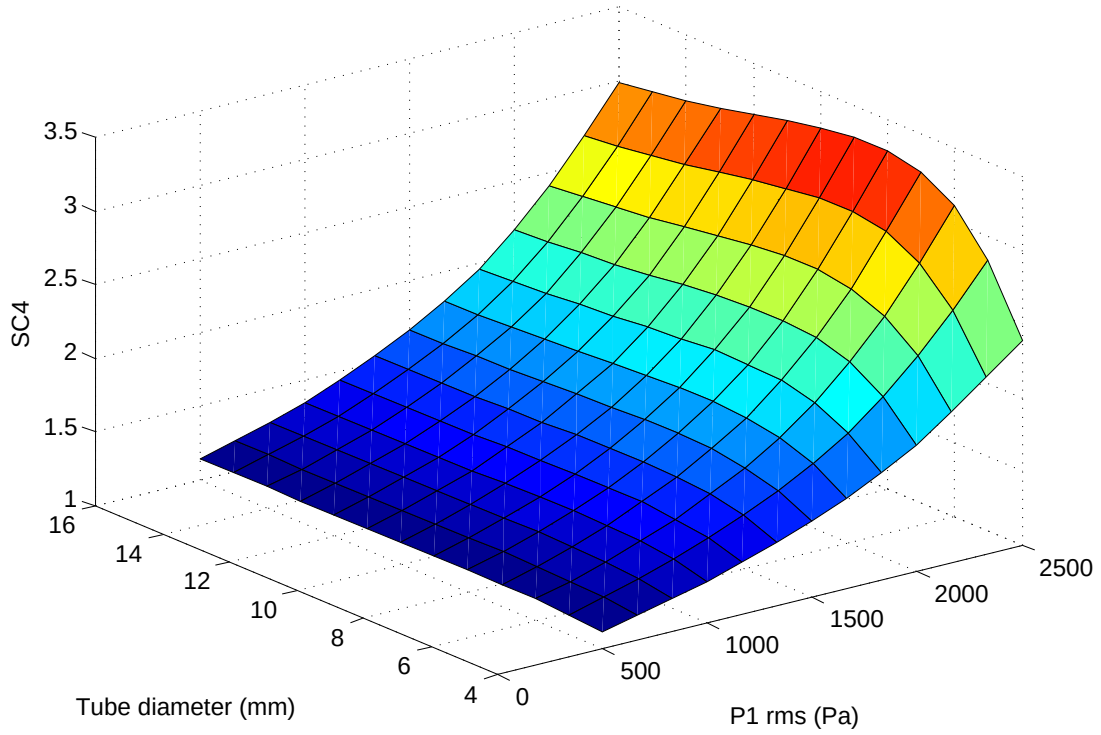

Figure 6.23: Simulated far field spectral centroid of tubes ranging in diameter from 4 - 16mm during an amplitude sweep at 764Hz.

It can be seen here that for high amplitude input signals there is a small but significant increase in the value of the spectral centroid with decreasing tube diameter, to a maximum point at 9 - 10mm diameter. The spectral centroid then falls off rapidly as the tube diameter decreased further. We might expect that for the same pressure amplitude at the input of the tube, and neglecting losses, the nonlinear distortion should be independent of tube diameter and hence produce similar spectral centroid values. However, this is not what is seen here.

This can be explained by the fact that, for larger diameter tubes, where wall losses are very small, for a constant input pressure at a transfer function

minima, the forward going wave and backward going wave will have similar amplitudes (and noting that the measured input pressure, $P1$, is the sum of the forward and backward going wave). As the tube diameter decreases, the wall losses increase and thus the contribution of the backward going wave to the input pressure is reduced. An increase in the amplitude of the forward going wave is then required to achieve a given value of $P1$, increasing the level of nonlinear distortion and hence increasing spectral centroid seen in Figure 6.23, reaching a maximum for the 9mm diameter tube. As tube size continues to decrease, the effect of viscothermal losses becomes the dominant effect and their damping of high frequency components is more prominent than the addition of these components due to nonlinear distortion.

In relation to real brass instruments, this could be why brass instruments are manufactured to have bore diameters in this range - any smaller than this and the wall losses take over, any larger and the amount of energy needed by the player to produce the same output pressure is too much because of the bigger diameter.

6.6 Conclusions

This chapter presented an experimental setup using cylindrical tubes as simple brass instruments, with a forced oscillation input, to explore the relative significance of viscothermal losses and nonlinear wave steepening within brass instruments. The analysis was split into two sets of results; transfer function and spectral centroid.

It was shown that the transfer function between the entrance to the tube and 5cm inside the tube, $T12$, was between 0.8 and 1 for all the tubes. The 6mm diameter tube showed the highest transfer function result at 1, suggesting that the viscothermal losses are dampening the pressure wave so much so that the amplitude difference between the nodes and antinodes is small. The simulation showed a similar result but with all five tubes results giving lower $T12$ results.

The transfer function between the entrance and the radiation measurement point, $T14$, showed clearly that the transfer function decreased with tube diameter. This is as expected, with the larger diameter tubes having a larger radiated pressure and less significant viscothermal losses. The simulation results showed very good qualitative results, but for all tubes, except the 6mm diameter,

had a smaller transfer function value. The assumed reason for this is that the monopole radiation approximation in the simulation is over simplified.

To eliminate the possible complications caused by the radiation model the internal transfer function, $T23$, was examined. In this case, the simulation results were larger than the experimental results for all tubes, suggesting that the losses are under predicted in the simulation. The radiated spectral centroid, $SC4$, showed that the simulation results had little dependence on tube diameter, while the measured results did to some extent. The simulation showed a lower spectral centroid value for each tube at the highest amplitudes. For the largest diameter tubes this effect could be due to the monopole radiation approximation, but this does not explain the difference for the smaller diameter tubes.

The internal spectral centroid, $SC3$, results are more consistent between simulation and experiment, and also show less variation with diameter. There is no clear trend associated with tube diameter for either the $SC4$ or $SC3$ results; it is thought that this could be because of phase differences arising due to the tuning of the measurement frequency for each individual tube. When we consider the associated error in the frequency of the transfer function minima, and the experimental errors discussed in Section 6.2.8 it becomes difficult to analyse the meaning of trends within such a small range. It is possible that, at the highest input amplitudes, these results could show a significantly different trend if the experimental errors are approaching the outermost bound of 6%. To eliminate phase difference effects the simulation was carried out at the same chosen frequency for a larger range of diameter tubes; these results showed that there is a peak in the spectral centroid around the 9mm and 10mm diameter tubes, with a rapid decrease for the smaller diameter tubes where the viscothermal losses become the dominant factor. There is also a drop in spectral centroid for the larger diameter tubes which is thought to be because of the extra energy needed by the player to produce a higher value spectral centroid.

Chapter 7

Conclusions and future work

7.1 Analysis of the mechanics and computational modelling of slurred transients

Chapters 3 and 4 have discussed experimental and computational approaches to slurred transients on brass instruments. It was found experimentally that players who, on the horn, employ different playing techniques do indeed show different characteristics in the results. In the lower register is is possible for players to smoothly and discreetly stop the first note and move to the second note. It was very surprising to find that it is possible for the frequency of the lips to change from one note, to an octave higher, within the time taken for one cycle. The player's lips are still very much an unknown quantity in the brass instrument system, with even the players not having a full understanding of how their lips are moving. It would have seemed unlikely that the player was able to manipulate the the lips such that the frequency of oscillation could change so quickly and produce a smooth sounding slur. It was also found that different horns did not make a difference to the characteristics of the results, showing that the player can implement their chosen technique on different instruments. Good players are very adept at manipulating the sound from an instrument to what they wish it to sound like. While a beginner, given a high quality instrument, will most likely struggle to make it sound flawless, an accomplished player will be able to make a low quality instrument sound good.

It was found that, although different players show different characteristics in the instantaneous frequency results, both player's results showed differences

when octave slurs were played in different registers, and also when being slurred upwards or downwards in frequency. While in the lower register the results varied with player and slur direction, in the upper register all slurs showed very similar frequency characteristics; it is not fully understood why this should be the case.

The computational model has been shown to be a useful tool in exploring such transients, and very successfully model the instrument in the case of forced oscillation. When employing the lip model, but not including viscothermal losses, the model did show reasonable results but these did not show the same subtle frequency characteristics of the player results during the transition.

7.1.1 Future work

This work has only scratched the surface of exploration into slurred transients on brass instruments. Firstly, presented here was only a small number of measurements, mainly on the horn by two different players. To fully understand transients, both starting and slurred, a much fuller set of experiments is required with a larger number of players, instruments and notes. Although it is advantageous to study competent players to ascertain what makes a good sound, it would also be very interesting, and hopefully enlightening, to study a wide range of players with varying skill levels. Is is also essential to study not only transitions that are deemed good, an exploration of the mechanics behind a 'split' note would be insightful.

This work was also concerned only with lip-slurs. There are a wide range of brass instruments that use different types of valves to move between different notes. Musicians are required to make any transition, that is marked as a slur, sound smooth and seamless, whether this be through the use of valves or solely through adjusting the lips and blowing characteristics.

An understanding of the player's lips and embouchure are vitally important in achieving a full understanding of transients, but so equally are other areas. Little is known about what is happening in the player's mouth cavity and tongue during transients. Ideally, the pressure would be measured at numerous points throughout the player/instrument system, including at various points along the instrument bore.

The computational model work presented here was only preliminary and the scope this could be used for is far reaching. Further work involving the model

includes using simplified player data as an input in the latest version of the model that contains treatment of the viscothermal losses. The input parameters for the lip model also need more work to deduce the correct and best values for these.

As previously discussed, players use transients to assess the quality of instruments. A computational model allows the bore profile to be modified without modifying the physical instrument. It would therefore be interesting to use the model to add defects to the instrument, a dent for example, and investigate how this would affect a transient played on the instrument.

7.2 Extreme high notes

Extreme high notes on trumpets were explored in Chapter 5. There has long been much mystery in the trumpet community over extreme high notes and how players go about playing these notes. Some players have theories as to why it is possible, whereas other believe it is simply a progression from the lower notes that requires pressing the lips tighter and blowing harder. This work showed the input impedance of a trumpet/mouthpiece combination that is used by players wishing to play in the highest register of the trumpet. It is clear from the input impedance that the peaks become much less significant above the 12^{th} resonant mode, and almost undiscernible above the 15^{th}.

Measurements of the transfer function of the same instrument and mouthpiece showed that between the 12^{th} and 16^{th} resonant mode frequencies there were clearly defined peaks and troughs in the results.

Using a similar high speed photography technique as for the transients work, a specialist player's lips were filmed playing the 8^{th} and the 12^{th} resonant modes. These results showed nothing out of the ordinary, in that the lips were opening and closing periodically at the sounding frequency.

7.2.1 Future work

In the high speed photography work, the mouthpiece used must be one which is chosen for high note playing. Although the mouthpiece used was transparent and had the outer cup wall machined down, the optical access was not optimal as the lips were viewed from an angle slightly off centre. For better quantitative results

the optical access to the lips needs to be improved, while retaining the specific mouthpiece dimensions.

It was also found by the player that the setup was not entirely comfortable, and for this reason there are no results shown higher than the 12^{th} resonant mode. Further work on this topic should include high speed filming of the lips at higher frequencies, taking in the 'super C' note.

It would also be interesting to investigate the lips in the third dimension. The lips protrude into the mouthpiece during playing and it would be interesting to explore in 3-dimensions the differences in lip motion at the highest playable frequencies.

7.3 Cylindrical tubes as a simple brass instrument

Chapter 6 presented experiments on cylindrical tubes, using a forced oscillation input, to investigate the relative importance of viscothermal losses and nonlinear distortion during amplitude sweeps.

The transfer function results showed that when analysing the difference between pressure signals in the radiation field, and at the entrance to the tube, the transfer function decreased with tube diameter. This shows that the smaller diameter tubes do indeed have more significant viscothermal losses than the larger diameter tubes, and that the larger tubes radiate the sound more effectively.

The spectral centroid showed that in the radiation field the results did differ with tube diameter but with no discernable trend. The internal spectral centroid, however, showed much less variation with diameter.

The computational simulation results showed generally good comparisons with the experimental data but the differences were taken to show that the monopole radiation approximation is not fully adequate, and that the viscothermal losses are under estimated.

When using the computational program to simulate tubes of diameters from 4mm to 16mm, at a fixed input frequency, it was found that there was a peak in the radiated spectral centroid at around 9-10mm. The spectral centroid drops off steadily at larger diameters and rapidly at smaller diameters. This is very interestingly related to real brass instruments - if these diameters are the optimum

for a brass instrument, this could be why brass instruments are manufactured with diameters around these values.

7.3.1 Future work

The simulation program has been shown to, on the whole, successfully model what is seen experimental. It would be interesting to explore the effects of changing the viscothermal loss parameters in the simulation to ascertain what value would be needed to produce results in line with those seen experimentally. The monopole radiation approximation is also a possible reason for inconsistencies between the simulation and experimental results as it is a simplified approximation of that radiation.

The obvious extension of this work is to move onto experimentally investigating real instruments, namely trombones as the tubes used here were chosen as a very simple trombone like instrument. It would be advantageous to explore in more detail the radiation field, in the anechoic chamber, from the end of the cylinders. With a more careful analysis of the radiation at different frequencies, possible reasons for the monopole model not being satisfactory could be explored.

This thesis has used a number of experimental techniques, along with computational simulations, to investigate various different issues within brass instrument acoustics, that are as yet not fully understood. There is still great scope for further analysis of these issues, that will hopefully lead to a full understanding of the playability of instruments and how this relates to the choices made by players on instruments. It is, understandably, difficult for players to verbalise and quantify their feelings on different instruments and the motion and dynamics of the lips during playing. Hopefully a full understanding of playability, and possibly the development of a playability factor, can be formed which will aid players, and makers alike, in the future.

Appendix A

Transients - narrow bore horn

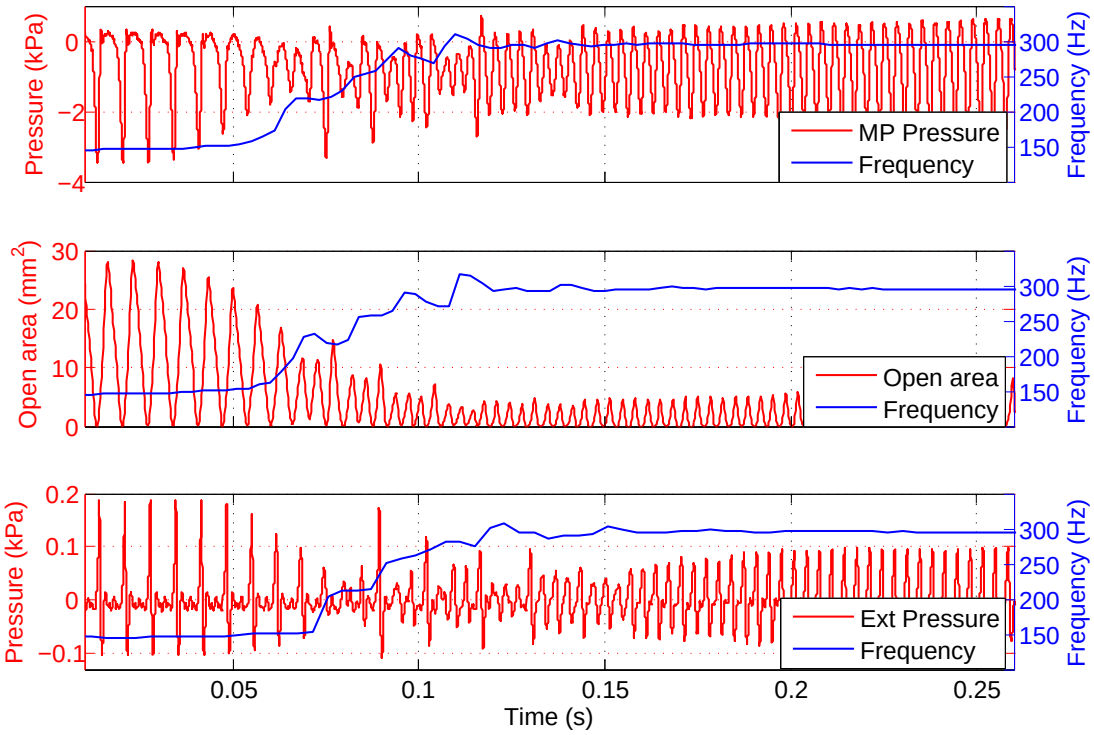

Figure A.1: Synchronised signals for lip-slur from D_3 to D_4 by Player A, on narrow bore horn by Boosey and Hawkes. **Top**: Mouthpiece pressure **Middle**: Lip open area **Bottom**: Radiated pressure.

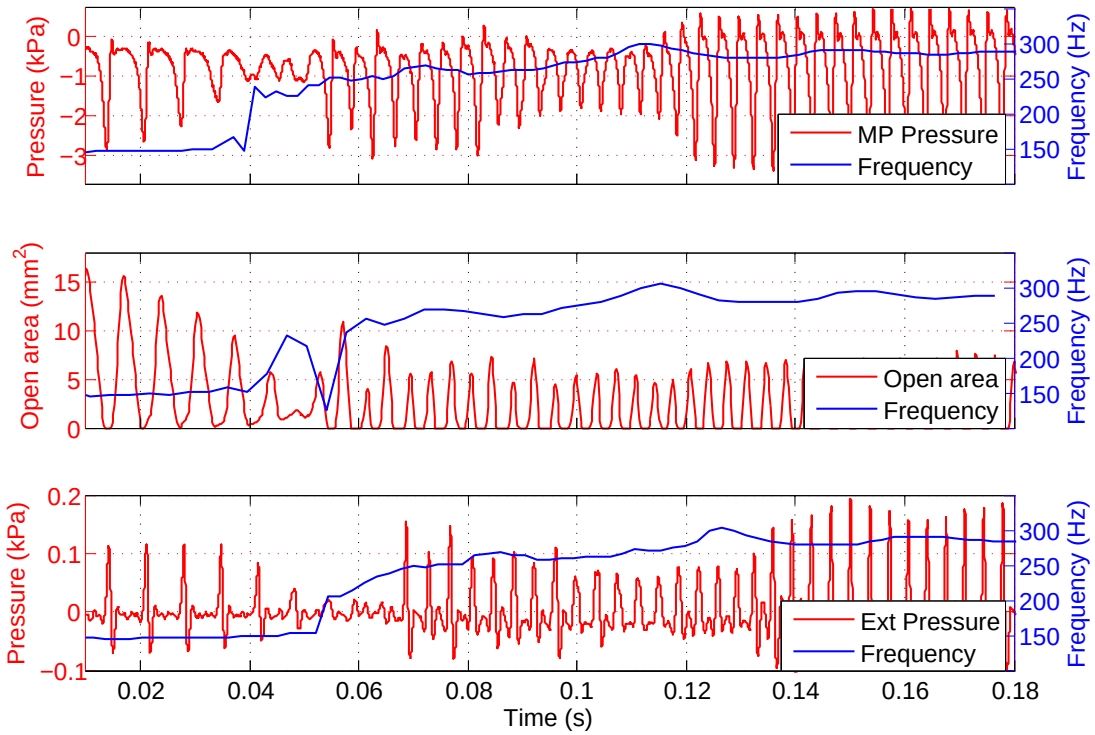

Figure A.2: Synchronised signals for lip-slur from D_3 to D_4 by Player B, on narrow bore horn by Boosey and Hawkes. **Top**: Mouthpiece pressure **Middle**: Lip open area **Bottom**: Radiated pressure.

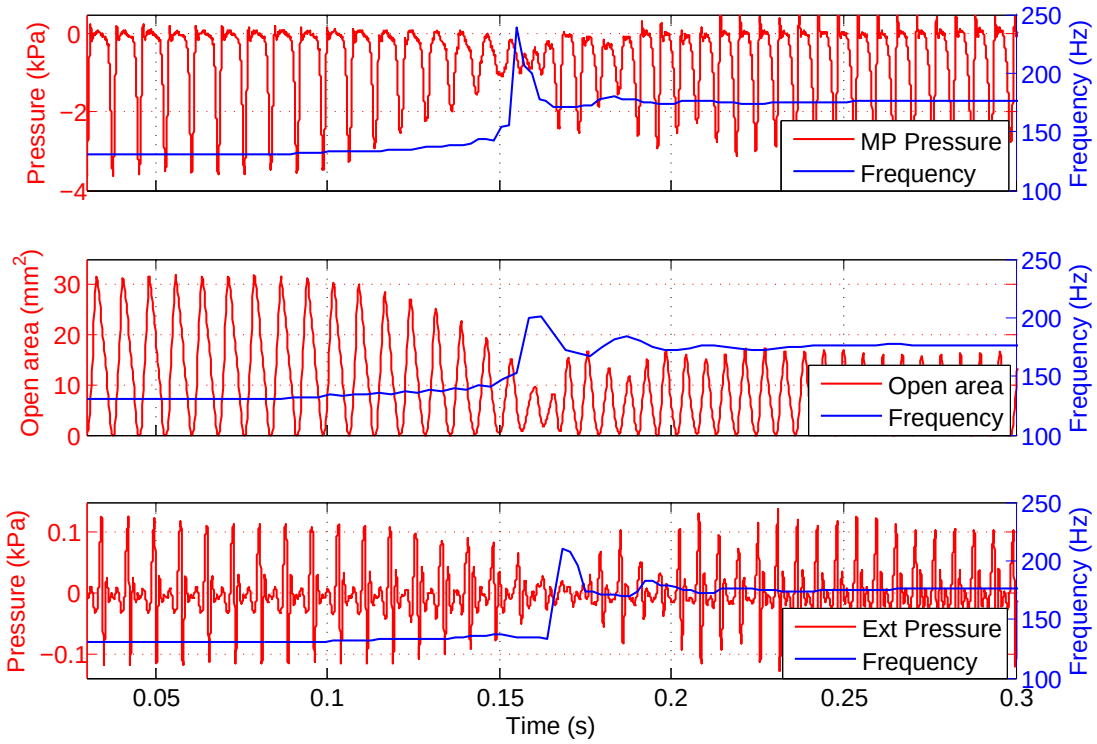

Figure A.3: Synchronised signals for lip-slur from C_3 to F_3 by Player A, on narrow bore horn by Boosey and Hawkes. **Top**: Mouthpiece pressure **Middle**: Lip open area **Bottom**: Radiated pressure.

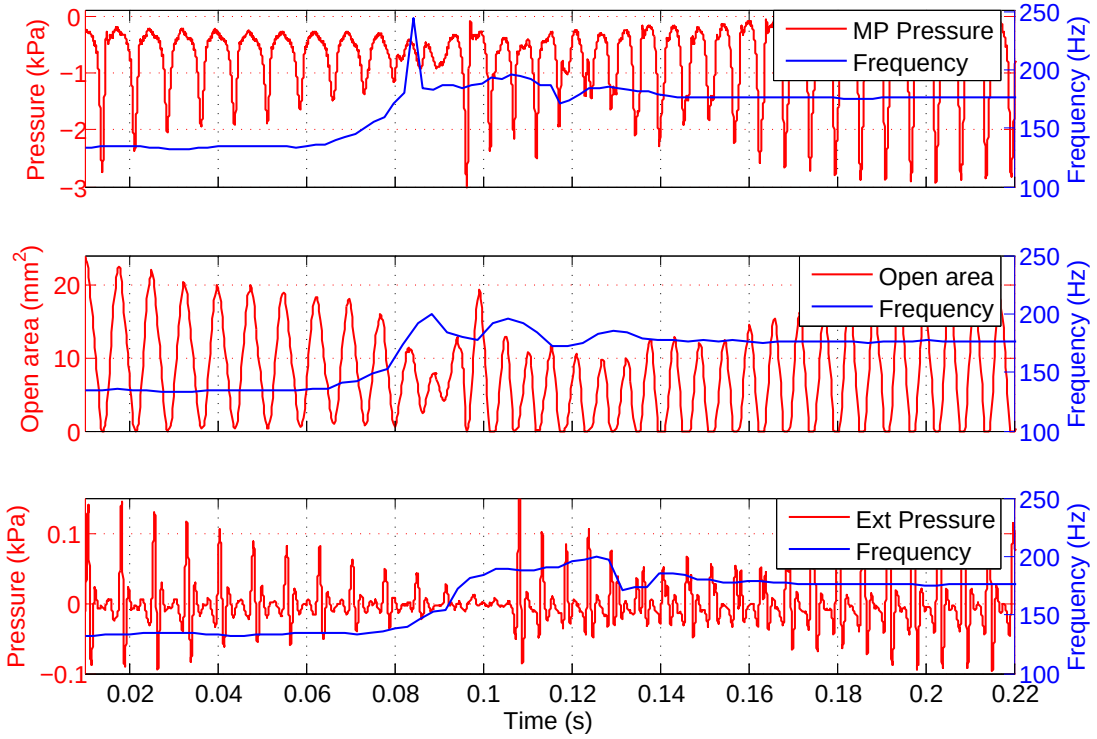

Figure A.4: Synchronised signals for lip-slur from C_3 to F_3 by Player B, on narrow bore horn by Boosey and Hawkes. **Top**: Mouthpiece pressure **Middle**: Lip open area **Bottom**: Radiated pressure.

Appendix B

Cylindrical tubes - spectral centroid

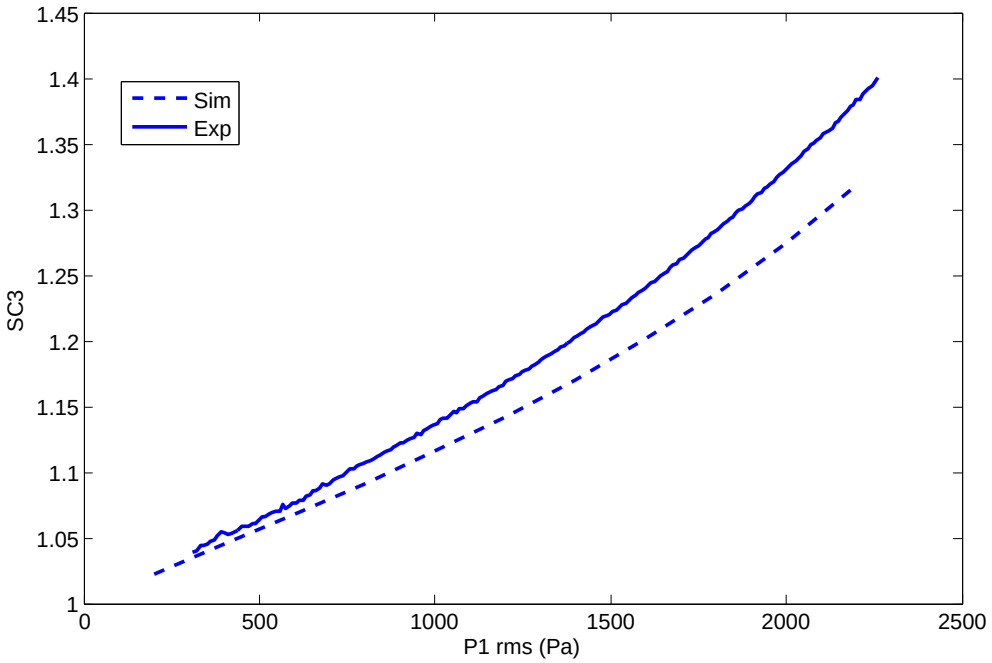

Figure B.1: Internal spectral centroid of the 6mm diameter tube during an amplitude sweep at frequencies corresponding to a minima of the transfer function, showing experiment and simulation results.

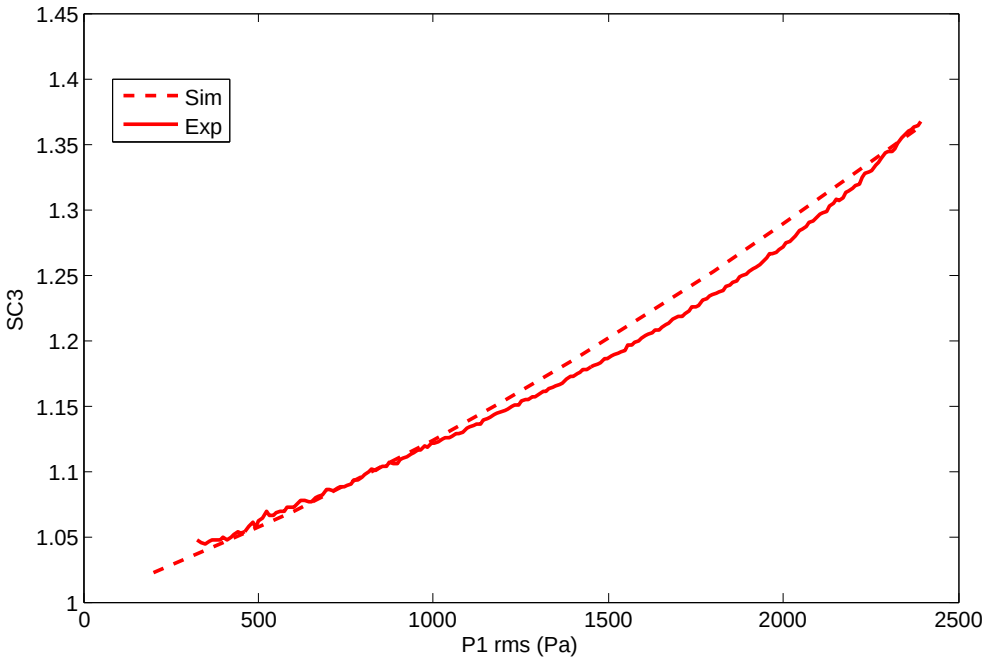

Figure B.2: Internal spectral centroid of the 8mm diameter tube during an amplitude sweep at frequencies corresponding to a minima of the transfer function, showing experiment and simulation results.

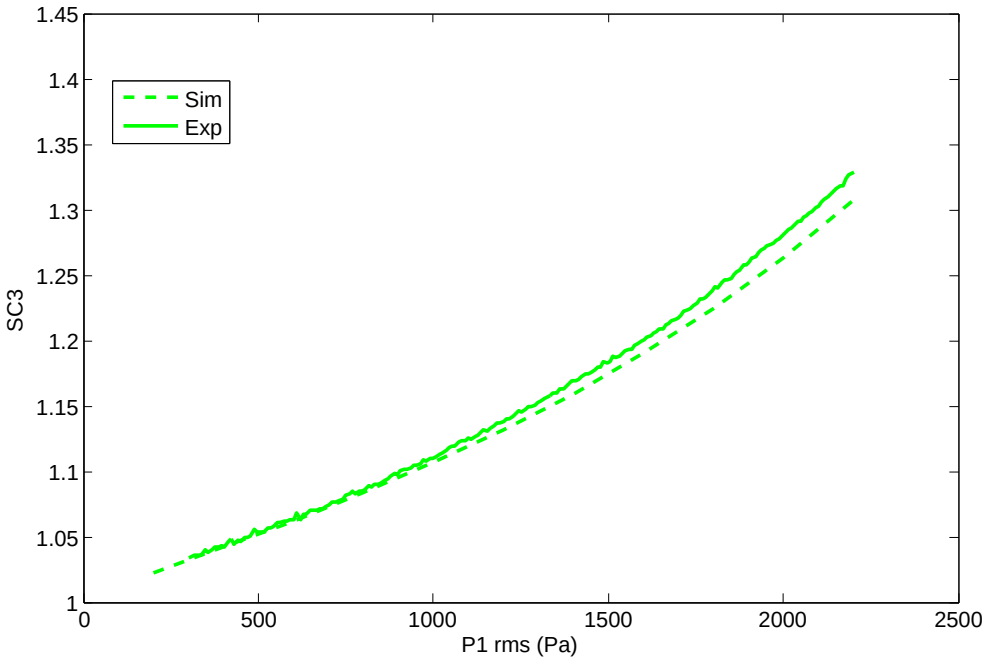

Figure B.3: Internal spectral centroid of the 10mm diameter tube during an amplitude sweep at frequencies corresponding to a minima of the transfer function, showing experiment and simulation results.

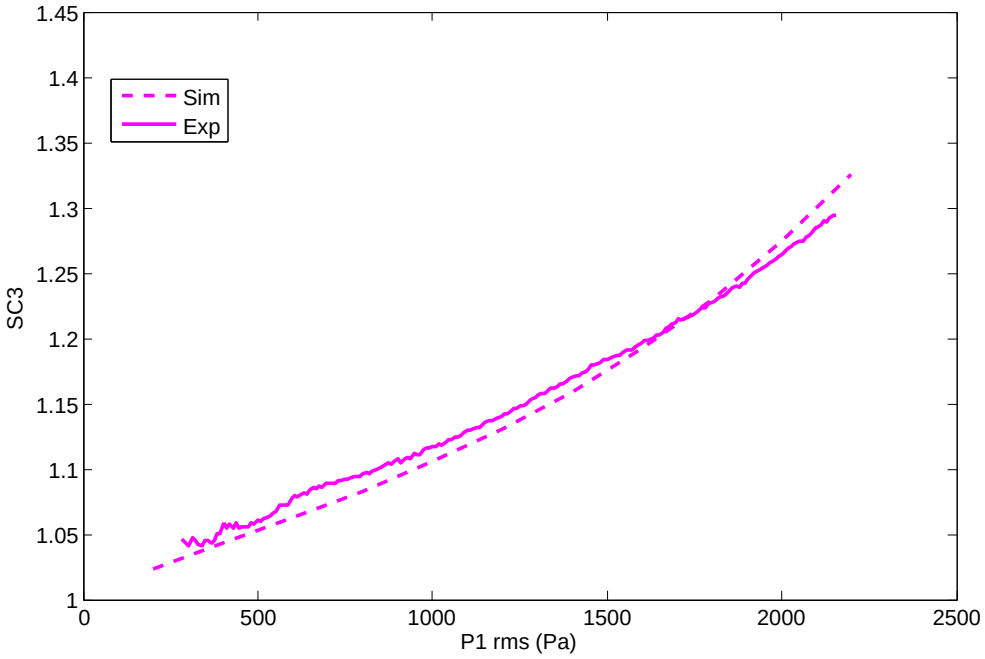

Figure B.4: Internal spectral centroid of the 12mm diameter tube during an amplitude sweep at frequencies corresponding to a minima of the transfer function, showing experiment and simulation results.

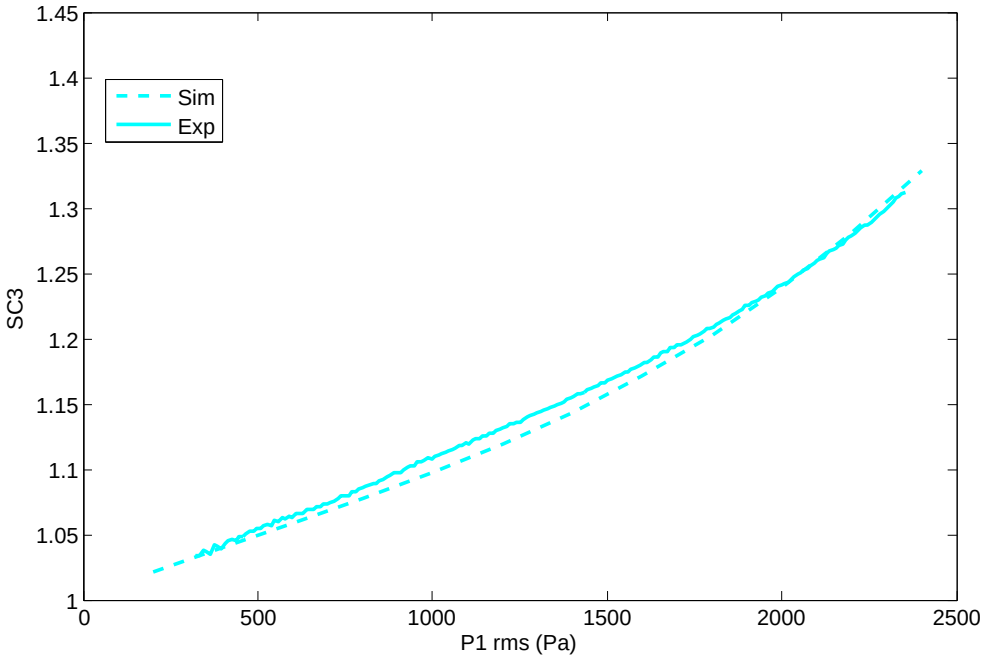

Figure B.5: Internal spectral centroid of the 14mm diameter tube during an amplitude sweep at frequencies corresponding to a minima of the transfer function, showing experiment and simulation results.

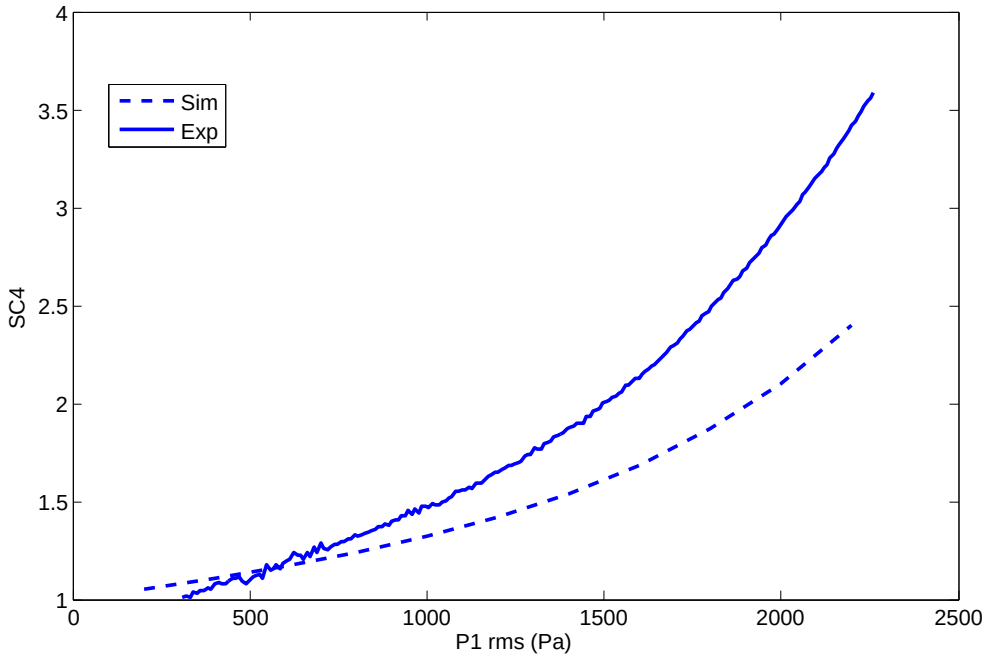

Figure B.6: Far field spectral centroid of the 6mm diameter tube during an amplitude sweep at frequencies corresponding to a minima of the transfer function, showing experiment and simulation results.

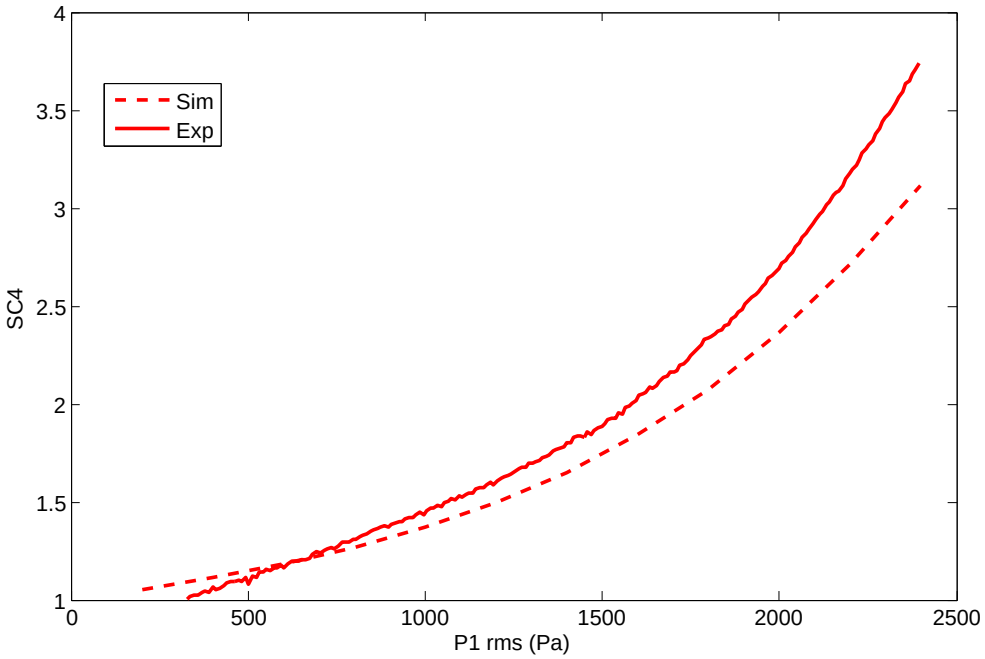

Figure B.7: Far field spectral centroid of the 8mm diameter tube during an amplitude sweep at frequencies corresponding to a minima of the transfer function, showing experiment and simulation results.

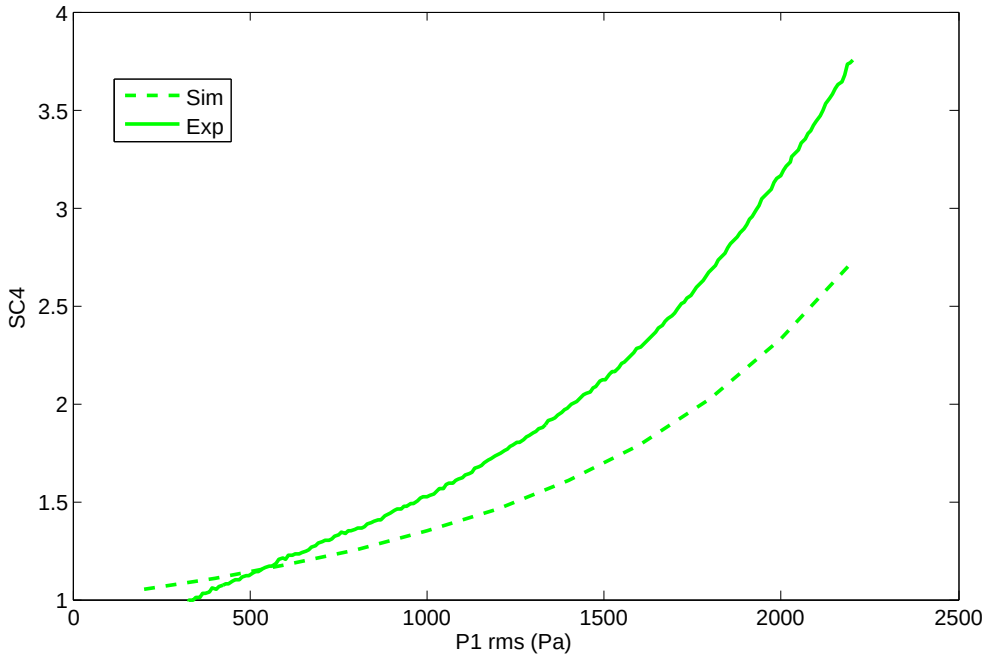

Figure B.8: Far field spectral centroid of the 10mm diameter tube during an amplitude sweep at frequencies corresponding to a minima of the transfer function, showing experiment and simulation results.

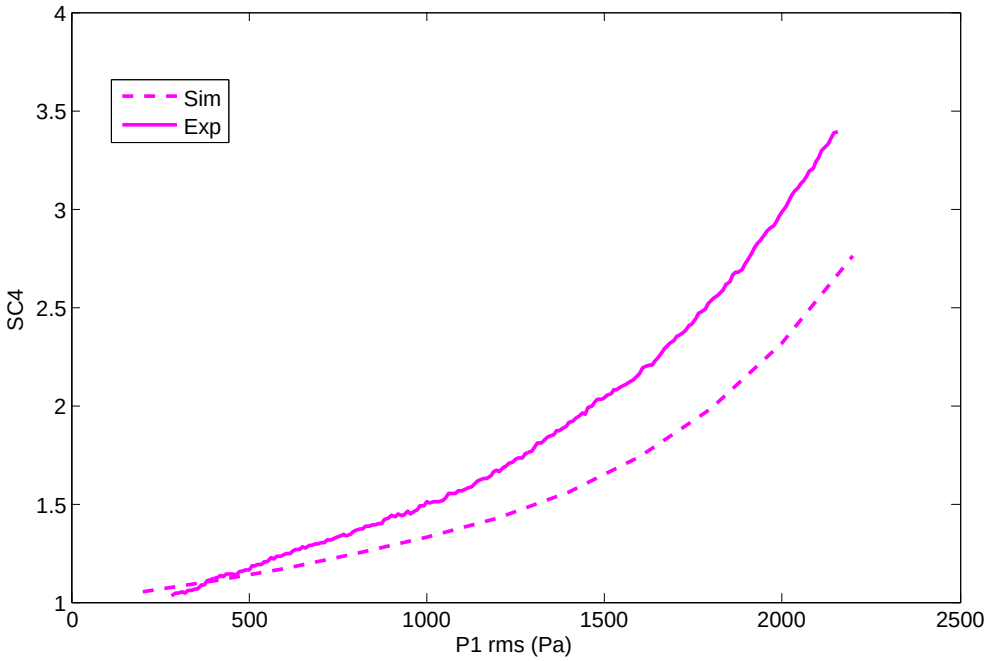

Figure B.9: Far field spectral centroid of the 12mm diameter tube during an amplitude sweep at frequencies corresponding to a minima of the transfer function, showing experiment and simulation results.

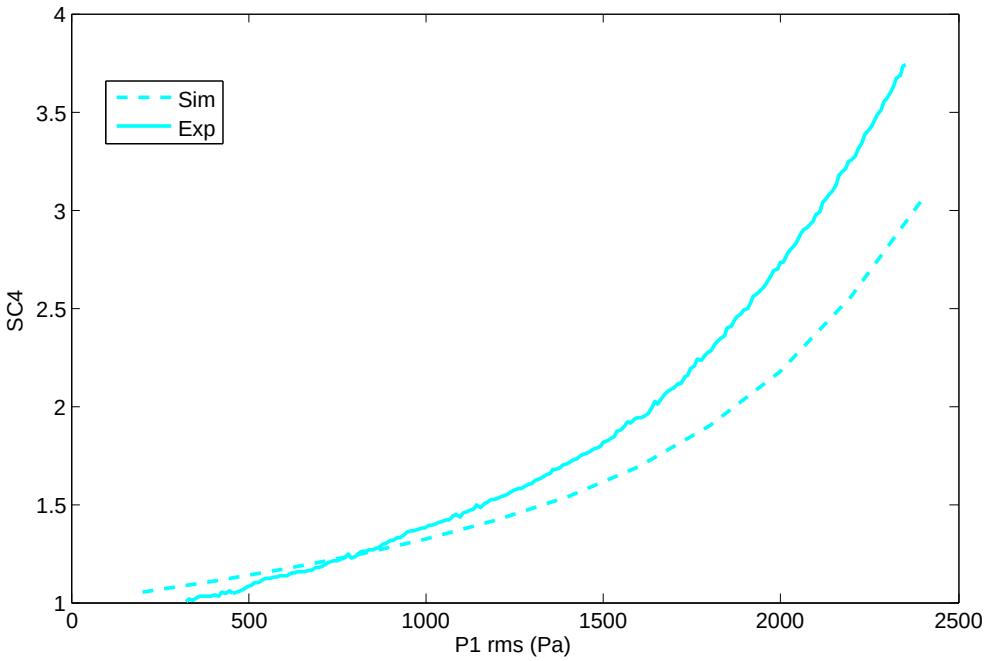

Figure B.10: Far field spectral centroid of the 14mm diameter tube during an amplitude sweep at frequencies corresponding to a minima of the transfer function, showing experiment and simulation results.

Bibliography

[Adachi 96] S. Adachi & M. Sato. *Trumpet sound simulation using a two-dimensional lip vibration model.* J. Acoust. Soc. Am., vol. 99(2), pages 1200–1209, 1996.

[Amir 95a] N. Amir, U. Shimony & G. Rosenhouse. *A discrete model for tubular acoustic systems with varying cross-section - The direct and inverse problems. Part 1: Theory.* Acta Acustica united with Acustica, vol. 81 (5), pages 450–462, 1995.

[Amir 95b] N. Amir, U. Shimony & G. Rosenhouse. *A discrete model for tubular acoustic systems with varying cross-section - The direct and inverse problems. Part 2: Experiments.* Acta Acustica united with Acustica, vol. 81 (5), pages 463–474, 1995.

[Atig 04] M. Atig, J.-P. Dalmont & J. Gilbert. *Termination impedance of open-ended cylindrical tubes at high sound pressure level.* Comptes Rendus Mecanique, vol. 332, pages 299–304, 2004.

[Ayers 98] R. D. Ayers. *New perspectives on brass instruments.* In International Symposium on Musical Acoustics, 1998.

[Backus 71] J. Backus & T.C. Hundley. *Harmonic generation in the trumpet.* J. Acoust. Soc. Am., vol. 45, pages 509–519, 1971.

[Backus 77] J. Backus. The acoustical foundations of music. W.W. Norton & Company Inc., 2 edition, 1977.

[Baines 93] A. Baines. Brass instruments: their history and development. Dover Publications, 1993.

[Beauchamp 80] J. Beauchamp. *Analysis of simultaneous mouthpiece and output waveforms*, 1980.

[Beauchamp 82] J.W. Beauchamp. *Synthesis by spectral amplitude and 'brightness' matching of analyzed musical instrument tones.* J. Audio Eng. Soc., vol. 30, pages 396–106, 1982.

[Benade 59] A.H. Benade. *On woodwind instrument bores.* J. Acoust. Soc. Am, vol. 31, pages 137–146, 1959.

[Benade 69] A.H. Benade. *Effect of dispersion and scattering on the startup of brass instrument tones.* J. Acoust. Soc. Am., vol. 45, pages 296–297, 1969.

[Benade 74] A.H. Benade & E.V. Jansson. *On plane and spherical waves in horns with nonuniform flare.* Acustica, vol. 31, pages 80–98, 1974.

[Benade 76] A.H. Benade. Fundamentals of musical acoustics. Oxford University Press, New York, 1976.

[Berger 64] K.W. Berger. *Some factors in recognition of timbre.* J. Acoust. Soc. Am., vol. 36, pages 1888–1891, 1964.

[BIAS 13] Brass Instrument Analysis System BIAS. *http://www.bias.at, Institute fur Wiener Klangstil, Vienna*, Date last viewed: 16/01/13.

[Bilbao 08] S. Bilbao. *Direct simulation for wind instrument synthesis.* In 11th conference on digital audio effects, Espoo, Finland, 2008.

[Bilbao 09] S. Bilbao. Numerical sound synthesis. Wiley, 2009.

[Bilbao 11] S. Bilbao. *Time domain simulation of brass instruments.* In Proceeding of Forum Acusticum, Aalborg, 2011.

[Blackstock 97] D.T. Blackstock & M.J. Crocker. 'nonlinear acoustics and cavitation' in encyclopedia of acoustics. John Wiley & Sons, New York, 1997.

[Bromage 03] S.R. Bromage, O.F. Richards & D.M. Campbell. *Reproducability and control of the embouchure of and artificial mouth for playing brass instruments.* In Proceedings of the Stockholm Musical Acoustics Conference, 2003.

[Bromage 06] S. Bromage, D.M. Campbell, J. Chick, J. Gilbert & S. Stevenson. *Motion of the brass player's lips during extreme loud playing.* In Proceedings of the 8eme Congres Francais d'Acoustique, 2006.

[Bromage 07] S. Bromage. *Visualisation of the lip motion of brass instrument players, and investigations of an artificial mouth as a tool for comparative studies of instruments.* PhD thesis, The University of Edinburgh, 2007.

[Bruël and Kjær 13] Bruël and Kjær. *http://www.bksv.co.uk/*, Date last viewed: 16/01/13.

[Campbell 87] D.M. Campbell & C. Greated. The musician's guide to acoustics. Oxford Univeristy Press, New York, 1987.

[Campbell 99] D.M. Campbell. *Nonlinear dynamics of musical reed and brass wind instruments.* Contemporary Physics, vol. 40, pages 415–431, 1999.

[Campbell 04] D.M. Campbell. *Brass instruments as we know them today.* Acta Acustica united with Acustica, vol. 90, pages 600–610, 2004.

[Carrall 06] S. Carrall. *Relationship between the physical parameters of musical wind instruments and the psychoacoustic attributes of the produced sound.* PhD thesis, The University of Edinburgh, 2006.

[Causse 84] R. Causse, J. Kergomard & X. Lurton. *Input impedance of brass musical instruments - camparison between experiment and numerical models.* J. Acoust. Soc. Am, vol. 75 no.1, pages 241–254, 1984.

[Chen 96] F. Chen & G. Weinreich. *Nature of the lip reed.* J. Acoust. Soc. Am., vol. 99(2), pages 1227–1233, 1996.

[Cheveigne 02] A. Cheveigne & H. Kawahara. *YIN, a fundamental frequency estimator for speech and music.* J. Acoust. Soc. Am, vol. 111, pages 1917–1930, 2002.

[Copley 95] D.C. Copley & W.J. Strong. *A stroboscopic study of lip vibration in a trombone.* J. Acoust. Soc. Am., vol. 99(2), pages 1219–1226, 1995.

[Cullen 00a] J. Cullen, J. Gilbert & M. Campbell. *Brass instruments: Linear stability analysis and experiments with an artificial mouth.* J. Acoust. Soc. Am., vol. 86, pages 704–724, 2000.

[Cullen 00b] J.S. Cullen. *A study of brass instrument acoustics using an artificial reed mechanism, laser doppler anemometry and other techniques.* PhD thesis, The University of Edinburgh, 2000.

[Dalmont 95] J.P. Dalmont, B. Gazengel, J. Gilbert & J. Kergomard. *Some aspects of tuning and clean intonation in reed instruments.* Applied Acoustics, vol. 46, pages 1155–1180, 1995.

[Dalmont 03] J.P. Dalmont, J. Gilbert & S. Ollivier. *Nonlinear characteristics of single-reed instruments: Quasistatic volume flow and reed opening measurements.* J. Acoust. Soc. Am, vol. 114(4), pages 2253–2262, 2003.

[Dietz 95] P. Dietz & N. Amir. *Synthesis of trumpet tones by physical modelling.* In Proceedings of the International Symposium on Musical Acoustics, Dourdan, France, 1995.

[Elliot 82] S. Elliot & J.M. Bowsher. *Regeneration in brass and woodwind instruments.* J. Sound Vib., vol. 83, pages 181–217, 1982.

[Farkas 56] P. Farkas. The art of french horn playing. Summy-Birchard, 1956.

[Fletcher 93] N.H. Fletcher. *Autonomous vibration of simple pressure-controlled valves in gas flows.* J. Acoust. Soc. Am., vol. 93(4), pages 2172–2180, 1993.

[Fletcher 98] N.H. Fletcher & T.D. Rossing. The physics of musical instruments. Springer-Verland, 2 edition, 1998.

[Fletcher 99a] N.H. Fletcher. *The nonlinear physics of musical instruments.* Rep. Prog. Phys., vol. 62, pages 723–764, 1999.

[Fletcher 99b] N.H. Fletcher & A. Tarnopolsky. *Blowing pressure, power, and spectrum in trumpet playing.* J. Acoust. Soc. Am., vol. 105(2), pages 874–881, 1999.

[Gilbert 97] J. Gilbert & J.-F. Petiot. *Brass instruments: some theoretical and experimental results.* In In Proceedings International Symposium on Acoustics, volume 19, pages 391-400, 1997.

[Gilbert 98] J. Gilbert, S. Ponthus & J.-F. Petiot. *Artificial buzzing lips and brass instruments: experimental results.* J. Acoust. Soc. Am., vol. 104, pages 1627–1632, 1998.

[Gilbert 07] J. Gilbert, D.M. Campbell, A. Myers & R.W. Pyle. *Difference between brass instrument arising from variations in brassiness due to non-linear propagation.* In Proceedings of the International Symposium on Musical Acoustics, Barcelona, 2007.

[Gilbert 08a] J. Gilbert & P. Aumond. *Pedal notes of brass instruments, a mysterious regime of oscillations.* In Proceedings of Acoustics '08, Paris, 2008.

[Gilbert 08b] J. Gilbert, L. Menguy & D.M. Campbell. *A simulation tool for brassiness studies.* J. Acoust. Soc. Am, vol. 123(4), pages 1854–1857, 2008.

[Grey 77] J.M. Grey & J.A. Moorer. *Perceptual Evaluation of Synthesized Musical Instrument Tones.* J. Acoust. Soc. Am., vol. 62(2), pages 454–462, 1977.

[Gromada 13] Gromada. *www.gromada.com*, Date last viewed: 16/01/13.

[Haddar 03] H. Haddar, T. Helie & D. Matignon. *A Webster-Lokshin model for waves with viscothermal losses and impedance boundary conditions: Strong solutions.* Mathematical and Numerical Aspects of Wave Propagation-WAVES 2003, Springer, Berlin, pages 66–71, 2003.

[Hamilton 98] M. Hamilton & D. Blackstock. Nonlinear acoustics. Academic Press, New York, 1998.

[Helie 03] T. Helie. *Unidimensional models of acoustic propagation in axisymmetric waveguides.* J. Acoust. Soc. Am, vol. 114, page 2633, 2003.

[Helmholtz 77] H.J.F. Helmholtz. On the sensation of tone. Translated by A.J. Ellis, reprinted by Dover (1954), 1877.

[Hirschberg 96] A. Hirschberg, J. Gilbert, R. Msallam & A.P.J. Wijnands. *Shock waves in trombones.* J. Acoust. Soc. Am., vol. 99 (3), pages 1754–1758, 1996.

[Kausel 08] W. Kausel & A. Mayer. *More experimental evidence favouring the hypothesis of significant wall vibration influence on radiated horn sound.* In Proceedings of Acoustics '08, Paris, 2008.

[Kausel 10] W. Kausel, D.W. Zietlow & T.R. Moore. *Influence of wall vibrations on the sound of brass wind instruments.* J.Acoust. Soc. Am., vol. 128, pages 3161–3174, 2010.

[Keefe 84] D. Keefe. *Acoustical wave propagation in cylindrical ducts: Transmission line parameter approximations for isothermal and nonisothermal boundary conditions.* J. Acoust. Soc. Am, vol. 75 no.1, pages 58–62, 1984.

[Kelly 62] J.L. Kelly & C.C. Lochbaum. *Speech Synthesis.* In Proceedings of Fourth International Congress on Acoustics, Copenhagen, Denmark, pp. 1-4, Paper G42, 1962.

[Kinsler 00] L.E. Kinsler, A.R. Frey, A.B. Coppens & J.V. Sanders. Fundamentals of acoustics. John Wiley & Sons, 2000.

[Knauss 41] H.P. Knauss & W.J. Yeager. *Vibration of the walls of a cornet.* J. Acoust. Soc. Am., vol. 13, pages 160–162, 1941.

[Lawson 85] B. Lawson & W. Lawson. *Acoustical characteristics of annealed french horn bells.* J. Acoust. Soc. Am., vol. 77, pages 1913–1916, 1985.

[Luce 67] D. Luce & M. Clark. *Physical correlates of brass-instrument tones.* J. Acoust. Soc. Am., vol. 42, pages 1232–1243, 1967.

[Lynch 84] J.H. Lynch. A new approach to altissimo trumpet playing. C.L. Barnhouse Company, 1984.

[Martin 42] D.W. Martin. *Lip vibrations in a cornet mouthpiece.* J. Acoust. Soc. Am., vol. 13, pages 305–308, 1942.

[Mathworks 13] Mathworks. *http://www.mathworks.co.uk/*, Date last viewed: 16/01/13.

[Mignot 09] R. Mignot. *Réalisation en guides d'ondes numériques stables d'un modèle acoustique réaliste pour la simulation en temps-réel d'instruments à vent.* PhD thesis, Telecom-Paris Tech, Paris, France, 2009.

[Moore 05] T.R. Moore, E.T. Shires, I.E.W. Codrey & A. Daniels. *The effect of bell vibrations on the sound of a modern trumpet.* Acta Acustica united with Acustica, vol. 91, pages 578–589, 2005.

[Moore 07] T. Moore, V. Jiawon & D. Zietlow. *How can bell vibrations affect the sound of brass instruments?* J. Acoust. Soc. Am., vol. 121(5), pages 3178–3178, 2007.

[Morse 68] P. Morse & U. Ingard. Theoretical acoustics. Princeton University Press, Princeton, New Jersey, 1968.

[Msallam 00] R. Msallam, S. Tassart, R. Causse & S. Dequidt. *Physical model of the trombone including non-linear propagation effects: application to the sound synthesis of loud tones.* Acta Acustica united with Acustica, vol. 86, pages 725–736, 2000.

[Myers 07] A. Myers, J. Gilbert, R.W. Pyle & D.M. Campbell. *Non-linear propagation characteristics in the evolution of brass musical instrument design.* In 19th International Congress on Acoustics, Madrid, 2007.

[Myers 12] A. Myers, R.W. Pyle, J. Gilbert, D.M. Campbell, J.P. Chick & S. Logie. *Effects of nonlinear sound propagation on the caracteristic timbres of brass instruments.* J. Acoust. Soc. Am, 2012.

[National Instruments 13] National Instruments. *http://www.ni.com/labview/*, Date last viewed: 16/01/13.

[Neal 01] M.A. Neal, O.F. Richards, D.M. Campbell & J. Gilbert. *Study of the reed mechanism of brass instruments using an artificial mouth.* In Proceedings of the International Symposium on Musical Acoustics, Perugia, Italy, 2001.

[Newton 08] M. Newton, D.M. Campbell & J. Gilbert. *Mechanical response measurements of real and artificial brass players lips.* J. Acoust. Soc. Am., vol. 123(1), pages EL14–EL20, 2008.

[Newton 09] M.J. Newton. *Experimental mechanical and fluid mechanical investigations of the brass instrument lip-reed and the human vocal folds.* PhD thesis, University of Edinburgh, 2009.

[Nief 08] G. Nief, F. Gautier, J.-P. Dalmont & J. Gilbert. *External sound radiation of vibrating trombone bells.* In Proceedings of Acoustics '08, Paris, 2008.

[Pandya 03] B.H. Pandya, G.S. Settles & J.D. Miller. *Schlieren imaging of shock waves from a trumpet.* J. Acoust. Soc. Am, vol. 114 (6), pages 3363–3367, 2003.

[Petiot 03] J.-F. Petiot, F. Tessier, J. Gilbert & D.M. Campbell. *Comparitive analysis of brass wind instruments using and artificial mouth: First results.* Acta Acustica united with Acustica, vol. 89, pages 103–106, 2003.

[Plitnik 99] G.R. Plitnik & B.A. Lawson. *An investigation of correlations between geometry, acoustic variables, and psychoacoustic parameters for French horn mouthpieces.* J. Acoust. Soc. Am, vol. 106(2), pages 1111–1125, 1999.

[Pyle 98] R.W. Pyle. *The effect of wall materials on the timbre of brass instruments.* In Proceedings of the 16th International Congress on Acoustics and 135th JASA Meeting, Seattle, 3:751-752, 1998.

[Rabiner 78] L. Rabiner & R. Schafer. Digital processing of speech signals. Prentice-Hall, Englewood Ciffs, New Jersey, USA, 1978.

[Richards 03] O.F. Richards. *Investigation of the lip reed using computational modelling and experimental studies with an artificial mouth.* PhD thesis, The University of Edinburgh, 2003.

[Saldanha 64] E.L. Saldanha & J.F. Corso. *Timbre cues and the identification of musical instruments.* J. Acoust. Soc. Am., vol. 36, pages 2021–2026, 1964.

[Saneyoshi 87] J. Saneyoshi, H. Teramura & S. Yoshikawa. *Feedback oscillations in reed woodwind and brasswind instruments.* Acta Acustica united with Acustica, vol. 62, pages 194–210, 1987.

[Smith 78] R.A. Smith. *Recent developments in trumpet design.* International Trumpet Guild Journal, vol. 3, pages 1–8, 1978.

[Smith 86] R. Smith. *The effect of material in brass instruments: a review.* In Proceedings of the Inst. of Acoust. Vol (8), pages 91-97, 1986.

[Smith 87] R. Smith. *Holographs of bell vibrations.* Nature, vol. 329, page 762, 1987.

[SmithWatkins 13] SmithWatkins. *http://www.smithwatkins.com*, Date last viewed: 16/01/13.

[Stevenson 09a] Stevenson. *An experimental investigation of the lips of brass instrument musicians during extremely loud playing and the starting transient.* PhD thesis, University of Edinburgh, 2009.

[Stevenson 09b] S. Stevenson, D.M. Campbell, J. Chick, J. Gilbert & S. Bromage. *Motion of the lips of brass players during extremely loud playing.* J. Acoust. Soc. Am., vol. 125(4), pages EL152–EL157, 2009.

[Thompson 01] M.W. Thompson & W.J. Strong. *Inclusion of wave steepening in a frequency-domain model of trombone sound production.* J. Acoust. Soc. Am., vol. 110 (1), pages 556–562, 2001.

[Vergez 00] C. Vergez & X. Rodet. *New algorithm for nonlinear propagation of a sound wave, application to a physical model of a trumpet.* J. Siganl Process, vol. 4, pages 79–87, 2000.

[Vision Research Inc 13] Vision Research Inc. *http://www.visionresearch.com*, Date last viewed: 16/01/13.

[Webster 19] A. Webster. *Acoustical impedance, and the theory of horns and of the phonograph.* In Proceedings of the National Academy of Sciences of the United States of America, 5(7):275-282, 1919.

[Whitehouse 08] J. Whitehouse & D. Sharp. *A psychoacoustical investigation into the effect of wall material on the sound produced by lip-reed instruments.* In Proceedings of Acoustics '08, Paris, 2008.

[Widholm 97] G. Widholm. *The influence of valve mechanism on the microstructure of slurs played with brass wind instruments.* In Proceedings of the Institute of Acoustics, Edinburgh, volume 19 (part 5), pages pp.407-412, 1997.

[Widholm 05] G. Widholm. *The vienna horn - a historic relic successfully used by top orchestras of the 21st century.* In Proceedings of Forum Acusticum Budapest, pages 441-445, 2005.

[Yoshikawa 95] S. Yoshikawa. *Acoustical behaviour of brass player's lips.* J. Acoust. Soc. Am., vol. 97, pages 1929–1939, 1995.

[Young 60] F.J. Young. *The natural frequencies of musical horns.* Acustica, vol. 10, pages 91–97, 1960.

Publications

S.M. Logie, S. Stevenson, A.G. Apostoli, J.P. Chick, and D.M. Campbell. Transient behaviour in the motion of the brass player's lips during a lip-slur. In Proceedings *NAG/DAGA International Conference on Acoustics, Rotterdam, Netherlands*, 2009.

A.G. Apostoli, S.M. Logie, A. Myers, J.A. Kemp, J.P. Chick, and A.C.P. Braden. Reconstructing the Lituus: A reassessment of impedance, harmonicity, and playability. In Proceedings *NAG/DAGA International Conference on Acoustics, Rotterdam, Netherlands*, 2009.

John P. Chick and Shona M. Logie. Comparison of the mechanics of brass player's lips during slurred note transients. In *J. Acoust. Soc. Am.* **125***, 2598*, 2009.

Shona Logie, Murray Campbell, John Chick, Arnold Myers and Joël Gilbert. Musical consequences of nonlinear sound propagation in brass instruments. In *J. Acoust. Soc. Am.* **128***, 2282*, 2010.

Jonathan A. Kemp, Shona M. Logie, John P. Chick, Richard A. Smith, and D. Murray Campbell. Analysis of transients for brass instruments under playing conditions using multiple microphones. In Proceedings *10ème Congrès Français d'Acoustique, Lyon, France*, 2010.

Shona Logie, John Chick, Sam Stevenson, Murray Campbell. Upward and downward slurred transients on brass instruments: why is one not simply the inverse of the other? In Proceedings *10ème Congrès Français d'Acoustique, Lyon, France*, 2010.

John Chick, Shona Logie, Jonathan Kemp, Murray Campbell, and Richard Smith. An exploration of extreme high notes in brass playing. In Proceedings *International Symposium on Musical Acoustics, Sydney, Australia*, 2010.

Shona M. Logie, Stefan Bilbao, John P. Chick, and D. Murray Campbell. The

influence of transients on the perceived playability of brass instruments. In Proceedings *International Symposium on Musical Acoustics, Sydney, Australia*. 2010.

L. Norman, J.P. Chick, S. Logie, and D.M. Campbell. Pitch bending on early brass instruments. In Proceedings *International Symposium on Musical Acoustics, Sydney, Australia*. 2010.

Shona Logie, John Chick, Murray Campbell, and Stefan Bilbao. The influence of bore profile on slurred transients in brass instruments. In Proceedings *Forum Acusticum, Aalborg, Denmark*, 2011.

John P. Chick, Shona Logie, D. Murray Campbell, Arnold Myers, and Joël Gilbert. Effects of viscothermal losses on wavefront distortion due to nonlinear propagation in trombones. In Proceedings *Forum Acusticum, Aalborg, Denmark*, 2011.

Arnold Myers, Robert W. Pyle, Joël Gilbert, D. Murray Campbell, John P. Chick, and Shona Logie. Effects of nolinear sound propagation on the characteristic timbres of brass instruments. In *J. Acoust. Soc. Am.* **131**, *678*, 2012.

John P. Chick, Shona Logie, Murray Campbell, and Joël Gilbert. Spectral enrichment and wall losses in trombones played at high dynamic levels. In Proceedings *11th Congrès Français d'Acoustique and 2012 IOA Annual Meeting, Nantes, France*, 2012.